

INFORMATION TO USERS

The most advanced technology has been used to photograph and reproduce this manuscript from the microfilm master. UMI films the text directly from the original or copy submitted. Thus, some thesis and dissertation copies are in typewriter face, while others may be from any type of computer printer.

The quality of this reproduction is dependent upon the quality of the copy submitted. Broken or indistinct print, colored or poor quality illustrations and photographs, print bleedthrough, substandard margins, and improper alignment can adversely affect reproduction.

In the unlikely event that the author did not send UMI a complete manuscript and there are missing pages, these will be noted. Also, if unauthorized copyright material had to be removed, a note will indicate the deletion.

Oversize materials (e.g., maps, drawings, charts) are reproduced by sectioning the original, beginning at the upper left-hand corner and continuing from left to right in equal sections with small overlaps. Each original is also photographed in one exposure and is included in reduced form at the back of the book.

Photographs included in the original manuscript have been reproduced xerographically in this copy. Higher quality 6" x 9" black and white photographic prints are available for any photographs or illustrations appearing in this copy for an additional charge. Contact UMI directly to order.

U·M·I

University Microfilms International
A Bell & Howell Information Company
300 North Zeeb Road, Ann Arbor, MI 48106-1346, USA
313 761 4700 800 521-0600

Order Number 9032553

A study of the chlorination of gold: The effect of nascent chlorine, mechanism determination, the role of sulfide minerals and carbon, and the effect of multivalent cationic chloride salts

Nesbitt, Carl C., Ph.D.

University of Nevada, Reno, 1990

U·M·I

300 N. Zeeb Rd.
Ann Arbor, MI 48106

University of Nevada

Reno

A Study of the Chlorination of Gold:
The Effect of Nascent Chlorine, Mechanism Determination, the Role of
Sulfide Minerals and Carbon, and the Effect of Multivalent Cationic
Chloride Salts


A dissertation submitted in partial fulfillment
of the requirements for the degree of
Doctor of Philosophy in Metallurgical Engineering

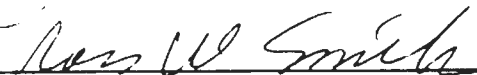
by


Carl C. Nesbitt

April 1990

The dissertation of Carl C. Nesbitt is approved:


Dissertation Advisor


Department Chair


Dean, Graduate School

University of Nevada
Reno

April 1990

ABSTRACT

A three-phase study has been conducted to investigate the effect of chlorine on the dissolution of elemental gold. The study lead to a conclusion that the existence of a "nascent chlorine" atom was not responsible for an observed increase in recovery and gold dissolution rate when chlorine was chemically formed *in situ*. Instead, the chloride reagents added to produce chlorine--HCl, NaCl, etc.--increased the ionic strength of the solution which increased the dissolution rate of gold. Also, the study concluded that the reason why flash chlorination is a successful pretreatment for carbonaceous gold ores is due to the adsorption of dissolved metals from sulfide minerals on the surface of the carbon. The adsorption of iron and copper reduces the adsorption of Au.

The first phase of the research investigated the existence of a reactive intermediate chlorine atom ($\text{Cl}\cdot$) which may be a more chemically reactive species than Cl_2 . The existence was investigated by photodecomposition of diatomic chlorine gas with ultraviolet light. The existence of nascent chlorine was not experimentally observed and was determined not to be the explanation of the earlier claims. However, during the course of the research, an anomalous peak in the gold concentration curves was noticed whenever fine gold was dissolved by chlorine. The observed Au concentration curve had a large peak, or spike, at the point at which a typical sigmoidal curve would have reached the maximum. The peak was determined to be caused by the interference of colloidal elemental gold with the atomic absorption spectrophotometer (AAS) spectra of dissolved gold

species at 242 nm. During the course of this research, it became obvious that the AuCl_2^- complex would reduce to Au^0 instantly if the exact conditions for stability were not achieved. This observation led to the determination that AuCl_2^- was an intermediate in the reaction of gold with chlorine and was reduced to Au^0 in the sample carrier stream to the AAS. Attempts to make the carrier stream amenable to the stability of AuCl_2^- failed as the stable range of pH and Eh is narrow and difficult to recreate exactly.

Another phase of the research investigated the effect that various multivalent cation chloride salts have on the dissolution of Au by sparging Cl_2 . By adding various amounts of HCl, NaCl, $\text{CaCl}_2 \cdot 2\text{H}_2\text{O}$, $\text{NiCl}_2 \cdot 6\text{H}_2\text{O}$ and $\text{FeCl}_3 \cdot 6\text{H}_2\text{O}$ to the leach solution in fine gold sparging experiments, the conclusion was drawn that an increase in chloride ion concentration, or ionic strength of the solution, resulted in an increased gold dissolution rate.

The final phase of the research investigated the "flash chlorination" process. The dissolution of five sulfide minerals by sparged chlorine gas was conducted individually in an attempt to see which, if any, dissolve faster than gold. The follow-up research was conducted to investigate the effect of chlorination on a synthetic refractory ore from Carlin. Studies showed that iron and copper dissolved from pyrite and chalcocite will adsorb on the carbon, reducing Au adsorption. The observed effect of iron and copper led to the development and testing of a pretreatment process using ferric chloride in conjunction with chlorine to hinder Au adsorption.

TABLE OF CONTENTS

ABSTRACT	i
ACKNOWLEDGEMENTS	v
LIST OF FIGURES	vi
LIST OF TABLES	xiv
 INTRODUCTION:	
I. Historical Background to Chlorination of Gold	2
a. Experiments and Patents of Chlorination of Gold	2
b. Industrial Applications of Chlorination	4
II. Flow Injection Analysis	7
III. Electrochemistry and Thermodynamics of Au-Cl-H ₂ O System The Eh-pH Diagram	11
 CHAPTER ONE: Nascent Chlorine and the Chlorination of Gold	
I. Introduction	20
a. Nascent Chlorine	20
b. Photochemistry of Cl ₂	22
c. Mechanism of Chlorination	23
II. Experimental	25
III. Results	34
IV. Discussion	69
a. Cl ₂ Addition and Nascent Chlorine	69
b. Mechanism of the Chlorination of Gold	76
V. Conclusions	81
 CHAPTER TWO: The Role of Carbon and Minerals in the Pretreatment of Refractory Gold Ores With Chlorine.	
I. Introduction	82
a. Chlorine Chemistry	82
b. Flash Chlorination Process Development	83
c. The Refractory Ore of Carlin, Nevada	88
II. Experimental	92
III. Results	99
IV. Discussion	159
a. Mineral Studies	159
b. Carbon Studies	162
V. Conclusions	170

CHAPTER THREE: The Effect of Multivalent Chloride Salts on the
Chlorination of Gold Ores

I. Introduction	171
a. Chloride Salts	171
b. Chlorine Activity	173
II. Experimental	178
III. Results	179
IV. Discussion	201
IV. Conclusions	217
 CHAPTER FOUR:	
Conclusions of Study	218
 BIBLIOGRAPHY	222

ACKNOWLEDGEMENTS

In recognizing all who were important to the author, this section has the greatest likelihood of being the longest section. The author particularly wishes to thank Drs. Jim Hendrix for financial and technical support and John Nelson for technical support and guidance.

I would also like to thank Ljiljana Solujić and Emil Milosavljević for their help in the chemistry of the dissertation. Their knowledge of inorganic chemistry, synthesis of rare compounds, and the insight of flow injection analysis were invaluable. And to Mojtaba Amadiantehrani for help in the analytical procedures used in this dissertation more gratitude is expressed.

Also, the support of the Newmont Metallurgical Services for funding this research is gratefully acknowledged. In particular, the author wishes to thank Dave Hill, Marc LeVier, and Marcel DeGuire for keeping this project funded through its entirety.

But most importantly, the author wishes to thank his family. I thank my wife, Lorrie, whose support and self-sacrifice was so much appreciated; my children, Lauren, Mark, and Ellen for accepting Dad's absence; and my mother, Merle, whose support (both financial and mental) made this all possible.

LIST OF FIGURES

Figure 1. Flowsheet of the Chlorination Pre-treatment Plant of the Newmont Gold Company for the period of operation from 1972 to 1976 and 1982 to 1985	6
Figure 2. Effect of plug flow on an injected sample volume	9
Figure 3. Typical FIA loop for sampling a batch process with sample recycle	9
Figure 4. Two position rotary valve for FIA injections	10
Figure 5. Eh-pH diagram for $[Au] = 10^{-4}$ M and $[Cl^-] = 2.0$ M	19
Figure 6. Eh-pH diagram for $[Au] = 10^{-4}$ M and $[Cl^-] = 10^{-2}$ M	19
Figure 1-1. Energy diagram for a typical reaction of reactants to products	21
Figure 1-2. Energy diagram depiction of the formation of chlorine gas from a chloride salt with a reaction intermediate ($Cl\cdot$)	22
Figure 1-3. FIA flowsheet for the simultaneous determinations of Au and Cl_2	27
Figure 1-4. Modified FIA flow diagram for Phase II of the experiments	29
Figure 1-5. Apparatus schematic for sparging experiment	31
Figure 1-6. Sample port for FIA system	33
Figure 1-7. Response of the initial FIA arrangement to step increase of Au concentration	45
Figure 1-8. Response of the second FIA arrangement to step increase of Cu concentration	45
Figure 1-9. Au dissolution by sparging chlorine under a UV 'Show N Grow' 60W-120V bulb	46
Figure 1-10. Au dissolution by sparging chlorine in total darkness	47
Figure 1-11. Au dissolution by sparging chlorine with a submersible UV lamp in a 1-L sample	48

Figure 1-12. Au dissolution by sparging chlorine in a 1-L experiment in total darkness	49
Figure 1-13. Au dissolution by sparging chlorine in a 1.5-L experiment with the G.E. flood light with an optic sensor to measure the amount of light absorbed	50
Figure 1-14. Au dissolution by sparging chlorine in a 1.5-L experiment with no light	51
Figure 1-15. Au dissolution of coarse gold (-20 mesh) in a 1.0-L experiment with sparging chlorine and room light	52
Figure 1-16. Au dissolution of fine gold (-325 mesh) in a 1.0-L experiment with sparging chlorine and room light	53
Figure 1-17. Au dissolution by chlorine for anodic formation of Cl_2 from a solution containing 0.2 M NaCl and 1 M HCl under a constant potential of 3.65 V	54
Figure 1-18. Dissolution data of Au by chlorine produced anodically from a solution of 0.2 M NaCl and 1.0 M HCl under variable potential ..	55
Figure 1-19. Dissolution data of Au by chlorine produced anodically from a solution of 0.1 M NaCl and 0.1 M HCl at a potential of 3.65 V	56
Figure 1-20. Dissolution data of Au by chlorine formed chemically by the acidification of NaOCl with H_2SO_4	57
Figure 1-21. Dissolution data of Au by chlorine formed chemically by the acidification of NaOCl with H_2SO_4	58
Figure 1-22. Dissolution of Au by chlorine formed chemically by the reaction of KMnO_4 and HCl (-325 mesh Au).....	59
Figure 1-23. Dissolution of Au by chlorine formed chemically by the reaction of KMnO_4 and HCl (-20 mesh Au).....	60
Figure 1-24. Comparison of the methods of manipulating FIA data	61
Figure 1-25. Observed Au AAS spectra of a solution of $\text{KMnO}_4/\text{HCl}/\text{H}_2\text{O}$ without gold.....	62
Figure 1-26. Au dissolution in the absence of mixing	63
Figure 1-27. Au dissolution with mixing by a 1-hp lab mixer and impellor	64

Figure 1-28. Results of an experiment using AuCl_2^- and AuCl_4^- to determine if AAS spectral interferences exist between Au(I) and Au(III) species	65
Figure 1-29. Effect of using 2M HCl in the carrier stream of the AAS ..	66
Figure 1-30. Effect of using 3.8M HCl in the carrier stream of the AAS .	67
Figure 1-31. Effect of using dissolved chlorine gas in the carrier stream.	68
Figure 1-32. Comparison of the chlorination of fine particle Au by sparging and the reaction of KMnO_4 with HCl	71
Figure 1-33. Comparison of the chlorination of coarse particle Au by sparging and the reaction of KMnO_4 with HCl	72
Figure 1-34. Comparison of the dissolution data from Figures 1-9 and 1-10	73
Figure 1-35. Comparison of the dissolution data from Figures 1-11 and 1-12	74
Figure 1-36. Comparison of the dissolution data from Figures 1-13 and 1-14	75
Figure 1-37. The effect of particle size on the chlorination of Au	79
Figure 2-1. Flowsheet of the "flash" chlorination process since 1987 ..	87
Figure 2-2. Cross-sectional view of a technique devised to secure the carbon in the mineral/carbon/gold experiments	94
Figure 2-3. Dissolution of coarse pyrite by sparging chlorine	112
Figure 2-4. Fine pyrite dissolution with chlorine gas	113
Figure 2-5. Comparison of the dissolution of coarse Au to coarse pyrite by sparging chlorine gas	114
Figure 2-6. Comparison of fine particle Au and pyrite dissolution by chlorine sparging	115
Figure 2-7. Coarse pyrite dissolution by the permanganate acidification reaction	116
Figure 2-8. Fine particle pyrite dissolution by KMnO_4/HCl reaction	117

Figure 2-9. Comparison of dissolution of coarse particle Au and pyrite by the acidification of KMnO_4	118
Figure 2-10. Comparison of permanganate acidification reaction dissolution of fine particle Au and pyrite	119
Figure 2-11. Sparged chlorine dissolution of coarse pyrrhotite	120
Figure 2-12. Sparged chlorine dissolution of fine pyrrhotite	121
Figure 2-13. Coarse particle Au and pyrrhotite dissolution comparison for sparging chlorine gas	122
Figure 2-14. Comparison of the dissolution of fine particle Au and pyrrhotite by sparging chlorine gas	123
Figure 2-15. KMnO_4 acidification of coarse pyrrhotite	124
Figure 2-16. KMnO_4 acidification of fine pyrrhotite.....	125
Figure 2-17. Comparison of the dissolution of coarse Au and pyrrhotite by the KMnO_4/HCl reaction	126
Figure 2-18. Comparison of the dissolution of Au by the KMnO_4/HCl of fine particle Au and pyrrhotite	127
Figure 2-19. Coarse particle chalcocite dissolution by gas sparging ..	128
Figure 2-20. Fine particle chalcocite dissolution by gas sparging ..	129
Figure 2-21. Comparison of the dissolution by sparging on coarse particles of Au and chalcocite	130
Figure 2-22. Comparison of fine particle Au and chalcocite dissolution by sparging	131
Figure 2-23. KMnO_4/HCl reaction dissolution of coarse chalcocite ..	132
Figure 2-24. KMnO_4/HCl reaction dissolution of fine chalcocite	133
Figure 2-25. Coarse particle dissolution comparison for Au and chalcocite in the acidification of potassium permanganate ..	134
Figure 2-26. Fine particle Au and chalcocite comparison by the KMnO_4/HCl reaction	135

Figure 2-27. Results of the dissolution of coarse chalcopyrite by Cl_2 sparging	136
Figure 2-28. Results of the dissolution of fine chalcopyrite by sparging..	137
Figure 2-29. Coarse Au and chalcopyrite dissolution comparison by sparging Cl_2 gas	138
Figure 2-30. Comparison of the dissolution by sparging of fine Au and chalcopyrite	139
Figure 2-31. Permanganate dissolution of coarse chalcopyrite	140
Figure 2-32. Permanganate dissolution of fine chalcopyrite	141
Figure 2-33. Comparison of the dissolution of coarse Au and chalcopyrite by the KMnO_4/HCl reaction	142
Figure 2-34. Comparison of the dissolution of fine chalcopyrite and Au by the permanganate method	143
Figure 2-35. Dissolution of coarse arsenopyrite by sparging Cl_2 gas	144
Figure 2-36. Dissolution of fine arsenopyrite by Cl_2 gas	145
Figure 2-37. Comparison of coarse particle dissolution of Au and arsenopyrite by Cl_2 gas	146
Figure 2-38. Fine particle dissolution comparing Au and arsenopyrite by gas sparging	147
Figure 2-39. Dissolution of coarse arsenopyrite by acidifying KMnO_4	148
Figure 2-40. Dissolution of fine arsenopyrite by acidifying KMnO_4 ..	149
Figure 2-41. Comparison of the dissolution of coarse Au and arsenopyrite by chlorine formed chemically by the reaction of KMnO_4 with HCl	150
Figure 2-42. Dissolution comparison for fine Au and arsenopyrite for the permanganate method of adding chlorine	151
Figure 2-43. Results of the dissolution of Au during the sparging of chlorine in a slurry of pyrite, chalcocite, Au with carbon in a vial apparatus	152
Figure 2-44. Metal adsorbance on carbon as a function of time	153

Figure 2-45. Au adsorbance on carbon with no pretreatment	154
Figure 2-46. Au adsorbance on carbon pretreated with sparged Cl_2 ..	155
Figure 2-47. Effect of 1.8 g/L Fe^{+3} ($\text{FeCl}_3 \cdot 6\text{H}_2\text{O}$) pretreatment of carbon in hindering the adsorption of dissolved Au	156
Figure 2-48. Effect of 1.8 g/L Fe^{+3} ($\text{Fe}(\text{NO}_3)_3 \cdot 9\text{H}_2\text{O}$) pretreatment of carbon in hindering the adsorption of dissolved Au	157
Figure 2-49. Effect of 1.8 g/L Fe^{+3} ($\text{FeCl}_3 \cdot 6\text{H}_2\text{O}$) and chlorine sparging pretreatment of carbon in hindering the adsorption of dissolved Au	158
Figure 2-50. The pH and Eh of the experiment using ferric chloride and Cl_2 pretreatment of carbon prior to Au addition	158
Figure 2-51. Comparison of the dissolution of coarse minerals by chlorine sparging	165
Figure 2-52. Comparison of the dissolution of fine minerals by chlorine sparging	166
Figure 2-53. Comparison of the dissolution of coarse minerals by chlorine produced by the KMnO_4/HCl reaction	167
Figure 2-54. Comparison of the dissolution of fine minerals by chlorine produced by the KMnO_4/HCl reaction	168
Figure 2-55. Comparison of gold dissolution experiment to the gold adsorption experiment	169
Figure 3-1. Effect of ionic strength by chloride ion on the rate of dissolution of gold for various chlorine concentrations	172
Figure 3-2. Plots of Meisner and Tester for ionic strength (μ) of 0 to 2M.	177
Figure 3-3. Family of plots from Meisner and Tester for high μ ...	177
Figure 3-4. Au dissolution by sparging Cl_2 with no salt added	183
Figure 3-5. Au dissolution by sparging Cl_2 with 0.05M chloride ion concentration from HCl	184
Figure 3-6. Au dissolution by sparging Cl_2 with 0.1 M $[\text{Cl}^-]$ from HCl .	185
Figure 3-7. Au dissolution by sparging Cl_2 with 0.5 M $[\text{Cl}^-]$ from HCl .	186

Figure 3-8. Au dissolution by sparging Cl_2 with 1.0 M $[\text{Cl}^-]$ from HCl .	187
Figure 3-9. Au dissolution by sparging Cl_2 with 0.05 M $[\text{Cl}^-]$ from NaCl.	188
Figure 3-10. Au dissolution by sparging Cl_2 with 0.1 M $[\text{Cl}^-]$ from NaCl ..	189
Figure 3-11. Au dissolution by sparging Cl_2 with 0.5 M $[\text{Cl}^-]$ from NaCl ..	190
Figure 3-12. Au dissolution by sparging Cl_2 with 1.0 M $[\text{Cl}^-]$ from NaCl ..	191
Figure 3-13. Au dissolution by sparging Cl_2 with 0.05 M $[\text{Cl}^-]$ from $\text{CaCl}_2 \cdot 2\text{H}_2\text{O}$	192
Figure 3-14. Au dissolution by sparging Cl_2 with 0.1 M $[\text{Cl}^-]$ from $\text{CaCl}_2 \cdot 2\text{H}_2\text{O}$	193
Figure 3-15. Au dissolution by sparging Cl_2 with 0.5 M $[\text{Cl}^-]$ from $\text{CaCl}_2 \cdot 2\text{H}_2\text{O}$	194
Figure 3-16. Au dissolution by sparging Cl_2 with 1.0 M $[\text{Cl}^-]$ from $\text{CaCl}_2 \cdot 2\text{H}_2\text{O}$	195
Figure 3-17. Au dissolution by sparging Cl_2 with 0.05 M $[\text{Cl}^-]$ from $\text{NiCl}_2 \cdot 6\text{H}_2\text{O}$	196
Figure 3-18. Au dissolution by sparging Cl_2 with 0.1 M $[\text{Cl}^-]$ from $\text{NiCl}_2 \cdot 6\text{H}_2\text{O}$	197
Figure 3-19. Au dissolution by sparging Cl_2 with 0.5 M $[\text{Cl}^-]$ from $\text{NiCl}_2 \cdot 6\text{H}_2\text{O}$	198
Figure 3-20. Au dissolution by sparging Cl_2 with 0.05 M $[\text{Cl}^-]$ from $\text{FeCl}_3 \cdot 6\text{H}_2\text{O}$	199
Figure 3-21. Au dissolution by sparging Cl_2 with 0.1 M $[\text{Cl}^-]$ from $\text{FeCl}_3 \cdot 6\text{H}_2\text{O}$	200
Figure 3-22. Comparison of the dissolution experiments for various $[\text{Cl}^-]$ from HCl addition and no salt addition	202
Figure 3-23. NaCl addition as compared to no salt addition for all $[\text{Cl}^-]$	203
Figure 3-24. CaCl_2 addition as compared to no salt addition	204
Figure 3-25. NiCl_2 addition as compared to no salt addition	205
Figure 3-26. FeCl_3 addition as compared to no salt addition	206

Figure 3-27. Comparison of 0.05 M [Cl ⁻] experiments to no salt	207
Figure 3-28. Comparison of 0.1 M [Cl ⁻] experiments to no salt	208
Figure 3-29. Comparison of 0.5 M [Cl ⁻] experiments to no salt	209
Figure 3-30. Comparison of 1.0 M [Cl ⁻] experiments to no salt	210
Figure 3-31. Typical dissolution profile for fine particle Au dissolution by Cl ₂ sparging	211
Figure 3-32. Graphical representation of the relation of μ to Au dissolution rate for the same sparging rate of chlorine	215
Figure 3-33. Graphical comparison of the dissolution rate and the chloride activity as calculated by the extended Debye-Hückel equation and the Meisner and Tester plots	216

LIST OF TABLES

Table I. Standard electrode potentials (E°) at 25°C for half-reactions pertinent to the Au-Cl-H ₂ O system arranged in decreasing oxidation potential	12
Table II. Theoretical chloride concentrations at which both AuCl ₂ ⁻ and AuCl ₄ ⁻ are thermodynamically stable.....	14
Table III. Reactions pertinent to the Au-Cl-H ₂ O system for which limited information is available	16
Table IV. Standard free energy of formation for species of the Au-Cl-H ₂ O system	17
Table V. Eh-pH expressions derived from the reactions defined for the Au-Cl-H ₂ O system	18
Table 2-I. Possible reactions of three minerals - (i) chalcocite, (ii) pyrite, and (iii) two forms of pyrrhotite - with chlorine and the associated standard free energies for the reactions (assuming S° or H ₂ S is produced)	84
Table 2-II. Possible reactions of three minerals - (i) chalcocite, (ii) pyrite, and (iii) two forms of pyrrhotite - with chlorine and the associated standard free energies for the reactions (assuming SO ₄ ⁻² produced)	85
Table 2-III. Calculated ore assay based on the analysis of Carlin ore by Dr. J. H. Nelson	91
Table 2-IV. Results of the analysis of the minerals by the acid digestion and inductively-coupled plasma (ICP) flame emission spectrophotometer	97
Table 2-V. Comparison of statistically generated mineral purity (based on initial weight and final metal assays for the dissolution experiments)	100
Table 2-VI. Results of the timed removal of carbon during the chlorination of pyrite, chalcocite and gold	109
Table 3-I. Comparison of the activity coefficients as calculated from the Extended Debye-Hückel equation and by the Meisner and Tester graphical analysis technique	176

Table 3-II. Average Au dissolution rate (mg/min) calculated from the various dissolution experiments	212
Table 3-III. Comparison of the dissolution rate of Au (mg/min) for chlorine sparging (~400 std. cc/min) at various ionic strengths (μ).....	212

Introduction

Cyanide is the gold and silver lixiviant of choice for nearly every commercial operation in the world. A wide range of ores are economically treated with cyanide. Special processes have been developed in recent years to treat refractory gold ores--such as carbonaceous ores, antimony- and arsenic- bearing ores, gold-telluride ores, sulfide ores, or combinations of these types. Autoclaving at 400°C and 2800 kPa, and pretreating with gaseous chlorine or hypochlorite solutions are becoming prevalent throughout the industry, but these processes are merely steps taken prior to cyanidation and may become prohibitively expensive to operate.

Many operators are, therefore, seeking alternative lixiviants, especially, inexpensive reagents that are potentially less environmentally hazardous. Several have been explored, such as thiourea, hypochlorite, and ammonium thiosulfate, but none has already been proven effective--chlorine. From 1850 through the turn of the century, chlorination of gold was the sole hydrometallurgical process in use. But since cyanide replaced chlorine, little has been done with chlorine with the exception of its use as a pretreatment for cyanidation.

This study is presented as a new look at an old process. To update our understanding of the chlorination process, the history of gold chlorination is presented. Also, brief descriptions of an improvement in sample acquisition and the thermodynamics of the Au-Cl-H₂O system are provided to improve our understanding of the process.

I. Historical Background to the Chlorination of Gold¹⁻¹⁸

Experiments and Patents of the Chlorination of Gold¹

The first discovery of gold dissolution from ores with chlorine has been attributed to Dr. John Percy of London whose research dates back to 1846. Two years later, Carl F. Plattner devised a process using chlorine water to extract gold from the arsenic residues of a roaster in Germany. The "Plattner Process" was first reported, however, by Wilhelm Guettler at the International Exhibition in London in 1851. Guettler reported the treatment of arsenical gold ores by the following method:

- (1) Roast the ore
- (2) Pass chlorine gas through the roasted ore
- (3) Wash with water to dissolve gold chloride
- (4) Precipitate gold from solution with H_2S .

This process was attributed to Plattner as being the inventor. However, Plattner had not published any such process or research. Instead, his research was limited to using chlorine water to dissolve gold. The first use of chlorine gas can be traced to the research of H. Lange in 1849.

The first U.S. Patent for chlorination was awarded in 1852 to Charles Spicker. The broad patent embodied gaseous Cl_2 , Cl_2 dissolved in water, and Cl_2 with alkaline salts (chlorinated lime) for "separation of gold from its ores, sands, or mixtures."¹ Edouard Primard was granted a patent in England in 1857 for a process of chlorination in barrels. Perhaps the forebearer to the "barrel process", chlorine was added to stationary barrels and subsequently washed with water. However, the "barrel process" was invented soon thereafter.

In 1848 Dr. Duflos described a technique for adding chlorine gas, water and ore to a glass bottle and "rolling it up and down a table for two hours". These experiments seem to be the first example of the barrel process. Later, the process permutated into various techniques. At first, the barrel process used gaseous chlorine generated externally by chemical reaction or, ultimately, by electrochemical generation. *In situ* formation of chlorine by acidification of calcium hypochlorite was also practiced.

William Henderson was granted a patent in 1859 for a process in which agitation was used in chlorination, but A.C.L. DeLacy is credited with the first barrel process patent in 1864. DeLacy used calcium hypochlorite and sulfuric acid to generate Cl_2 *in situ*.

In 1877 Mears patented a process by which chlorine gas was produced in an enclosed barrel. The high pressure was maintained for several hours. The contention was that the higher Cl_2 pressure improved the reaction rate and increased gold recovery.

Several processes have been used through the years for recovering the gold from solution. The first experiments by Percy used "sodium hyposulfate" (sodium thiosulfate). Duflos evaporated some samples, and added HCl with "arsenious" acid to precipitate gold in others. Guettler recommended the use of H_2S . And in 1880, W.M. Davis was granted a U.S. Patent for "the decomposition of gold chloride (AuCl_3) by carbon." Sulfur dioxide and iron sulfate (green vitriol) were also recommended for reduction of Au^{+3} to Au^0 . All of these methods found application in some commercial operations through the turn of the century.

Since 1900, very little research has been done on the chlorination of gold. Putnam¹⁹ demonstrated a kinetic effect of chloride ions in the chlorination of gold leaf in 1944. Walker²⁰ determined the heats of reactions for the chlorination of gold, silver, zinc, lead, mercury, and copper. Nagy and others²¹ compiled work on chlorination in 1966 (including the work of Jackson and Strickland²² of 1933). The U.S. Bureau of Mines studied the use of chlorine and hypochlorite for the oxidation of carbonaceous gold ores from 1966 to 1971.²⁵⁻³⁰ The lab and pilot plant studies considered the use of these reagents to oxidize carbon prior to cyanidation.

Industrial Applications of Chlorination

Guido Küstel² has attributed G.F. Deetkin with first introducing the Plattner Process in Nevada and California in 1858. For the next 50 years, chlorination was the main hydrometallurgical process for gold and silver recovery. However, the boom began declining by the turn of the century. Cyanide (discovered to be a lixiviant for gold and silver in 1843) was cheaper than the reagents needed to produce chlorine. While chlorine was limited to finely disseminated gold in oxide ores or roasted sulfide ores, cyanide had better recovery of gold and silver from sulfide ores without roasting.

Several textbooks chronicled the decline of chlorination as an industrial process. For instance, Austin's textbook (The Metallurgy of the Common Metal) appeared in six editions from 1907 to 1926³⁻⁵. In the 1st edition (1907) chlorination was allotted some 12 pages. In the 3rd edition

(1911) it was allotted 18 pages. But in the 6th edition (1926), only 2 pages were devoted to the chlorination process. In T.K. Rose's Metallurgy of Gold⁶⁻¹², the first four editions (1894 to 1902) devoted nearly 90 pages each to chlorination. However, by the fifth and sixth editions (1906 and 1915) only 43 pages and 20 pages, respectively, described chlorination. And by the seventh edition (1937) there was no mention of chlorination. Liddell¹³, in 1926, referred to chlorination as an "obsolete process".

Not until the late 1960's did the use of chlorine in gold hydrometallurgy reappear. From 1966 to 1971, the U.S. Bureau of Mines in conjunction with Carlin Gold Mining Company (later, called Newmont Gold) studied the use of various reagents for the oxidation of carbonaceous materials found in refractory gold ores prior to cyanidation.²⁵⁻³⁰ The laboratory and subsequent pilot plant studies showed good results with chlorine. So good, in fact, that construction began in 1971 for a chlorination circuit at the Carlin Gold Mine in Carlin, Nevada. By early 1972 the process was in operation. Figure 1 shows the plant flow diagram.²⁹ The plant operated in this mode until 1976 when an oxidation step prior to chlorination was added. By sparging air into pulp at 90°C prior to chlorination, the consumption of Cl₂ was dramatically reduced. But due to a large amount of equipment damage and high energy costs, the process was abandoned and replaced by original design in 1982.

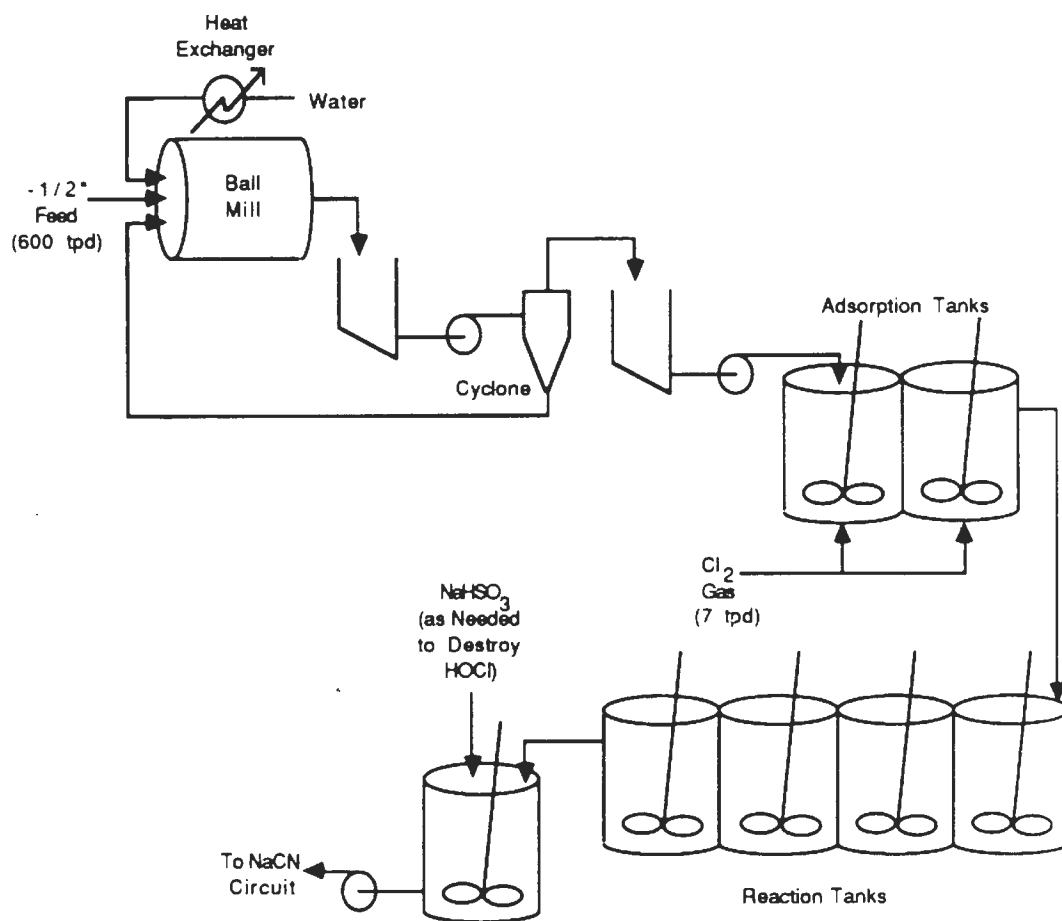


Figure 1. Flowsheet of the Chlorination Pre-treatment Plant of the Newmont Gold Company for the periods of operation; 1972 to 1976, and 1982 to 1985²⁹.

Later, in 1985, additional research showed that the optimum conditions for chlorination (short, big bursts of Cl_2 followed by long conditioning times) were much better than the prolonged exposures previously used. "Flash" chlorination improved gold extraction through cyanidation by 6%, and reduced the Cl_2 requirements per ounce by nearly 25% over the previous method.

II. Flow Injection Analysis

Flow injection analysis (FIA) was used extensively throughout the studies reported herein. FIA uses the principle of plug-flow injection of a sample into a constantly monitored stream. Changes in the pH, color, potential, absorption spectra, or fluorescence of the stream can be easily monitored and correlated to analyte concentrations in the sample stream. When the sample is continually pumped through a sample loop and periodically injected, kinetic data are readily obtained by use of FIA in conjunction with such instruments as atomic absorption spectrophotometers, monochromatic UV-Vis spectrophotometers, potentiometers, or any other constant monitoring detectors using flow through cells.

FIA was pioneered in the mid-1970's by Dr. Jaromir Ružička and Dr. Elo Harald Hansen³¹ and others.³²⁻⁴⁰ While FIA was initially used for biological applications, by the late 1980's, more than 1400 articles⁴¹ had been published dealing with a wide range of fields including metallurgy,⁴² chemistry,⁴³ biotechnology,⁴⁴ medicine,³⁶ pharmaceuticals,⁴⁵ and

environmental engineering.⁴⁶ Articles describe uses ranging from laboratory scale⁴⁷ to on-line industrial process control applications.⁴⁸ Specific uses of the technique have been applied to liquid-solid,⁴⁹ liquid-liquid,⁵⁰ liquid-gas,⁵¹ and even gas-solid⁵² interactions.

FIA operates on the principle that there is a low degree of mixing in a plug flow profile. When a sample is injected into a carrier stream, the "plug" of sample is carried to a detector as seen in Figure 2. The instrument will report the sample as a spike whose peak height is directly related to the sample concentration. By increasing the diameter or length of the tube in which the carrier flows to the detector, the degree of mixing (or dilution by the carrier) is increased. Likewise, if reagents must be added to form detectable products, increased mixing is achieved in this manner. Mixing coils are sections of tubing of various length and diameter which may be placed in the stream for this purpose. Figure 3 is an example of an FIA loop for sampling a batch system. The sample is pumped through a sample volume in the injection valve. This volume is injected into the carrier stream where it mixes with the reagent in the mixing coil. The final reaction products are then detected in the flow cell detector.

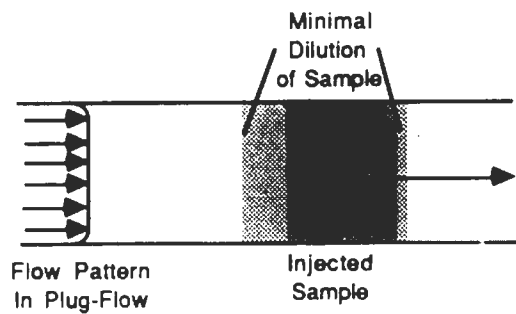


Figure 2. Effect of Plug Flow on an injected sample volume.

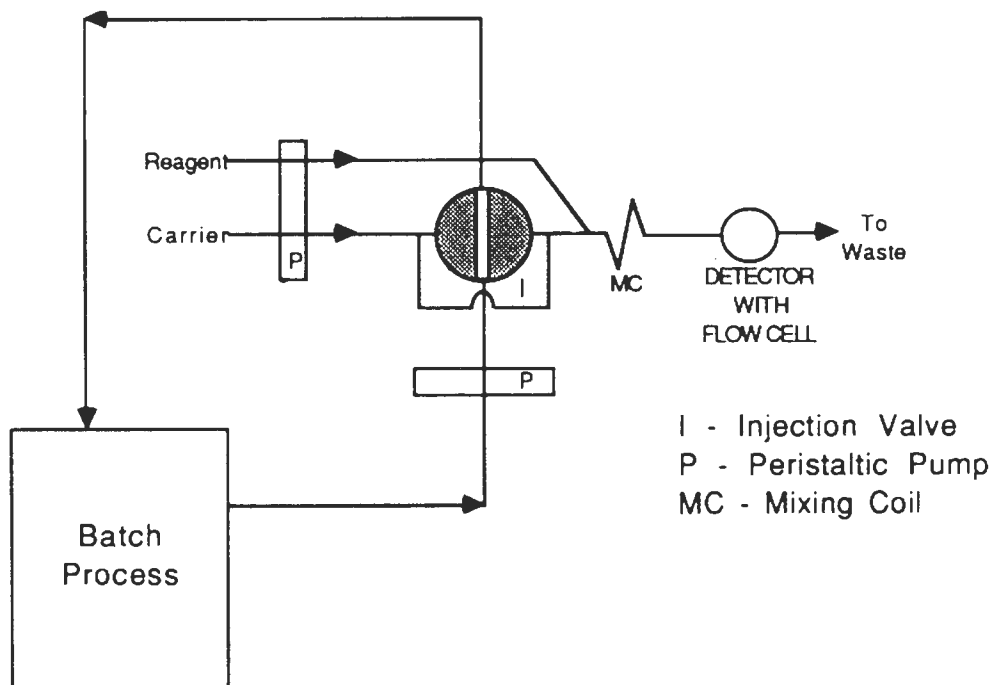


Figure 3. Typical FIA loop for sampling a batch process with sample recycle.

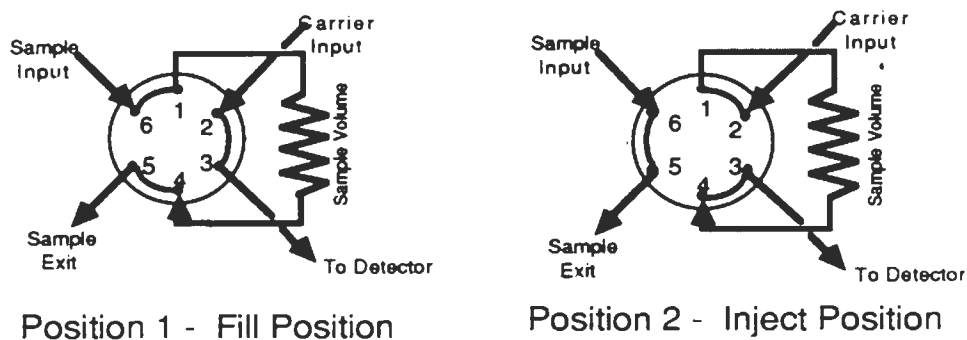


Figure 4. Two Position Rotary Valve for FIA Injections.

Rather than "injection" a more accurate description would be that the carrier stream is rerouted through a portion of the sample stream which is accomplished by using a two-position, 4-way rotary valve. Figure 4 is a schematic depiction of such a valve showing the two positions for sample filling and injection. When the valve is in Position 1 (Fill) the sample stream flows into port 6 and out of 1 then flows through a specific length of tubing (the length and diameter of the tubing determines the total volume of the sample). The sample then continues into port 4 and exits through port 5 to be either discarded or recycled to the process. Meanwhile, the carrier stream flows into port 2 and out of port 3 to the detector. With the valve in Position 2 (Inject) the carrier stream is rerouted from port 2 into port 1 and through the sample volume. The carrier and "injected" sample then flow into port 4 thence to port 3 and on to the detector. The sample stream now bypasses the sample loop from ports 6 to 5. When returned to the fill position, the small volume of carrier is returned with the sample, maintaining the total volume of the batch process being studied,

and diluting the total volume by a minimum amount. Typical sampled loop volumes are 25 to 1000 microliters.

The total time required for this operation is limited by only three factors:

- (1) speed of the detector,
- (2) flow rate of the carrier,
- (3) flow rate of the sample.

If relatively high flow rates are used (1-5 ml/min) little time is required to exchange the 25-1000 μL sample volumes. If the detector can manipulate the data instantly, the fill-inject-fill cycle could be completed as fast as 15 seconds, or, in other words, four samples may be analyzed every minute. Such sampling rates are ideal for kinetic data acquisition of moderately rapid reactions.

III. Electrochemistry and Thermodynamics of the Au-Cl- H_2O System: The Eh-pH Diagram

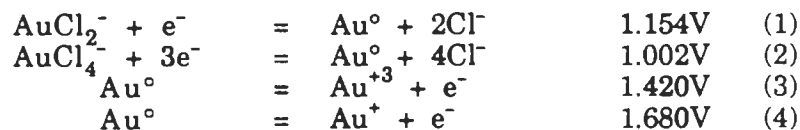
The equilibrium species involved in chlorination may be thermodynamically predicted. The electrochemical series which apply are arranged in Table I in order of increasing oxidizing potential. The oxidized form of a couple will react readily with the reduced form of a couple above it in the table. For example, Au^{+3} will be reduced by H_2 to elemental gold.

The question arises as to which species of gold (Au^+ , Au^{+3} , AuCl_2^- , or AuCl_4^-) is most stable for any given set of conditions. To determine

Couple	E° Volts	Reference
$2\text{H}^+ + 2\text{e}^- = \text{H}_2$	0.000	b
$\text{AuCl}_2^- + 2\text{e}^- = \text{AuCl}_2^- + 2\text{Cl}^-$	0.926	a
$\text{AuCl}_4^- + 3\text{e}^- = \text{Au}^\circ + 4\text{Cl}^-$	1.002	b
$\text{AuCl}_2^- + \text{e}^- = \text{Au}^\circ + 2\text{Cl}^-$	1.154	a
$\text{O}_2 + 4\text{H}^+ + 4\text{e}^- = 2\text{H}_2\text{O}$	1.229	b
$\text{Cl}_2 + 2\text{e}^- = 2\text{Cl}^-$	1.358	b
$\text{Au}^{+3} + 3\text{e}^- = \text{Au}^\circ$	1.420	b
$\text{Au}^+ + \text{e}^- = \text{Au}^\circ$	1.680	b

Table I. Standard oxidation potentials (E°) at 25°C for half-reactions pertinent to the Au-Cl-H₂O system arranged in decreasing oxidation potential. [Reference notes: a = Bard, et al⁵⁴ and b = Krauskopf⁵³.]

this, the individual half-reactions must be looked at independently.



(It will be shown later that Au⁺ and Au⁺³ will not be present.)

The following definition may be made:

$$E^\circ = -\Delta F / (n\mathcal{F}) \quad (5)$$

where: E° = the electrochemical potential
 ΔF = the free energy of formation
 n = gram-equivalents of electrons transferred
 \mathcal{F} = Faraday's Constant.

We may also write the Nernst equation as follows:

$$\Delta F = \Delta F^\circ + RT(\ln K) \quad (6a)$$

or,
$$\Delta F = \Delta F^\circ + [2.303RT](\log K) \quad (6b)$$

where: ΔF = the free energy of formation
 ΔF° = the free energy of formation under standard conditions
 R = the gas constant
 T = temperature, in K, and
 K = the equilibrium constant for the reaction.

Dividing equation (6b) by $(-n\mathcal{F})$ determines the Eh (oxidation potential in Volts) by the following equation:

$$E_h = E^\circ - [2.303RT/(n\mathcal{F})]\log K \quad (7)$$

And by incorporating the values for the constants ($R = 1.987 \text{ cal}/(\text{mole})(K)$, $T = 298 \text{ K}$, and $\mathcal{F} = 23,060 \text{ cal}/(V)(\text{gr. eq.})$), equation (7) is reduced to the following:

$$E_h = E^\circ - (0.059/n) \log K \quad (8).$$

Equation (8) can now be applied directly to equations (1) and (2).

From (1) the equilibrium constant is defined as follows:

$$K_{(1)} = [\text{Au}^\circ][\text{Cl}^-]^2/[\text{AuCl}_2^-]$$

where: $[X]$ is defined as the activity (or concentration in an ideal solution) of species X.

Likewise from (2), the equilibrium constant may be written:

$$K_{(2)} = [\text{Au}^\circ][\text{Cl}^-]^4/[\text{AuCl}_4^-].$$

By definition, the activity of a solid or element in its natural state is 1.

Therefore, we can write:

$$K_{(1)} = [\text{Cl}^-]^2/[\text{AuCl}_2^-]$$

$$K_{(2)} = [\text{Cl}^-]^4/[\text{AuCl}_4^-].$$

$K_{(1)}$ and $K_{(2)}$ may now be substituted into equation (8) with the standard electrode potential (E°) for each reaction to give the following equations:

$$E_{h(1)} = 1.154 + 0.059\log[\text{AuCl}_2^-] - 0.118\log[\text{Cl}^-] \quad (9)$$

$$E_{h(2)} = 1.000 + 0.020\log[\text{AuCl}_4^-] - 0.079\log[\text{Cl}^-] \quad (10).$$

Equations (9) and (10) show the importance of the chloride ion concentration for each reaction in determining the more stable species. The relative

stability of AuCl_2^- and AuCl_4^- depend on the amount of chloride ion present. By setting the activities of $[\text{AuCl}_2^-]$ and $[\text{AuCl}_4^-]$ equal to a constant, namely the total concentration of gold $[\text{Au}]$, the theoretical chloride concentration necessary for both species to be stable can be determined as a function of gold concentration by setting equations (9) and (10) equal. The simplified results of equating (9) and (10) are as follows:

$$\log[\text{Cl}^-] = 3.949 + \log[\text{Au}] \quad (11).$$

The values of $[\text{Cl}^-]$ for various concentrations of gold were calculated from equation (11) and are presented in Table II.

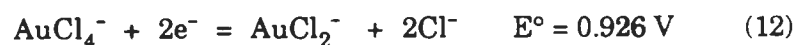
In general, at $[\text{Cl}^-]$ lower than the calculated value, AuCl_4^- is the stable species. At higher $[\text{Cl}^-]$, AuCl_2^- is more stable. This may be illustrated for $[\text{Au}] = 10^{-4}$ mole/L (~20 ppm gold) for two concentrations of Cl^- spanning the 0.89 M theoretical chloride concentration. For a $[\text{Cl}^-]$ of 2 moles/L, the Eh of AuCl_2^- is 0.883V, while that for AuCl_4^- is 0.896V. Therefore, at this higher $[\text{Cl}^-]$, AuCl_2^- is more stable. But for 0.5 M Cl^- , the Eh of AuCl_2^- is 0.954V, while that for AuCl_4^- is 0.944V. Now, AuCl_4^- is more stable. For the gold concentration of the previous example ($[\text{Au}] = 10^{-4}$ M), the Eh for Au^{+3} is 1.34 V and for Au^+ the Eh is 1.44 V. Both are

$[\text{Au}]$, moles/L	(~ppm)	$[\text{Cl}^-]$, moles/L	(~g/L)
10^{-3}	(200)	8.89	(320)
10^{-4}	(20.)	0.89	(32.0)
10^{-5}	(2.0)	0.09	(3.2)
10^{-6}	(0.2)	0.009	(.32)
10^{-7}	(0.02)	0.0009	(0.032)

Table II. Theoretical chloride concentrations at which both AuCl_2^- and AuCl_4^- are thermodynamically stable.

considerably higher than the gold chloride species for any chloride concentration.

When the $[\text{Cl}^-]$ is greater than the calculated transition concentration, then the AuCl_4^- field is determined by the manipulation of the $\text{AuCl}_4^-/\text{AuCl}_2^-$ couple equation:



From this equation, the following Eh relation may be derived as shown before:

$$E_h = E^\circ + 0.029\log[\text{AuCl}_4^-] - 0.029\log[\text{AuCl}_2^-] - 0.059\log[\text{Cl}^-] \quad (13)$$

The AuCl_4^- species will be more stable above the point at which the activities of the two gold species are equal, or in other words,

$$E_h = 0.926 - 0.059\log[\text{Cl}^-]$$

For $[\text{Cl}^-] = 2\text{M}$, the transitional Eh is 0.908 V.

Other important reactions in the Au-Cl- H_2O system are included in Table III. Either no electrochemical information is available, or no electron transfer is involved. For these reactions, the following procedure is used to obtain thermodynamic data for the Eh-pH diagram.

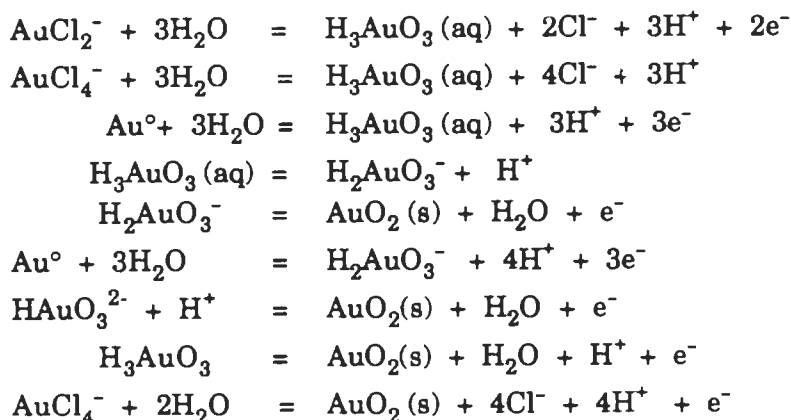


Table III. Reactions pertinent to the Au-Cl-H₂O system for which limited information is available.

First, determine the standard free energy of the reaction using the following definition:

$$(\Delta F^\circ)_{\text{reaction}} = \sum(v\Delta F^\circ)_i - \sum(v\Delta F^\circ)_j \quad (14)$$

where, ΔF°_x = standard free energy of formation of species x
 v_x = stoichiometric coefficient of x
 subscript i = product species i
 subscript j = reactant species j.

Table IV provides the values used to calculate the free energy for the reactions in Table III.

For the redox reactions, the standard electrode potential for the reaction has been defined in equation (5). But for reactions with no e⁻ transfer, the following definition applies:

$$\log K = -(\Delta F^\circ / (2.303RT)) \quad (15)$$

where K is the equilibrium constant, R is the gas constant, and T is the temperature. When T = 298 K, this simplifies to the following:

$$\log K = -\Delta F^\circ / 1.364 \quad (\text{for } \Delta F^\circ \text{ in kcal}) \quad (16).$$

<u>Species</u>	<u>ΔF° (kcal/mole)</u>	<u>References</u>
AuCl_4^-	-56.20	a
AuCl_2^-	-36.15	b,d
$\text{H}_2\text{O}(l)$	-56.69	a
$\text{Cl}^-(aq)$	-31.35	c
$\text{H}_3\text{AuO}_3(aq)$	-61.80	c
$\text{H}_2\text{AuO}_3^-(aq)$	-45.80	c
$\text{HAuO}_3^{-2}(aq)$	-27.60	c
$\text{AuO}_2(s)$	48.00	c

Table IV. Standard free energy of formation for species of the Au-Cl-H₂O system. [Reference: a = Krauskopf⁵³, b = Bard, et al⁵⁴, c = Garrels and Christ⁵⁵, d = Langmuir⁵⁶]

From the techniques described, equations can be derived that define the equilibrium regions of the different species on an Eh-pH diagram. Table V gives the equations derived from the reactions in Tables I and III. The lines may be defined for any given activity (or concentration) of gold and chloride ion. For $\text{Au}^\circ \rightarrow$ dissolved species, the activity of the dissolved species is considered to be the concentration of gold ($[\text{Au}]$). For the case of one dissolved species converting to another, the activities of each are considered to be equal. With these two stipulations, two Eh-pH diagrams have been created. The first (see Figure 5) was determined for a gold concentration of 10^{-4} M and a chloride concentration of 2 M. The second diagram (Figure 6) was for $[\text{Au}] = 10^{-4}$ M and $[\text{Cl}^-] = 10^{-2}$ M. From Table II for 10^{-4} M Au, the transition concentration of $[\text{Cl}^-]$ above which AuCl_2^- is stable is 0.89 M. And as expected, Figure 5 shows the area for which AuCl_2^- is stable.

<u>Equations</u>	<u>Conditions</u>
1a) $Eh = 1.000 + 0.020\log[AuCl_4^-] - 0.079\log[Cl^-]$	If $[Cl^-] < [Cl^-]_{Eqn. (11)}$
1b) $Eh = 0.926 + 0.029\log[AuCl_4^-] - 0.029\log[AuCl_2^-] - 0.059\log[Cl^-]$	If $[Cl^-] > [Cl^-]_{Eqn. (11)}$
2) $Eh = 1.154 + 0.059\log[AuCl_2^-] - 0.118\log[Cl^-]$	If $[Cl^-] > [Cl^-]_{Eqn. (11)}$
3) $Eh = 1.772 + 0.059\log[Cl^-] - 0.089pH$	If $[Cl^-] > [Cl^-]_{Eqn. (11)}$
4) $3pH = 4\log[Cl^-] + 28.6$	
5) $Eh = 1.565 - 0.059pH + 0.020\log[H_3AuO_3]$	
6) $pH = 11.73 + \log[H_2AuO_3^-] - \log[H_3AuO_3]$	
7) $Eh = 1.609 - 0.059\log[H_3AuO_3]$	
8) $Eh = 1.796 + 0.020\log[H_2AuO_3^-] - 0.079pH$	
9) $pH = 13.34 + \log[H_2AuO_3^-] - \log[H_3AuO_3]$	
10) $Eh = 2.059 - 0.098pH + 0.020\log[HAuO_3^{-2}]$	
11) $Eh = 0.820 + 0.059pH - 0.059\log[HAuO_3^{-2}]$	
12) $Eh = 2.303 - 0.059pH - 0.059\log[H_3AuO_3]$	
13) $Eh = 3.997 - 0.236pH + 0.236\log[Cl^-] - 0.059\log[AuCl_4^-]$	

Table V. Eh-pH expressions derived from the reactions defined for the Au-Cl-H₂O system.

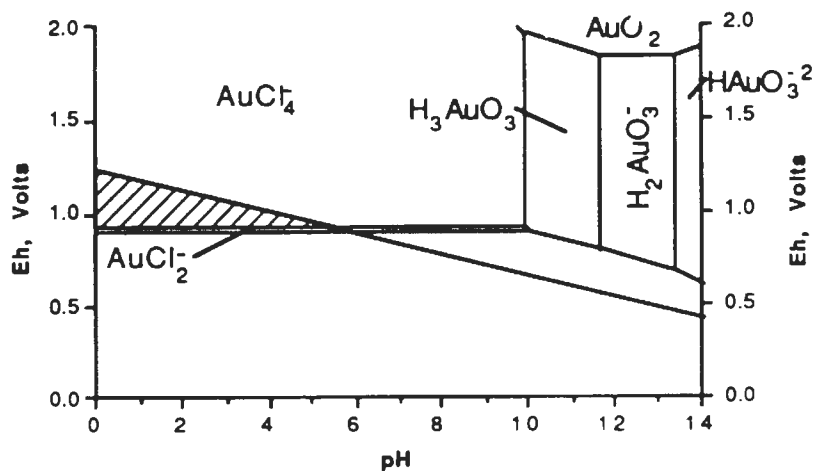


Figure 5. Eh-pH diagram for $[\text{Au}] = 10^{-4}$ M and $[\text{Cl}^-] = 2.0$ M. The diagonal line represents the upper stability limit of water. Above this line, water will decompose to oxygen gas. Shaded area represents where chloride complexes are stable in water. (All potentials are based on the standard hydrogen electrode.)

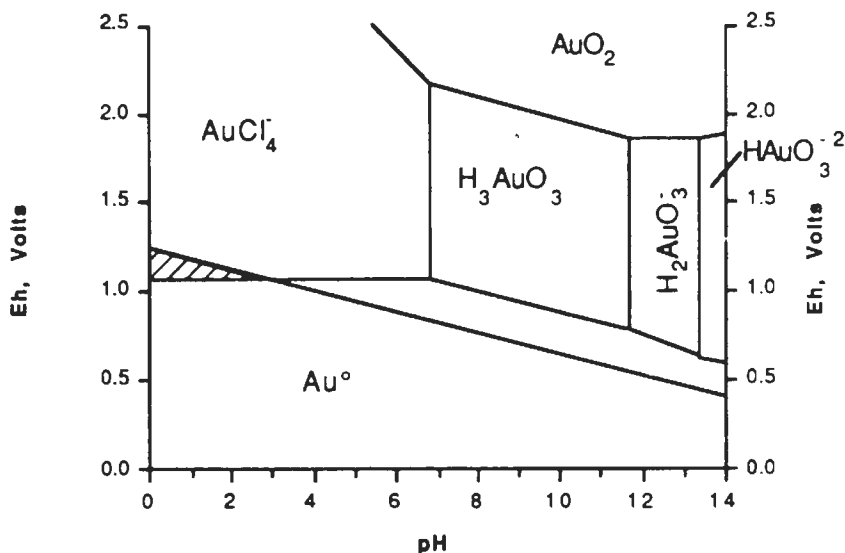


Figure 6. Eh-pH diagram for $[\text{Au}] = 10^{-4}$ M and $[\text{Cl}^-] = 10^{-2}$ M. The diagonal line represents the upper stability limit of water. Above this line, water will decompose to oxygen gas. Shaded area represents where chloride complexes are stable in water. (All potentials are based on the S.H.E.)

Chapter One

Nascent Chlorine and the Chlorination of Gold

I. Introduction

Nascent Chlorine

During the period in which the barrel process was in use (1864-1920), many of the scientists of the day felt that chlorine produced *in situ* was more reactive than added Cl_2 . Austin wrote "the chlorine, in formation in the nascent condition, acts with greater energy upon the gold,..."³ Their contention was that nascent chlorine (or "new born" chlorine) produced with the ore was a more reactive species than chlorine produced outside the vessel (as in the Plattner process). While several scientific explanations may be used to explain this, two theories will be explored to determine if these early observations can be explained. One explanation is that during the chemical production of chlorine gas, chloride ions are present in the water in excess. This will be further explored in Chapter Three of this dissertation.

Another proposed explanation comes from kinetic rate theory. In both the Absolute Rate Theory⁵⁷ and RRKM Rate Theory⁵⁸, a reactive intermediate is thought to exist during the course of a chemical reaction. A typical energy level diagram for a chemical reaction is shown in Figure 1-1. For the reaction shown, ΔE_0 represents the energy required for the reaction to proceed, or, more correctly, the activation energy for the reaction. The

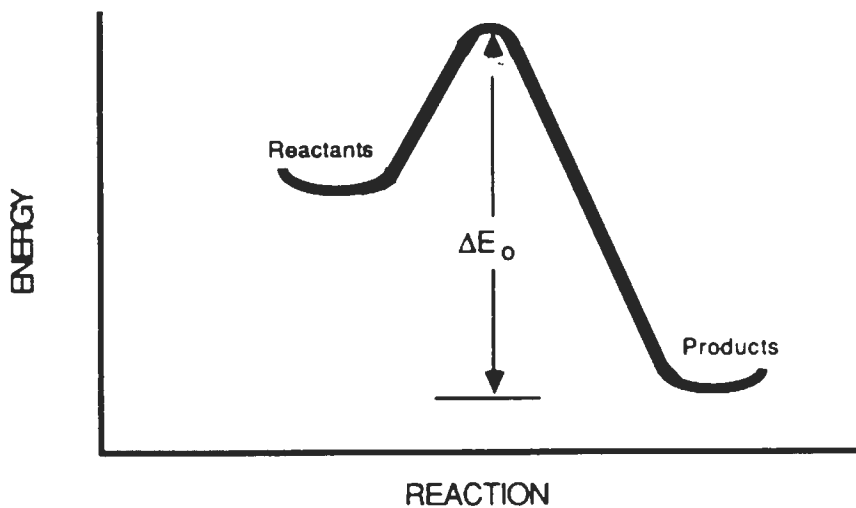
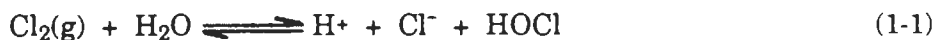


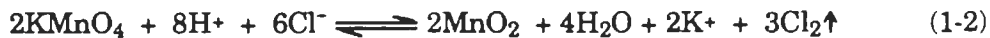
Figure 1-1. Energy diagram for a typical reaction of reactants \rightarrow products.

reaction of chlorine with water is given in Mortimer⁵⁹ by Equation (1-1):



The energy diagram for this reaction would be similar to that in Figure 1-1.

But suppose the reaction proceeds with the formation of a reactive intermediate ($\text{Cl}\cdot$). This chlorine atom could react with others to form Cl_2 or with other species to form new chemical compounds. For the sake of explanation, reaction (1-2) shows the case in which potassium permanganate is mixed with hydrochloric acid.



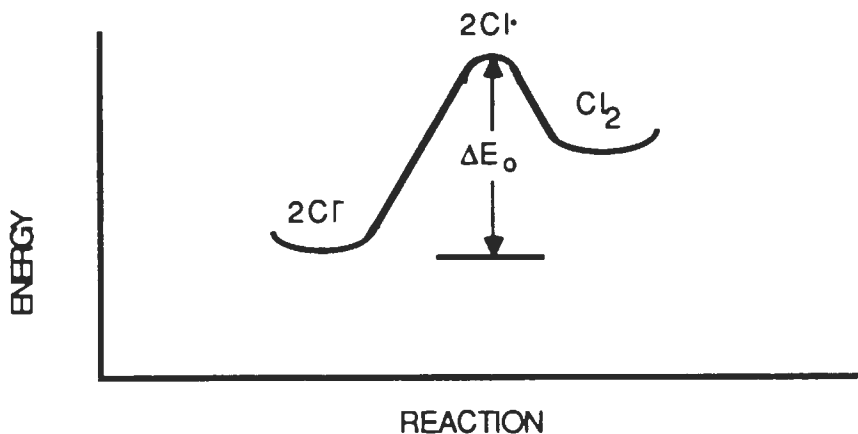


Figure 1-2. Energy diagram depiction of the formation of chlorine gas from a chloride salt with a possible reaction intermediate ($\text{Cl}\cdot$).

But suppose one of the participating reactions is similar to reaction (1-3):



This reactive intermediate may be present in sufficient quantities to react with other elements in the system. This may account for the "greater energy upon the gold."³

Photochemistry of Cl_2

Methods for producing an activated chlorine atom have been demonstrated by photochemical dissociation of chlorine gas.⁶⁰⁻⁶³ Calvert and Pitts⁶⁰ have reported that light with a wavelength less than 3300\AA (UV range) will be absorbed by chlorine gas. They state, "all available evidence suggests that the act of absorption of a quantum of light by a halogen

molecule ... results largely in the formation of halogen atoms." The dissociation usually results in one ground state ($^2P_{3/2}$) atom and one excited ($^2P_{1/2}$) halogen atom. At too high of an energy, namely within the vibrational energy realm (for Cl_2 , 4989\AA), the molecule dissociates into two ground state ($^2P_{3/2}$) atoms.

To prove or disprove the existence of nascent chlorine, several tests may be conducted. Formation of $\text{Cl}\cdot$ by photochemical decomposition of the gas could be verified in a leach test by detecting differences in the dissolution rate of Au when light is present, and in the absence of light. Also, changes in Au dissolution when Cl_2 is formed chemically as compared to gas sparging may add some evidence to back this hypothesis. If a reactive intermediate is present, theoretically, the rates of Au dissolution should be enhanced.

Mechanism of Chlorination

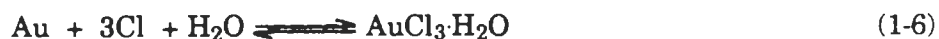
Conflicting theories have been proposed to describe how chlorine reacts with gold. Some^{20,21,22} contended that dissolution is described by equation (1-4):



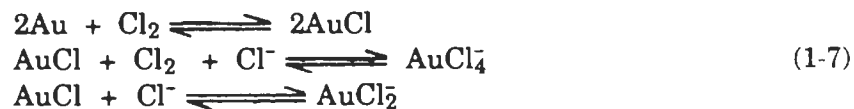
Austin⁴ theorized the reaction to follow mechanism (1-5)* when chlorine was introduced as a gas:



But, he felt that nascent chlorine reacted by equation (1-6)*:



Putnam¹⁹ contended that a complex is formed as by mechanism (1-7):



Although many^{1,14,17,18,20} thought that AuCl_3 was the soluble form of gold chloride, the Pourbaix diagram of the Au-Cl- H_2O system²⁴ shows that AuCl_4^- is the equilibrium species of gold at low Cl^- concentrations. It is stable in the 0 to 6 pH range in an oxidation potential range of greater than 0.9 volts, depending on the gold and chloride concentration.

Few have actually tackled this controversy through the years. However, with recent developments in sampling by flow-injection analysis (FIA), more insight may be gained on the actual mechanism of gold chlorination.

* - Both mechanism (1-5) and equation (1-6) were quoted directly from Austin⁴ as reported in the text.

II. Experimental

Experimental Procedures

Each experiment was conducted in the same general manner. The solid gold was weighed to the nearest 0.1 mg. The gold was added to a clean, dry 2-L Pyrex reactor vessel. A 5 cm. magnetic stir bar was added just before a volume of water (mandated by the method of chlorine addition) was added. In tests using sparged gas or anodic formation of Cl_2 , an exact volume of water (.50-L, 1.00-L, 1.50-L or 2.00-L) was added. Two chemical formation techniques were tested. In the permanganate experiments, 0.91-L of water was added to the gold and permanganate. In the hypochlorite experiments, water (300 mL or 1.80-L) was added to the gold. A volume (determined by the experimental parameters) of 5% (by vol.) NaOCl was added to the water.

In each experiment, platinum tip and pH electrodes (pre-calibrated) were then placed in the vessel and the stirrer was started at a rate of about half of the ultimate speed. At this point, the FIA pumps were started so that initial values of Au and Cl_2 (when needed) could be measured. In the Cl_2 gas experiments, the sparger was placed into the vessel and the stirring was increased to full speed. The pH and the oxidation-reduction potential (ORP) were allowed to restabilize before another set of Au and Cl_2 samplings were made. For each of the three methods of Cl_2 addition, different events constituted the "start" of the experiment, the Cl_2 valve was opened to the sparger, the potentiostat was started, HCl was added to the

water/ KMnO_4 or H_2SO_4 was added to the water/ NaOCl mixtures.

Analytical and Experimental Equipment

FIA techniques were employed extensively throughout this study. Figure 1-3 shows the flowsheet of the FIA as it was used for the initial phase of this study. The two (2) two-position, 4-way Teflon rotary valves injected samples for simultaneously measuring both the dissolved gold and chlorine concentrations.

To measure the gold concentration, a 4-way Rheodyne Type 50 Teflon rotary valve was used to inject a 500 μL sample into a water carrier stream. The carrier stream fed a Model 2380 Perkin Elmer atomic absorption spectrophotometer (AAS) equipped with a Perkin-Elmer Au hollow cathode lamp. The carrier stream was pumped at a rate of 4 mL/min by a Model 7615-80 Ismatec peristaltic pump using a 1.75 mm diameter Tygon tube. All of the lines from the water reservoir to the AAS were 0.50 mm in diameter.

To measure the chlorine concentration, an FIAstar Model 5020 Analyzer flow injection unit was used. This instrument has two peristaltic pumps and a 4-way Teflon rotary valve included. The rotary valve was used to inject a 25 μL sample into a water stream flowing to a diffusion unit. At the diffusion unit, dilution water was added. The dissolved chlorine in the sample diffuses through a Teflon membrane into a cocurrent water stream. The chlorine is then reacted with a solution of 3mM *o*-tolidine and

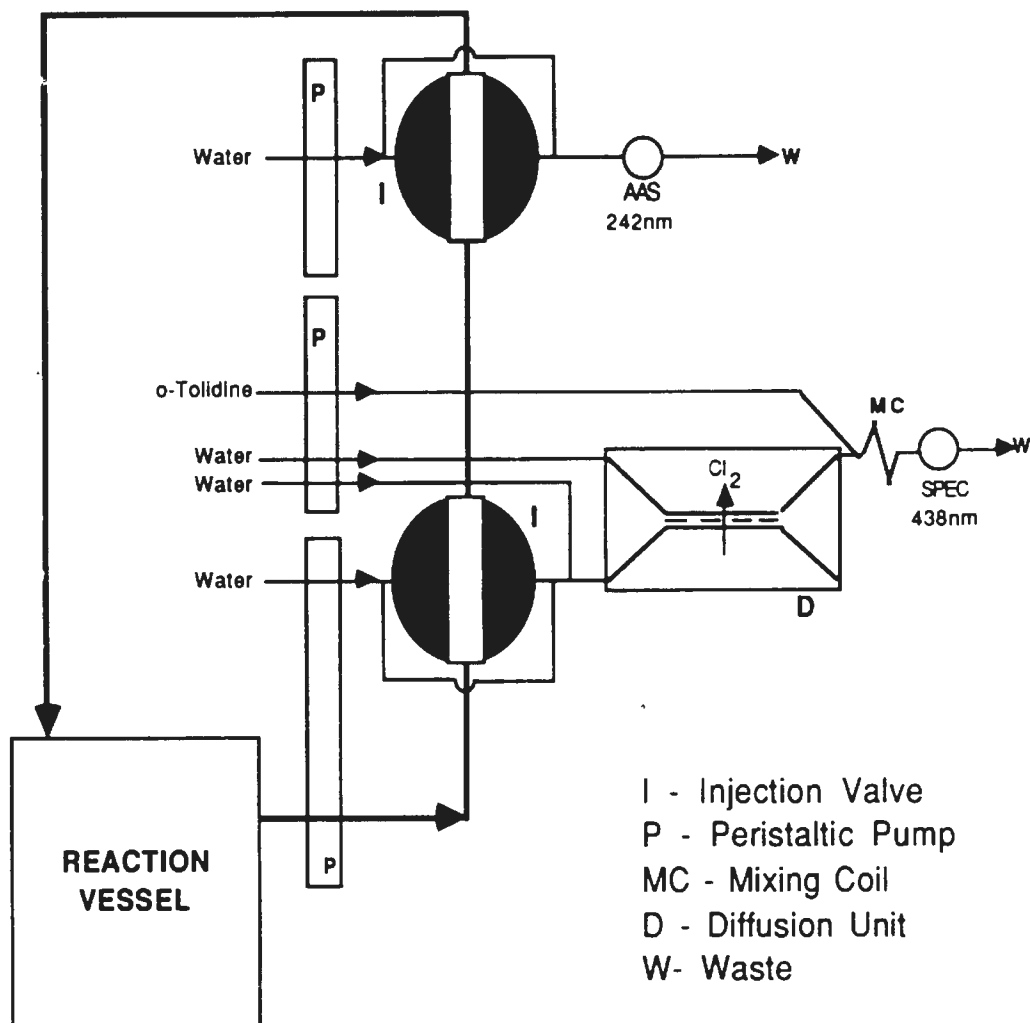
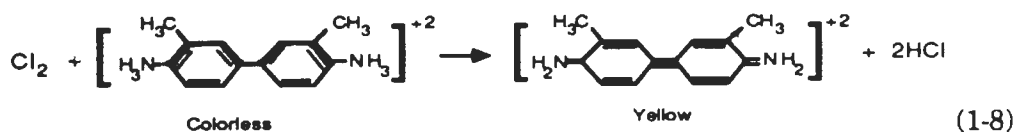


Figure 1-3. FIA flowsheet for the simultaneous determinations of Au and Cl_2 . This scheme was used only in the first phase of the research.

2M HCl. The result is the production of a yellow color as by reaction (1-8)⁸⁷ which is detected in an FIAstar Model 5023 Spectrophotometer at a wavelength of 438 nm.



This procedure is detailed in Leggett, et al.⁸⁴

One of the peristaltic pumps on the Model 5020 Analyzer was used to pump the sample stream through a recycle loop and the carrier water to the diffusion unit. The other pump was used to supply the dilution water to the chlorine circuit, the *o*-tolidine solution prior to the spectrophotometer and the water to the adsorption side of the diffusion unit. All streams were pumped at a flow rate of 1.5 mL/min. Both pumps used 0.89 mm Tygon tubing, and 0.5 mm diameter tubing was used for the solution transport.

The second phase used a modified version of the first phase FIA setup. A Hastings Model TALL-50K mass flow meter monitored the chlorine gas flow with a type H-50KM Hastings Mass Flow Transducer. The chlorine diffusion system was abandoned for this simpler and more accurate method of metering the chlorine gas flow. By monitoring the Cl₂ gas flow directly, the need for the FIAstar Model 5023 Spectrophotometer and the Model 5020 Analyzer was eliminated. Another Ismatec model 7615-80 pump was used to circulate the sample through the loop. A 0.89 mm Tygon tube was used to pump the sample at a 1.9 mL/min flow rate. Figure 1-4 is a schematic diagram of the modified FIA flow diagram.

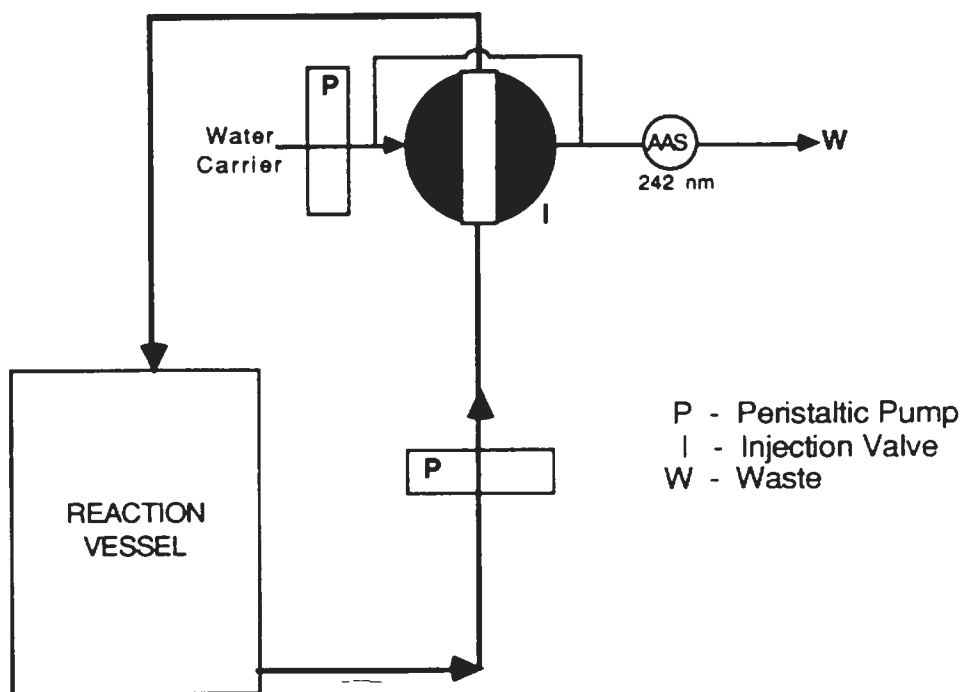


Figure 1-4. Modified FIA flow diagram for Phase II of the experiments.

A Corning Model 610A portable pH meter with a Fisher Scientific combination pH electrode was used to measure the pH. A Corning Model 7 pH meter with a Fisher platinum wire electrode was used to measure the oxidation-reduction potential (ORP). Fisher standards of pH 7 and 4 were used to calibrate the pH meter. A Zoebell's solution (0.0033 M each of potassium ferrocyanide and potassium ferricyanide, and 0.045 M potassium iodide) was used to calibrate the ORP readings by providing a +240 mV standard relative to the $H_2/2H^+$ couple.

Experiments were conducted with various parameter changes. Mixing speed was varied with a Thermix stirring hot plate Model 215T from Fisher Scientific with 5 cm Teflon coated magnetic stir bars. The available light was varied with one of the following: (1) a 60W-120V "Plant Grow N Show" ultraviolet light bulb, (2) a Cole-Parmer water-tight submersible UV lamp, or (3) a 250W-120V General Electric flood light. The electrical current for forming Cl_2 from NaCl and HCl mixtures was generated by an AIS Model PEC-1 potentiostat connected to ultrapure graphite rods. A Fisher Scientific Ag/AgCl reference electrode was used with the potentiostat.

Throughout the experiments, several chart recorders were used to help in accumulating the analytical data from each run. A Perkin-Elmer Model 023 recorder was connected to the AAS to monitor metal ion concentration. A Servogor 210 recorder was initially used to monitor the output of the Hastings mass flow meter for chlorine addition data. However, a Soltec 1243 three port recorder was used to monitor the chlorine flow, the pH and the ORP of the reaction.

Chlorine was sparged into the reaction vessel through a 10-20 μm pore glass bubbler. A similar bubbler was used to clean the reactor off-gas. The off-gas was drawn from the reactor vessel by vacuum through another of the 10-20 μm bubblers into a solution of NaOH, CaO, or $\text{Ca}(\text{OH})_2$. Figure 1-5 is a schematic depiction of the equipment setup as in the sparging experiments.

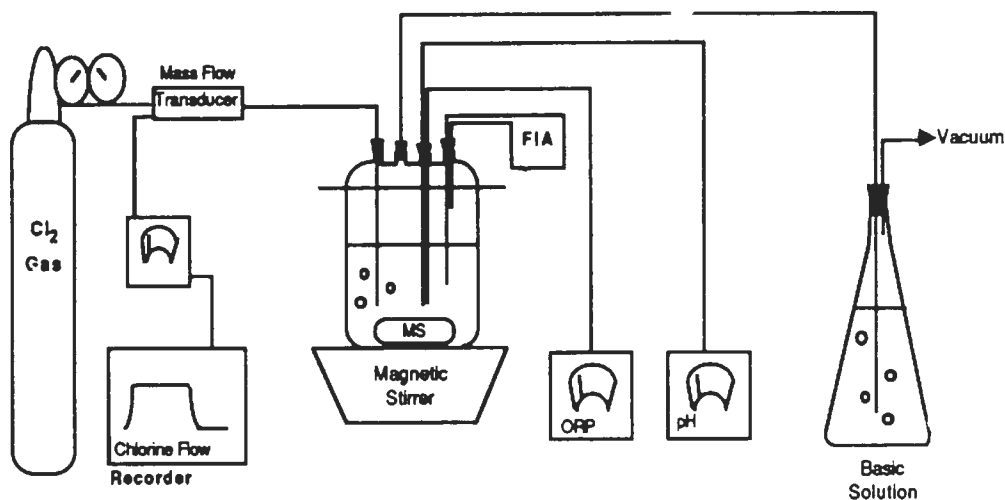


Figure 1-5. Equipment set up for the chlorination study (sparging arrangement).

Analytical Procedures

Dissolved chlorine may be determined by titrating a diluted sample mixed with potassium iodide and starch solution indicator against a 0.1N sodium thiosulfate standard. The endpoint is attained when the blue color disappears. The procedure, as described in Vogel,⁶⁵ was employed to standardize the chlorine diffusion process described previously, and to determine the final concentration of chlorine in the reactor volume.

Standards of gold were prepared by diluting measured volumes of a 1000 ppm standard with solutions made from the experimental parameters. After each experiment, two standards were used to develop an absorbance/concentration curve for the AAS. As a double check for the Au

data, either of two methods were used to manipulate the absorbance data from the FIA. The first method used the final Au concentration of the reaction and divided it by the average absorbance from the last FIA absorbance values. This conversion factor (ppm/absorbance units) was then applied to the rest of the FIA data points. In the second method, two or more standards ranging from 4 - 20 ppm Au were aspirated into the sample loop. The absorbances detected by FIA injection were averaged and divided into the corresponding standard concentration for the ppm/A.U. factor. Without changing the AAS parameters (flame, burner alignment, lamp current, gain, etc.) and after flushing the system with water, a gold dissolution experiment was performed. The conversion factors would be applied to convert the FIA absorbance data of the experiment to Au concentration.

Before and after each experiment, the FIA was flushed with distilled water. In some instances, dilute aqua regia was also flushed through the FIA to remove any precipitates, undissolved gold, or other possible contaminants.

The sample was pumped from a sample port located in the top of the reactor. The bottom of a 5 mm glass tube was filled with glass wool to filter any solids. The tube was stoppered into the reactor so that the liquid level was at least 5 cm above the glass wool. The FIA tubing was then placed into the glass tube and the liquid pumped into the loop. Figure 1-6 is a sketch of this apparatus.

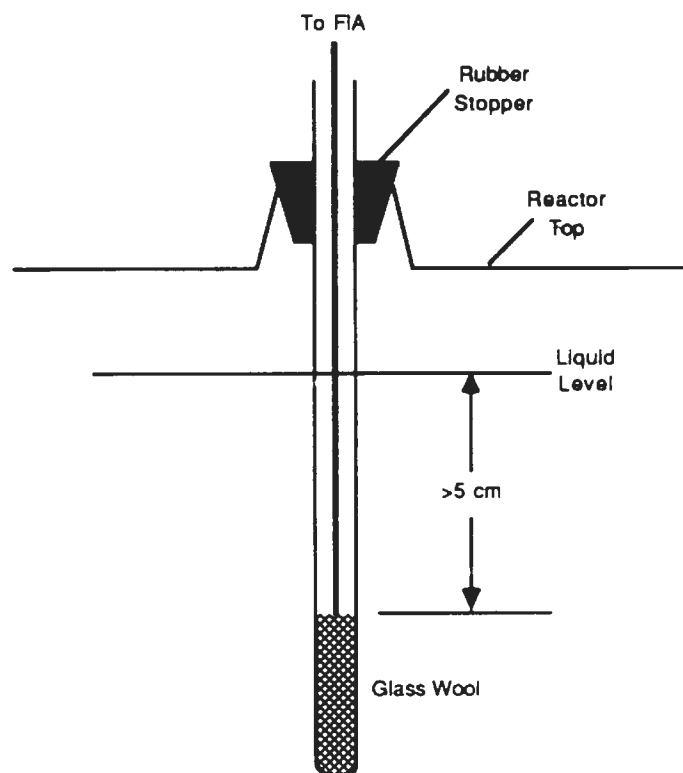


Figure 1-6. Sample port for FIA system.

Reagents

Aldrich Chemical Company, Inc. was the supplier used for the gold powder (-325 mesh, and -20 mesh) and the *o*-tolidine dihydrochloride hydrate. All other reagents and standards were from Fisher Scientific. Deionized-distilled water was used throughout the experiment.

Synthesis of the Complexes of AuCl_2^- and AuCl_4^-

Tetraethylammonium dichloroaurate ($[\text{Et}_4\text{N}]\text{AuCl}_2$) and tetraethylammonium tetrachloroaurate ($[\text{Et}_4\text{N}]\text{AuCl}_4$) are two complexes of gold chloride which have been isolated. The synthesis of the Au(I) complex is particularly difficult given the fact that AuCl_2^- readily decomposes to metallic gold in water and room light. Therefore, to produce the very sensitive $[\text{Et}_4\text{N}]\text{AuCl}_2$, phenylhydrazinium chloride ($\text{PhNH}\cdot\text{NH}_2\cdot\text{HCl}$) was used to reduce the Au(III) complex to the Au(I) species. The method used to synthesize both complexes is somewhat complicated, but it is detailed by Braunstein and Clark⁶⁶

III. Results

All experiments had final Eh values within the 1.1 - 1.2 V range, and pH values between 1.5 and 2.0. The experiments reached these values within the first minute.

In order to make accurate comparisons of data acquired by either FIA arrangement, a test was devised to check the relative response time of each set up. Two mL increments of 1000 ppm AAS standards (Au and Cu) were added to 1-L of constantly stirred water. In the first test, Au was used; in the second FIA arrangement, Cu was used. The AAS absorbance from FIA was read after each step-increase of metal concentration and was plotted as a function of time where zero time represents the time of the addition. Figure 1-7 shows the response curves for the FIA setup as seen in

Figure 1-3; Figure 1-8 contains the response curve for the second FIA setup (see Figure 1-4) using Cu ion. Both FIA arrangements report at least 90% of the final concentration within 1 minute of the addition of the metal.

Many experiments were conducted to decide on the best method of introducing Cl_2 to react with Au. The sparging of Cl_2 and the *in situ* formation of Cl_2 by both electrochemical and chemical reactions were tested. Many parameters were varied for each method, including stir rate, light/dark, concentration of reactants, electrode potential, gas feed rate, particle size of Au, and reactor volume. As the results were compiled, further tests were performed to determine the effect of Au(I) and Au(III) on the concentration data. The tetraethylammonium salts of Au(I) chloride and Au(III) chloride were synthesized for these tests.

(a) Cl_2 Gas Sparging

Many experiments were conducted in which Cl_2 gas was bubbled into the water/gold mixture. After the first few experiments of sparging, it was decided that the method for determining chlorine concentration needed improvement. After less than 1 minute of sparging, the chlorine concentration exceeded the detection limit of the spectrophotometer. Increased dilution of the sample and reduction of the sample size did not lower the readings. The second FIA set-up was adopted for this reason. The mass flow meter allowed for constant monitoring of the chlorine as it was delivered to the reaction. This created a means of more accurately

reproducing the chlorine flow from experiment to experiment.

One parameter studied in the experiments was the effect of available light on the photodecomposition of Cl_2 to $2\text{Cl}\cdot$. The object was to determine the existence and effect of nascent chlorine. Several light sources were used. A UV "Plant Grow N Show" 60W-120V bulb was placed next to the vessel. Similarly, a submersible fluorescent UV light was used. A 250W-120V General Electric flood light was also used. The specific volume of water used in the reaction was also varied during these experiments.

A peculiar peak was noted as the sparging experiments progressed. Dissolved gold was detected within the first 2 to 3 minutes of the experiment. The reported concentration by the FIA-AAS analytical equipment increased steadily to a peak, then dropped to a value near the maximum calculated concentration based on complete dissolution of the initial weight of gold in the total volume of water. This trend was noted only when fine Au powder (-325 mesh, $44\mu\text{m}$) was used. When a coarser (-20 mesh, $841\mu\text{m}$) gold was used, the Au concentration curve observed was a sigmoidal shape.

The results of a 0.50-L UV bulb experiment and the corresponding dark experiment are presented in Figures 1-9 and 1-10. These experiments were conducted on gold particles that were neither -325 mesh nor -20 mesh. The estimated particle size of this material was -100 mesh, but an exact analysis was not performed. The particle size variation may account for the lack of a peak in the dark experiment. The results of a 2-L submersed UV light and the corresponding dark experiment are given in Figures 1-11 and

1-12. The -325 mesh gold was used in these experiments. Figures 1-13 and 1-14 show the results of a 1-L GE flood light and the corresponding dark experiment which also used -325 mesh Au. In general, dissolved gold was not detected until after at least five minutes of sparging. This basic characteristic held regardless of the volume of the experiment. Also in all of the experiments in which -325 mesh Au was used, a concentration somewhat greater than expected from the calculated concentration based on complete dissolution of the initial Au added was always observed.

The results from a coarse (-841 μ m) and a fine (-44 μ m) gold experiment are seen in Figures 1-15 and 1-16, respectively. As previously noted, the dissolved gold was observed after five minutes of sparging in both experiments. However, the coarse particle dissolution was slower (represented by the decreased slope of the concentration line) and had a sigmoidal shape. The fine particles dissolved much faster (complete dissolution in less than 10 minutes as opposed to the 20 minutes needed for the coarse particles to dissolve) but was characterized by a sigmoidal shape with the anomalous peak at the point at which the maximum calculated concentration would have been reached.

(b.) Electrochemical Formation

Several experiments were conducted in which Cl_2 was produced anodically. Solutions containing various amounts of HCl and NaCl underwent electrochemical reactions to produce Cl_2 .

The baseline experiment used a constant potential (3.65 V) applied to

a solution of 0.2M NaCl and 1M HCl with 0.0075 g of fine gold in 500 mL of water. The sigmoidal shaped dissolution curve from this experiment is presented in Figure 1-17.

An experiment to test the effect of Cl₂ production rate was conducted for 500mL of a .1M NaCl/.1M HCl solution with 7.5 mg of Au powder. An increase of the applied potential relates to an increase in the chlorine production rate. The electrode potential was stepped from 3.65 V to 4.0 V and finally to 4.5 V. The results are shown in Figure 1-18. As seen in the figure, the rate of dissolution increased (noted by increase of the slope of the concentration curve) as the potential was increased.

An experiment to test the effect of the stirring rate on Au dissolution was performed on a 500mL solution of .2M NaCl and 1M HCl with a constant electrode potential of 3.65 V. The stirring rate was increased from 60 rpm to nearly 130 rpm. The results of this test are shown in Figure 1-19. As seen in the results, the slope of the dissolution curve increased with an increase in the stirring rate.

(c.) Chemical Formation

Two reactions for the formation of Cl₂ were tested to determine if either method was effective in dissolving Au. Reaction (1-9) shows the acidification of sodium hypochlorite (NaOCl) by sulfuric acid (H₂SO₄):



In one such test, a 300 mL solution containing 0.25% (by volume) NaOCl

was prepared. To this, 7.8 mg of Au powder (-325 mesh) was added. The gold concentration was monitored for five (5) minutes to ensure that no gold reacted with the OCl^- . Then 25 mL of concentrated (96%) sulfuric acid was added. The results of the dissolution of gold are presented in Figure 1-20. The results show that gold dissolution begins only two minutes after the acid was added, but less than 80% of the gold was ultimately dissolved.

As a follow-up to this experiment, a similar test was conducted in which 1.8-L of water and 100 mL of H_2SO_4 was mixed. To this, 25.36 mg of Au was added. The mixture was then mixed with 100 mL of bleach (5% NaOCl) solution. However, because the pH and ORP were not at sufficient levels (pH < 2 with the ORP > 100 mV), an additional 80 mL of H_2SO_4 and 25 mL of bleach were added. The results of this experiment are presented in Figure 1-21. As in the previous experiment, dissolution began soon after the sulfuric acid was added, but not until an excess of both reagents were added to attain the necessary pH and ORP levels for dissolution.

The second method of chemical formation was the reaction between potassium permanganate and HCl as in reaction (1-10):



Because of the industrial success of this procedure in the late 1890's and early 1900's, the initial ratios of $\text{H}_2\text{O}:\text{KMnO}_4:\text{HCl}$ were taken from Liddell³

For every 910 mL of water, 0.36 g of KMnO_4 and 90 mL of HCl were added.

As in the experiments in which Cl_2 gas was sparged, a peak developed when fine gold was used. Therefore, experiments with both fine and coarse

gold were conducted. Results from two of these tests are given in Figures 1-22 and 1-23. The results of these tests show that the dissolution of Au begins within one minute of the HCl addition. However, only 50% of the coarse gold was ultimately dissolved.

(d.) Effect of Au(I) and Au(III) on Dissolution Data -
Determining the Cause of the Anomalous Peak

Initially the peak was explained by assuming that some of the solid gold particles were lodging themselves in the glass wool at the base of the sample port. This would create an unusually high concentration of gold in the feed line to the FIA. But this was discounted by conducting an experiment in which the FIA samples were drawn directly from the leach solution instead of through the sample port.

Contributions by FIA to the anomalous peak were discounted by comparing the two FIA data manipulation schemes described earlier. Figure 1-24 shows the plot of the results of an experiment determined in both ways. The relative error of the two methods is minimal as seen in the figure.

Another possible explanation of the peak was that metal contaminants were being introduced into the vessel through the Cl₂ delivery system. To eliminate any possible metal contamination, the stainless steel lines used in the chlorine delivery system were replaced with Teflon and Tygon tubing. But no change in the peak was observed.

The possible interferences of KMnO₄/HCl or Cl₂ were also

investigated. Chlorine was sparged into water without gold and monitored with the AAS by direct aspiration of the solution. The absorbance varied from 0.002 to -0.001 through the course of the experiment. FIA was used in the experiments of permanganate acidification with no Au. The results of this experiment are provided in Figure 1-25 and show that the interference is minimal.

Another explanation for the peak came from the possibility that the magnetic stirrer was not adequate for complete mixing of the 1-L, or greater, experiments. If the gold remained near the bottom of the vessel, the sampler would draw a sample with a larger Au concentration until the dissolved gold diffused into the upper portion of the reactor vessel. To investigate this explanation, three experiments were conducted:

- (1) Injection of dye into the reactor while operating under standard experimental conditions (~300 std cc/min chlorine rate, pH and ORP probes, and stirring by magnetic stirrer.)
- (2) Repeat an experiment in which no stirring was used, and
- (3) Repeat the experiment using an overhead mixer with a Teflon impellor for agitation. For this experiment, the sample inlet for FIA was placed near the top, but below the level at which air was aspirated.

The results of the first experiment will be discussed in the next section of this chapter. But the results of experiments (2) and (3) are presented in Figures 1-26 and 1-27, respectively. The results of experiment (2) show no peak, but the peak is still observed despite the increased mixing from the

lab mixer/impellor of test (3).

The next possible explanation was related to the gold ions present. From thermodynamics it is suggested that only AuCl_4^- can exist for the concentrations of the various species present. However, if AuCl_2^- is present in small quantities as an intermediate, then perhaps the Au(I) and Au(III) species may lead to interferences in the AAS spectra. This speculation may not be so incredulous. The Perkin-Elmer operations manual⁶⁷ makes mention of the possibility of ionization interferences. The manual also describes techniques for preparing standards of some metals with excess barium salts to eliminate this interference. However, most of these interferences result in false low readings, not a false increase. By the same token, the Au(I) may reduce to colloidal elemental Au. These small particles may have a dramatic effect on the absorption spectra of the AAS.

To test the idea of Au(I) and Au(III) interference, the chloride complexes of Au(I) and Au(III) were needed. Tetraethylammonium dichloroaurate ($[(\text{C}_2\text{H}_5)_4\text{N}]\text{AuCl}_2$) and tetraethylammonium tetrachloroaurate ($[(\text{C}_2\text{H}_5)_4\text{N}]\text{AuCl}_4$) were synthesized. Because of the extreme instability of $[(\text{C}_2\text{H}_5)_4\text{N}]\text{AuCl}_2$, special experimental conditions had to be used. Because the reduction to elemental gold is so rapid, FIA could not be used. Instead, the sample was pumped directly to the AAS from the reaction vessel for constant monitoring of the Au concentration. Also, because light causes rapid reduction to Au^0 all experiments were conducted in total darkness. And because AuCl_2^- is only thermo-

dynamically stable in high chloride concentrations, 0.3 to 0.5 M NaCl solutions were used.

Several experimental techniques were attempted. One experiment used .3M NaCl solution with about 10 ppm Au(I) from the $[(C_2H_5)_4N]AuCl_2$ added prior to Cl_2 sparging. Most of the gold, however, precipitated as Au^0 . Another experiment began with about 10 ppm Au(III) as $AuCl_4^-$ in a .5M NaCl solution. The $[(C_2H_5)_4N]AuCl_2$ was then added, but most of the gold again instantly precipitated as Au^0 . In all experiments with the $AuCl_2^-$ complex, the AAS absorbance signal was more noisy than the signal received during the dissolution experiments.

Finally, an experimental procedure was devised to exactly duplicate the dissolution experiments described in the sparging section. Equal amounts of $[(C_2H_5)_4N]AuCl_2$ and $[(C_2H_5)_4N]AuCl_4$ were weighed and combined. Chlorine was sparged into 1-L of distilled water for about 5 minutes. Then, the two complexes were added simultaneously. The results showed a peak of nearly twice the height of the final concentration. The peak was 0.045 absorbance units, while the final level was only 0.025 absorbance units. Figure 1-28 shows the results of one such experiment.

In an attempt to identify the interfering species, Au dissolution tests were repeated as in the previous experiments. However, the deionized-distilled water previously used as the carrier solution to the AAS was replaced by various combinations of salts, HCl, or dissolved chlorine in water. The premise tested was that after injection of the sample from the

reactor, the water medium caused the immediate reduction of AuCl_2^- to Au° by reducing the stability of the species. The salt and chlorine was expected to provide an environment that maintained the stability of the Au(I) species. Because of the interferences caused by sodium, calcium and potassium chloride, the chloride concentration was varied by addition of HCl to the carrier stream. A standard solution of chlorine water ($\sim 2.5 \text{ g/L}$) was also tested. HCl concentrations of 2M and 3.8M were used in the carrier. The results of these tests are presented in Figures 1-29, 1-30 and 1-31. None of the experiments resulted in the elimination of the peak.

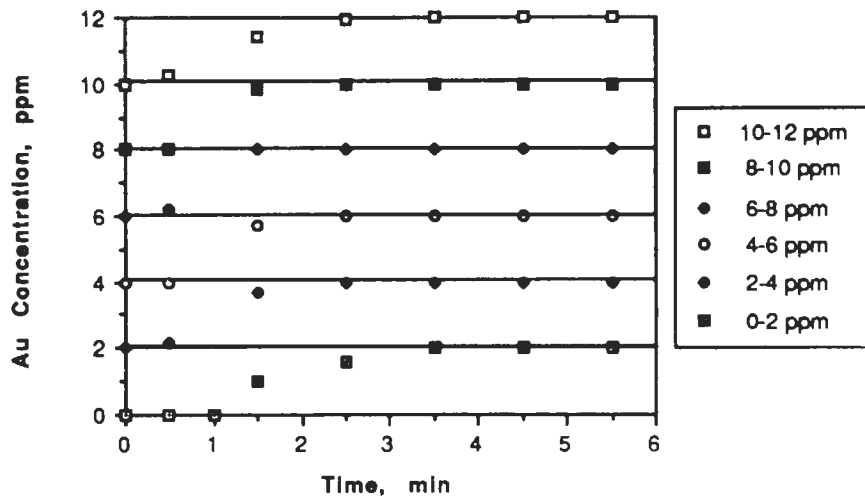


Figure 1-7. Time for the first FIA arrangement to respond to a 2 ppm step increase in Au concentration, added incrementally from 0 to 12 ppm.

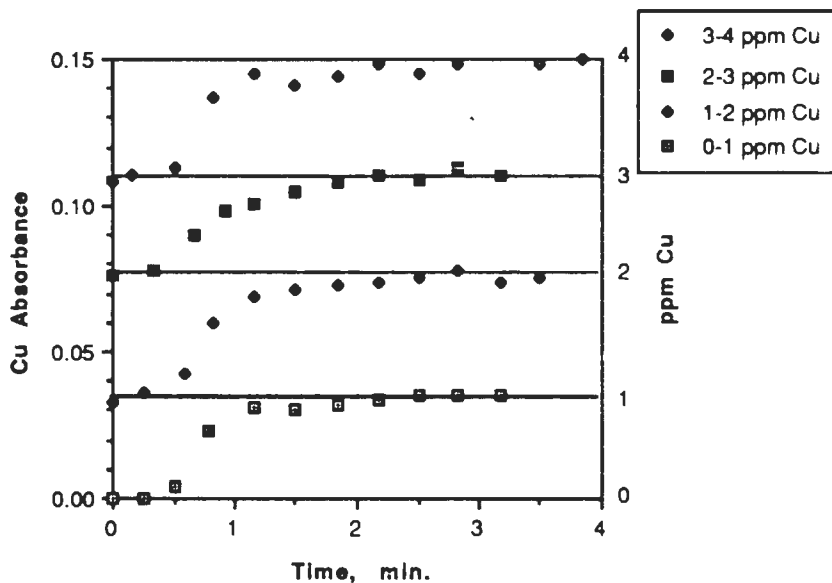


Figure 1-8. Time for the second FIA arrangement to respond to a 1 ppm step increase in Cu concentration, added incrementally from 0 to 4 ppm.

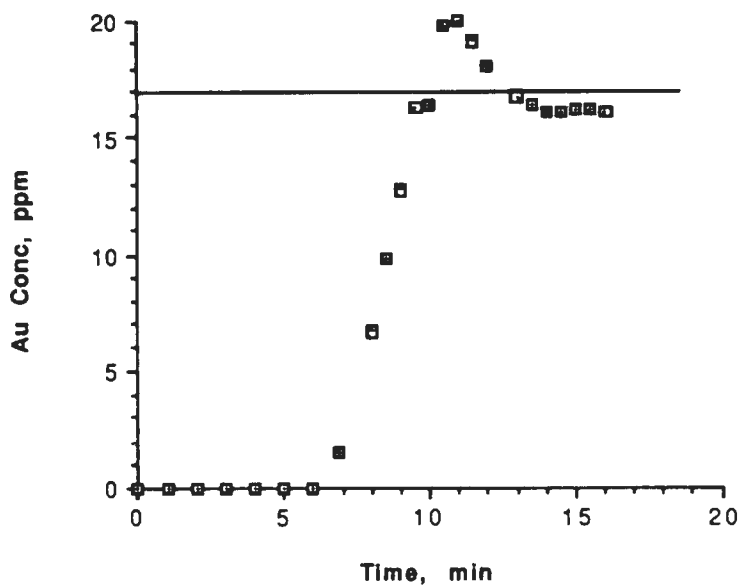


Figure 1-9. Au dissolution by sparging chlorine under a UV 'Show N Grow' 60W-120V Bulb. The sample volume was 0.5-L for this experiment. The line at 16.9 ppm represents the maximum concentration calculated on the basis of complete dissolution of the initial weight of Au. The particle size of Au used in this experiment had not been quantified prior to the dissolution (estimated average particle size ~100 mesh).

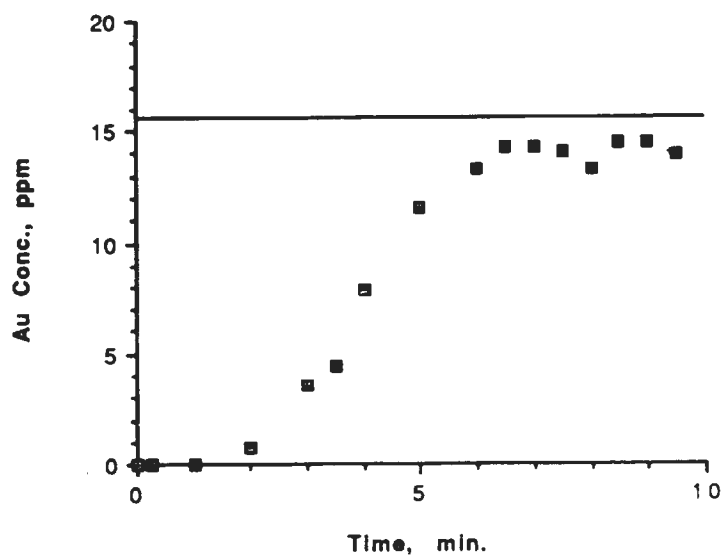


Figure 1-10. Au dissolution by sparging chlorine in total darkness. Sample volume was 0.5-L. The line at 15.3 ppm represents the maximum concentration calculated on the basis of complete dissolution of the initial weight of Au. The particle size of Au used in this experiment had not been quantified prior to the dissolution (estimated average particle size ~100 mesh).

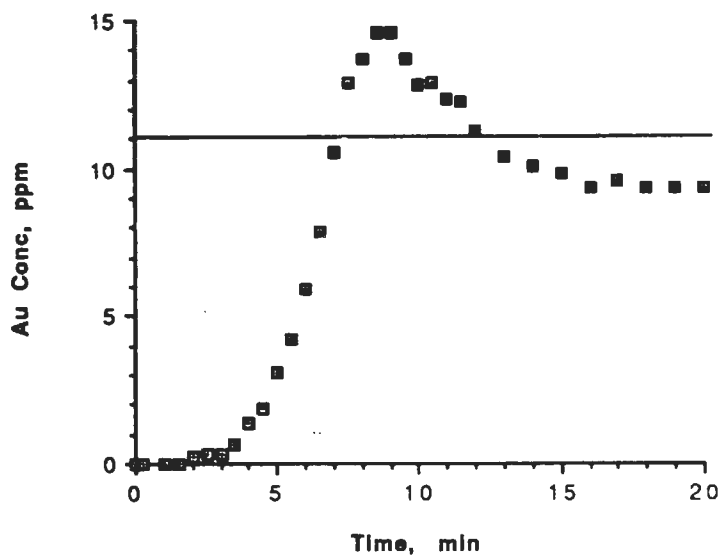


Figure 1-11. Au dissolution by sparging chlorine with a submersible UV lamp in a 2-L sample. The line at 11.0 ppm represents the maximum concentration calculated on the basis of complete dissolution of the initial weight of Au. Fine Au (-325 mesh) was used in this experiment.

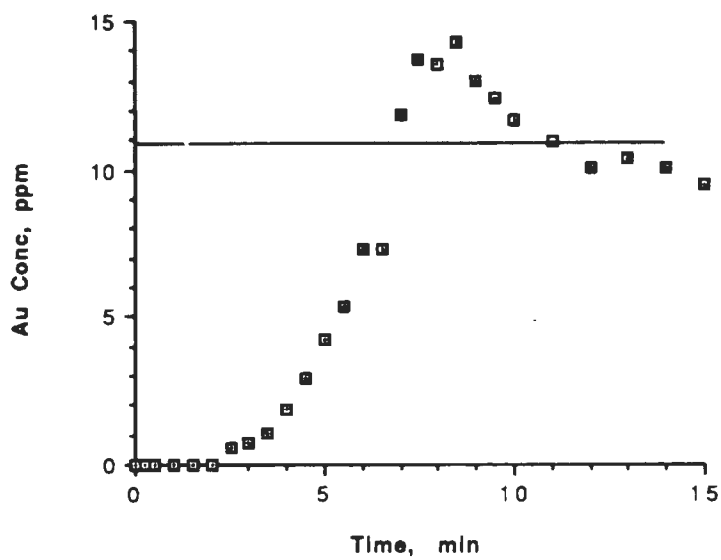


Figure 1-12. Au dissolution by sparging chlorine in a 1-L experiment in total darkness. The line at 10.9 ppm represents the maximum concentration calculated on the basis of complete dissolution of the initial weight of Au. Fine Au (-325 mesh) was used in this experiment.

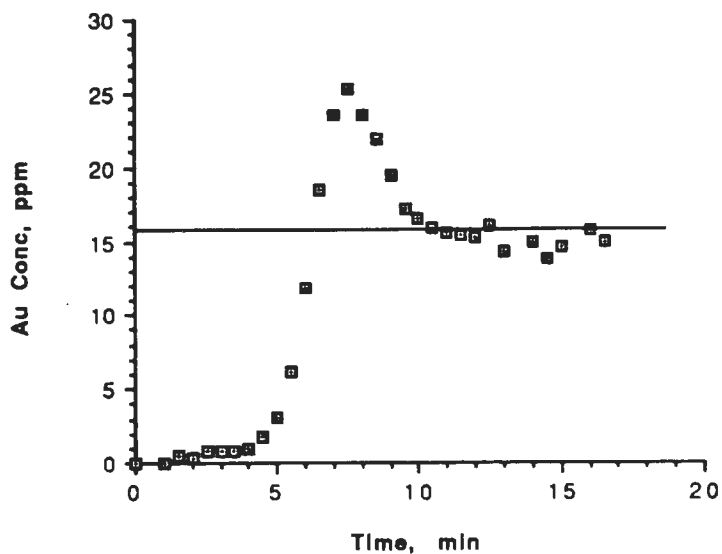


Figure 1-13. Au dissolution by sparging chlorine in a 1.5-L experiment with the G.E. flood light with an optic sensor to measure the amount of light absorbed. The line at 15.8 ppm represents the maximum concentration calculated on the basis of complete dissolution of the initial weight of Au. Fine Au (-325 mesh) was used in this experiment.

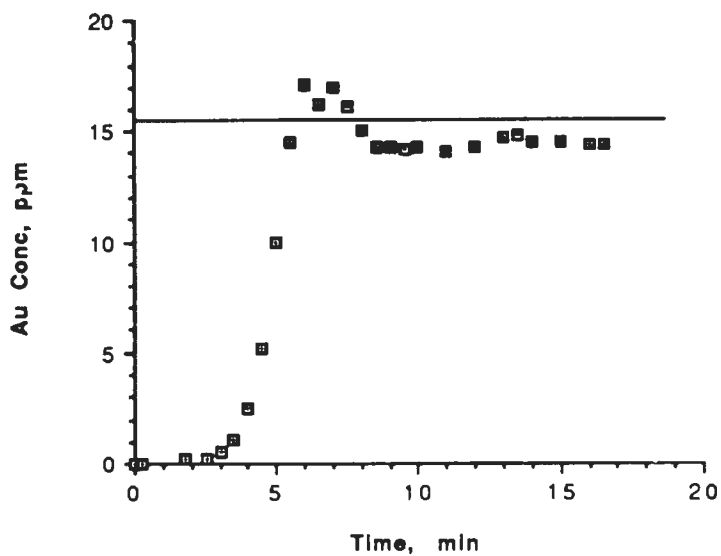


Figure 1-14. Au dissolution by sparging chlorine in a 1.5-L experiment with no light. The line at 15.5 ppm represents the maximum concentration calculated on the basis of complete dissolution of the initial weight of Au. Fine Au (-325 mesh) was used in this experiment.

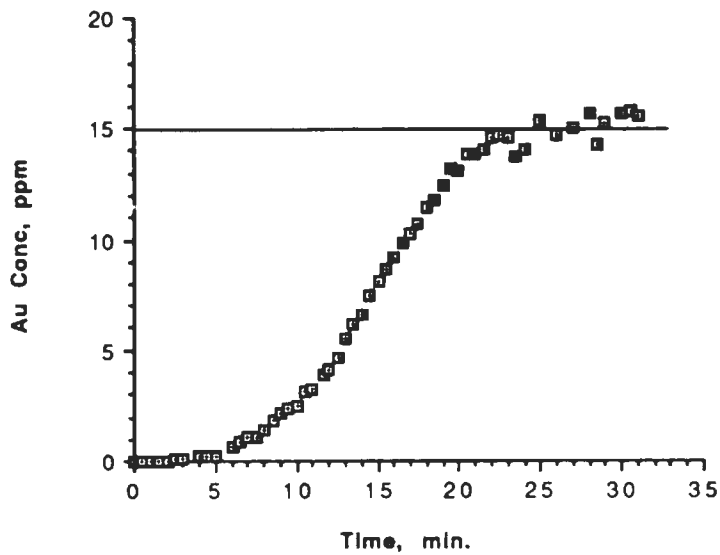


Figure 1-15. Au dissolution of coarse gold (-20 mesh) in a 1.0-L experiment with sparging chlorine and room light. The line at 14.9 ppm represents the maximum concentration calculated on the basis of complete dissolution of the initial weight of Au.

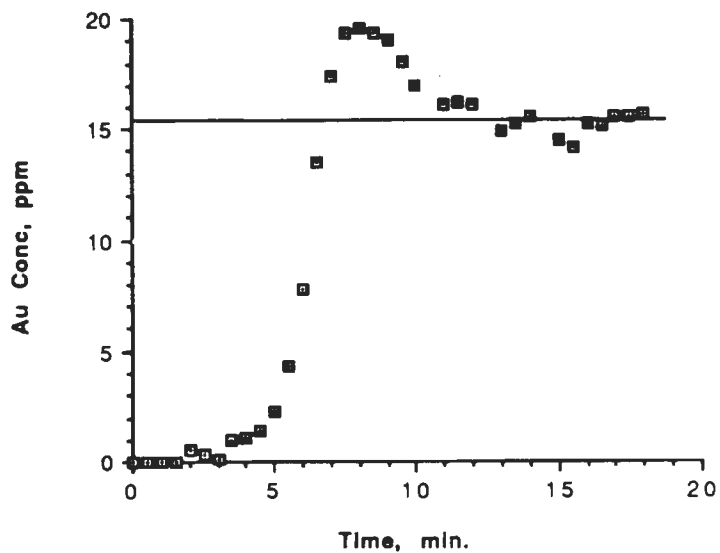


Figure 1-16. Au dissolution of fine gold (-325 mesh) in a 1.0-L experiment with sparging chlorine and room light. The line at 15.4 ppm represents the maximum concentration calculated on the basis of complete dissolution of the initial weight of Au.

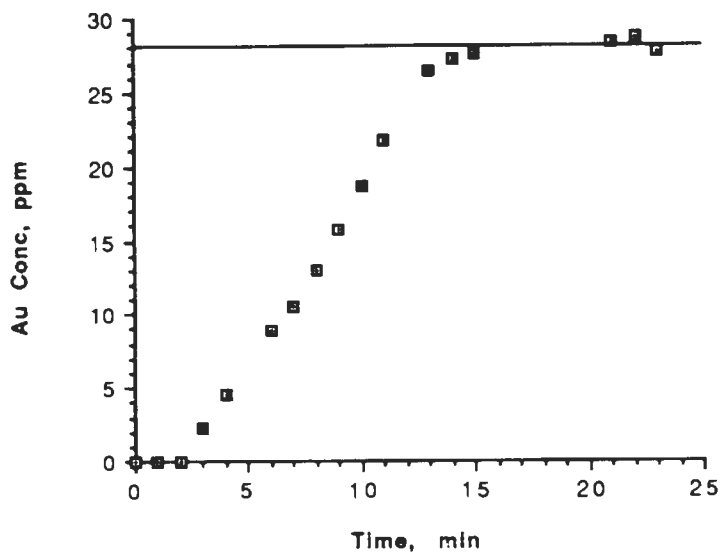


Figure 1-17. Au dissolution by chlorine for anodic formation of Cl_2 from a solution containing 0.2M NaCl and 1 M HCl under a constant potential of 3.65 V. The line at 28.0 ppm represents the maximum concentration calculated on the basis of complete dissolution of the initial weight of Au. The particle size of Au used in this experiment had not been quantified prior to the dissolution (estimated average particle size ~100 mesh).

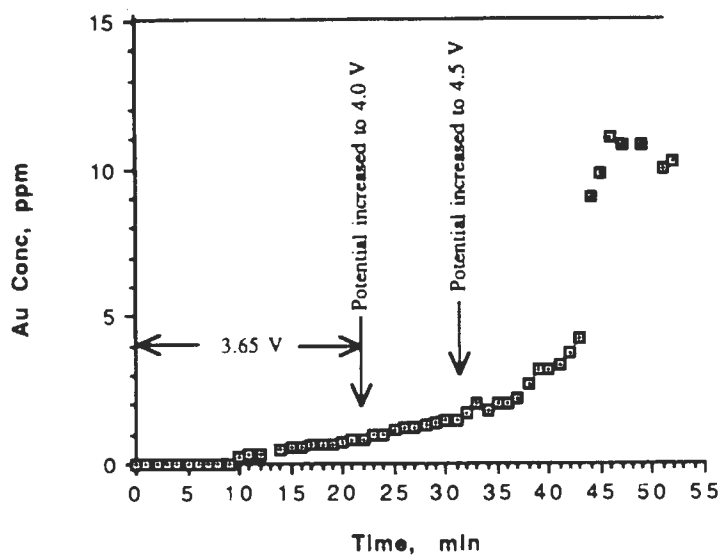


Figure 1-18. Dissolution data of Au by chlorine produced anodically from a solution of 0.2 M NaCl and 1.0 M HCl under variable potential. The line at 15 ppm represents the maximum concentration calculated on the basis of complete dissolution of the initial weight of Au. The particle size of Au used in this experiment had not been quantified prior to the dissolution (estimated average particle size ~100 mesh).

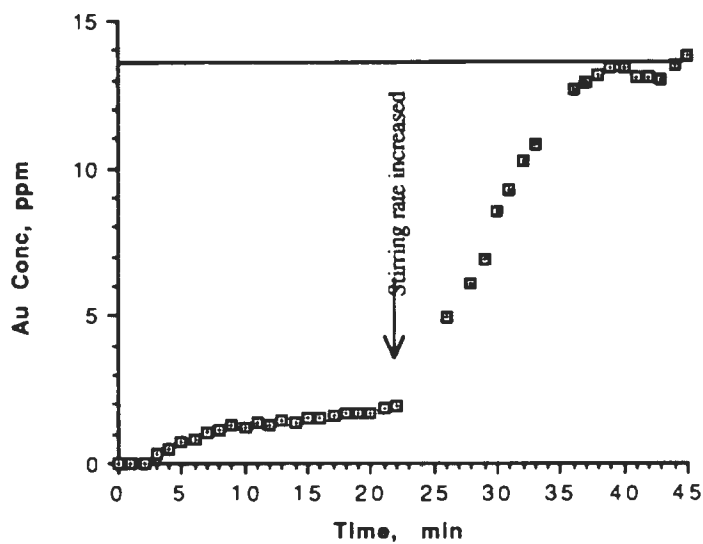


Figure 1-19. Dissolution of Au by chlorine formed anodically from a solution of 0.1 M NaCl and 0.1 M HCl at a potential of 3.65 V. The line at 13.5 ppm represents the maximum concentration calculated on the basis of complete dissolution of the initial weight of Au. The particle size of Au used in this experiment had not been quantified prior to the dissolution (estimated average particle size ~100 mesh).

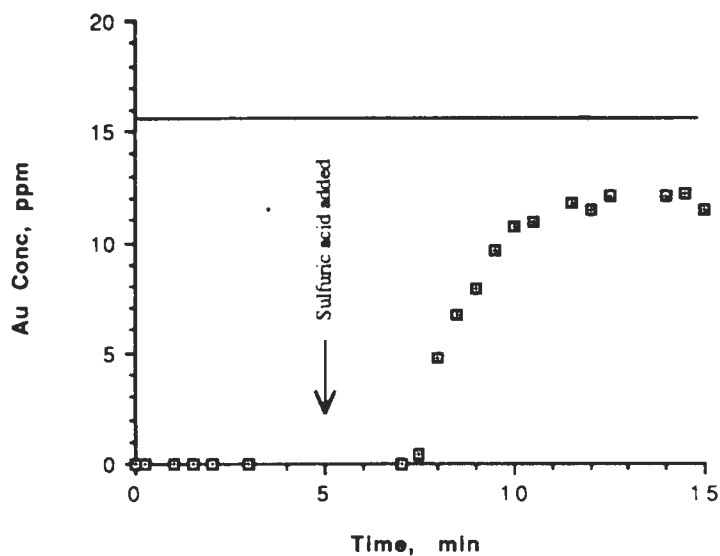


Figure 1-20. Dissolution of Au by chlorine formed chemically by the acidification of NaOCl with H_2SO_4 . Experiment volume was 0.5-L. Time = 0 represents the time NaOCl was added. The line at 15.6 ppm represents the maximum concentration calculated on the basis of complete dissolution of the initial weight of Au. Fine Au (-325 mesh) was used in this experiment.

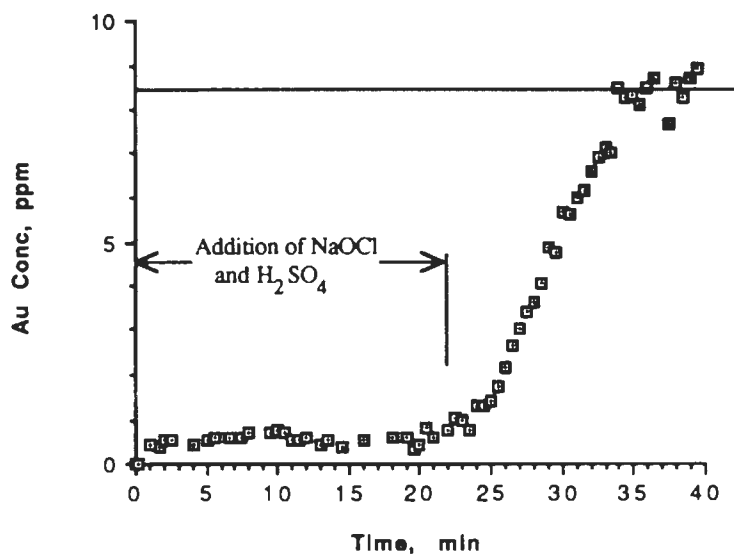


Figure 1-21. Dissolution of Au by chlorine formed chemically by the acidification of NaOCl with H₂SO₄. Experiment volume was 2.0-L. Initially, sulfuric acid was added to the gold, then at t=0, NaOCl was added. More of each was added over the first 22 minutes of the experiment to attain an ORP greater than 1.0V and pH below 2. The line at 8.5 ppm represents the maximum concentration calculated on the basis of complete dissolution of the initial weight of Au in the final reaction volume. Fine Au (-325 mesh) was used in this experiment.

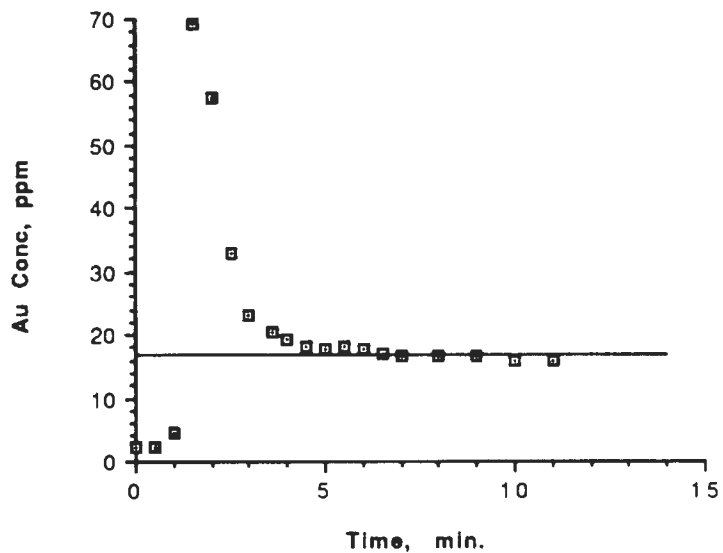


Figure 1-22. Dissolution of Au by chlorine formed chemically by the reaction of KMnO_4 and HCl . Experiment volume was 1.0-L and fine gold (-325 mesh) initially used. The line at 16.3 ppm represents the maximum concentration calculated on the basis of complete dissolution of the initial weight of Au.

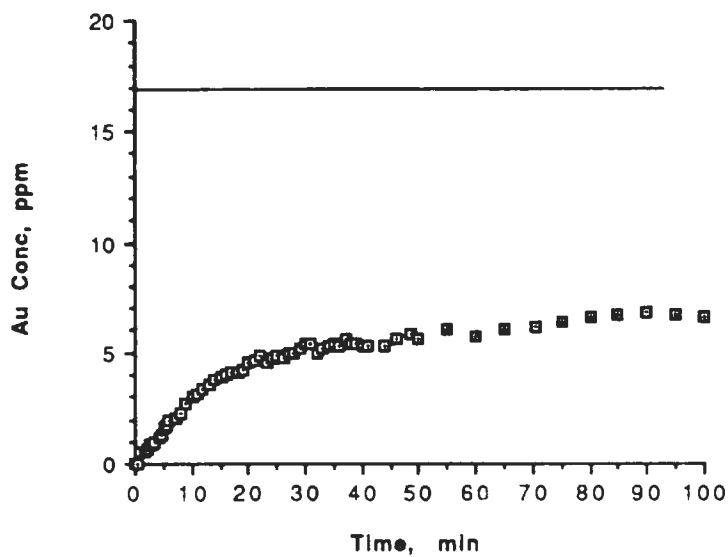


Figure 1-23. Dissolution of Au by chlorine formed chemically by the reaction of KMnO_4 and HCl . Experiment volume was 1.0-L and 16.9 mg of coarse gold (-20 mesh) initially used. The line at 16.9 ppm represents the maximum concentration calculated on the basis of complete dissolution of the Au.

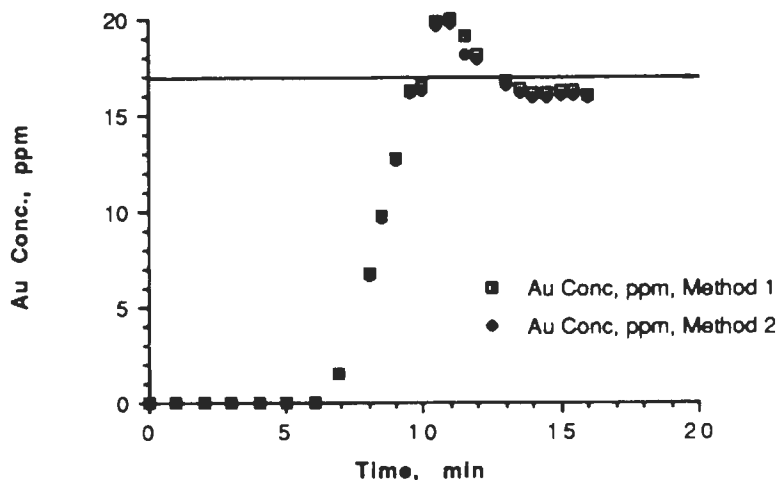


Figure 1-24. Comparison of the manipulation of FIA data.

Method 1: A conversion factor for determining the Au concentration from the absorption data from FIA was calculated by dividing the final solution assay (ppm) by the average peak height of the last FIA absorbance data.

$$(\text{ppm/A.U.}) = \text{Final Conc./Final FIA}$$

Method 2: The conversion factor relating the concentration to the FIA data was determined by comparing the FIA absorbances of standard gold concentrations to the FIA data of the experiment.

$$(\text{ppm/A.U.}) = \text{Initial Standards/FIA absorbance}$$

The line at 16.9 ppm represents the maximum concentration calculated on the basis of complete dissolution of the Au. Fine particle gold (-325 mesh) was used.

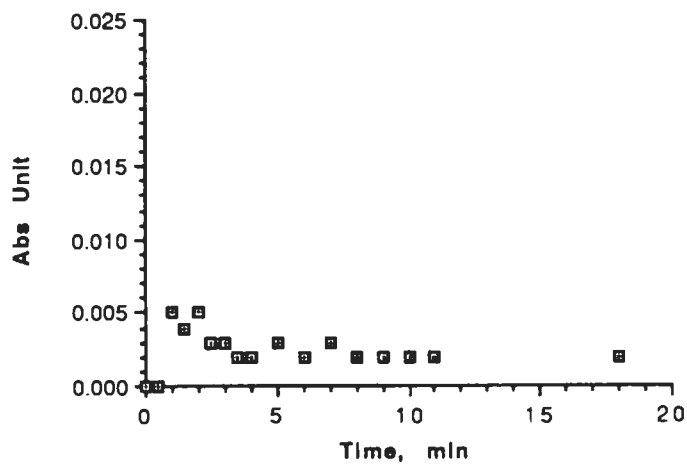


Figure 1-25. Observed Au AAS absorbance spectra at 242 nm of a solution of $\text{KMnO}_4/\text{HCl}/\text{H}_2\text{O}$ without gold. (Typically, a 15 ppm Au sample will have an absorbance of ~ 0.14 A.U. at this wavelength.)

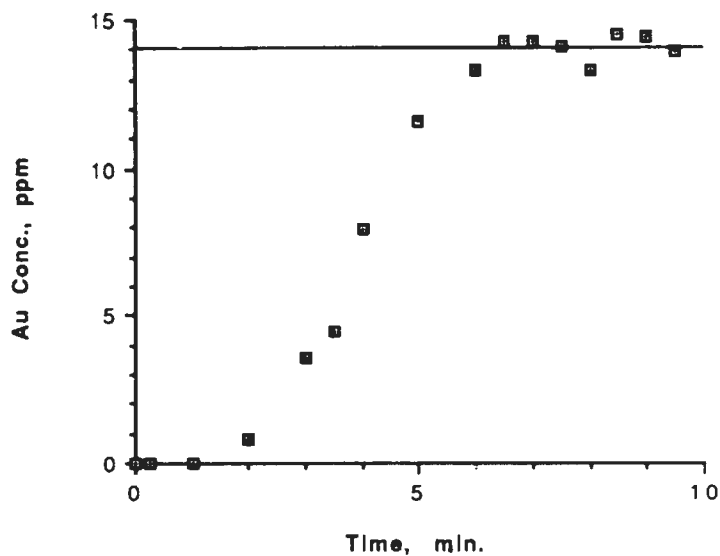


Figure 1-26. Au dissolution in the absence of mixing. (14.0 mg of fine Au and 1-L of water was used in conjunction with Cl_2 sparging at ~ 400 std. cc/min. The line represents the maximum concentration for the initial conditions.)

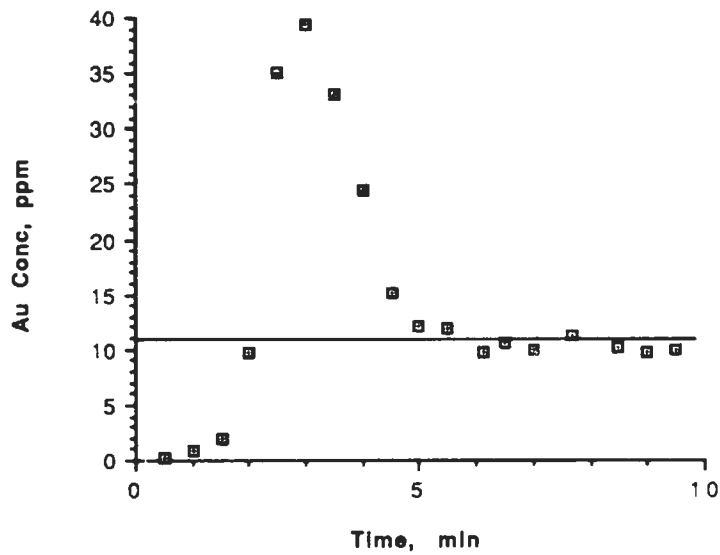


Figure 1-27. Au dissolution by Cl_2 sparging (~ 400 std. cc/min) of fine Au in 1-L of water with increased mixing by a 3-prong Teflon impellor driven by a 1-hp lab mixer. The line at 10.8 ppm represents the maximum concentration calculated on the basis of complete dissolution of the initial weight of Au.

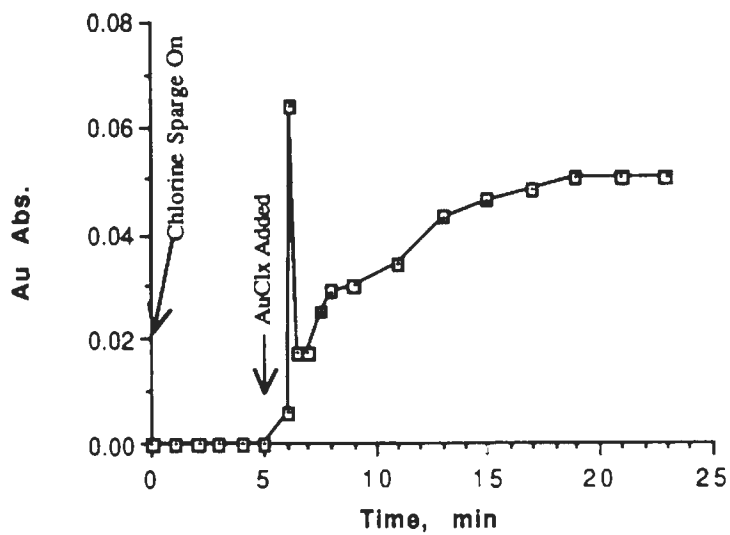


Figure 1-28. Results of an experiment using AuCl_2^- and AuCl_4^- to determine if AAS spectral interferences exist between the Au(I) and Au(III) species.

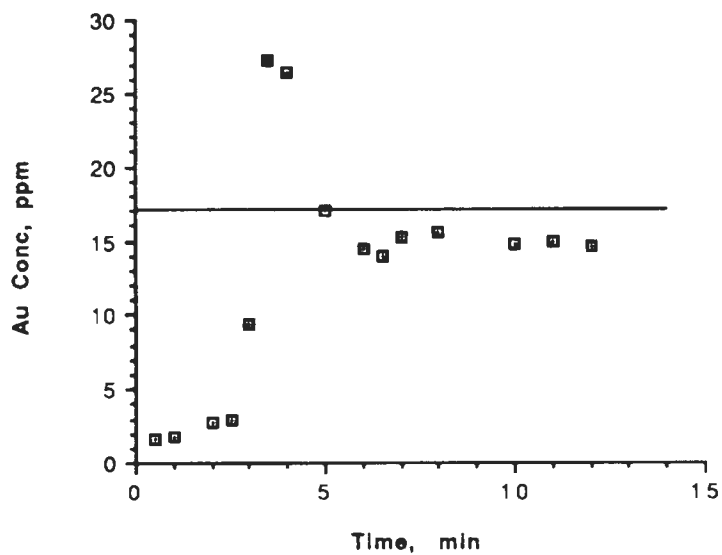


Figure 1-29. Effect of using 2 M HCl in the carrier stream of the AAS. The line at 17.4 ppm represents the maximum concentration calculated on the basis of complete dissolution of the initial weight of Au. Fine Au (-325 mesh) was used in this experiment.

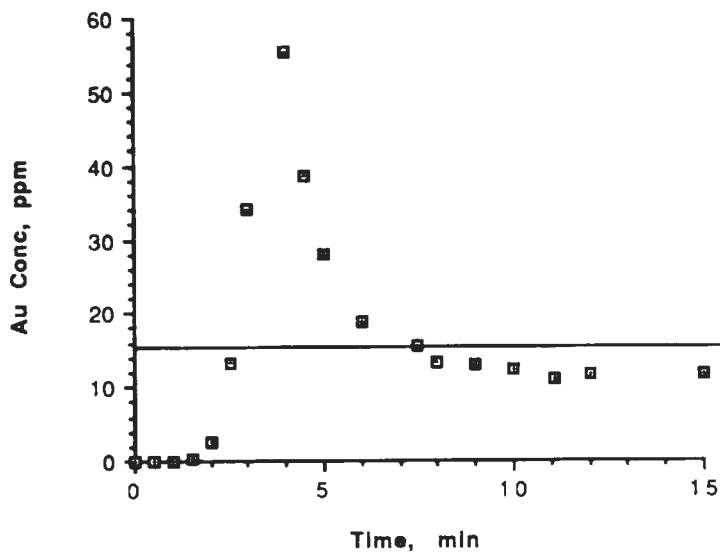


Figure 1-30. Effect of using 3.8 M HCl in the carrier stream of the AAS. The line at 15.5 ppm represents the maximum concentration calculated on the basis of complete dissolution of the initial weight of Au. Fine Au (-325 mesh) was used in this experiment.

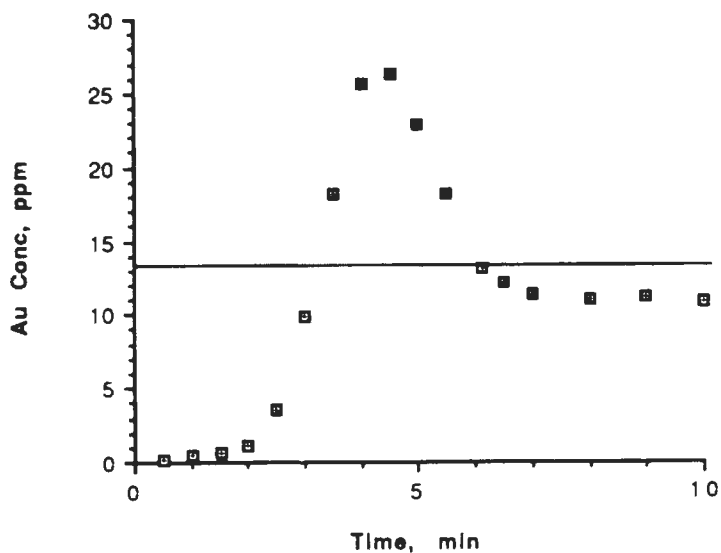


Figure 1-31. Effect of using dissolved chlorine gas in the carrier stream of the AAS. The line at 13.6 ppm represents the maximum concentration calculated on the basis of complete dissolution of the initial weight of Au. Fine Au (-325 mesh) was used in this experiment.

IV. Discussion

Cl₂ Addition and Nascent Chlorine

The method by which chlorine was introduced played a major role in the dissolution rate of gold powder. Anodic formation of chlorine, sparging of chlorine gas, and *in situ* chemical formation of chlorine by several methods produced different results.

The experiments in which chlorine was produced electrochemically showed that the rate of formation of Cl₂ was important. It follows that the fastest means of introducing Cl₂ would have the best Au dissolution rate. This corroborates the conclusion that Cl₂ sparging or production of Cl₂ by the permanganate reaction with hydrochloric acid are the best methods due to the speed at which chlorine is introduced. However, the final recoveries of coarse gold by each method showed that sparging had a definite advantage. In the experiments using coarse gold in the permanganate process, gold recoveries were never higher than 60%; in the sparging experiments with coarse gold, however, all of the gold was ultimately dissolved. Figure 1-32 shows the comparison of the two methods of addition (sparging and permanganate) on the fine Au. Figure 1-33 shows the comparison of the methods on the coarse gold. In both cases, the permanganate method put Au into solution faster than did chlorine gas sparging. The fact that Au was not detected until after 5 minutes of sparging would lead to the conclusion that time is necessary for chloride ion to form [see reaction (1-1)] before dissolution will take place. Comparing

the results of the $\text{NaOCl}/\text{H}_2\text{SO}_4$ and KMnO_4/HCl reactions would justify that the Cl^- species is more important than the OCl^- in the reaction of Cl_2 with gold.

The best explanation for the lower recovery of coarse particle gold by the permanganate method of addition can be traced to the reaction products. Manganese dioxide is precipitated as a result of the acidification process. This precipitate formed on all exposed surfaces of the reaction vessel, sample port, and the electrodes. The gold dissolution curve usually levelled soon after the precipitate was observed. Most likely, this protective coating of MnO_2 forms on the surface of the gold, inhibiting further reaction with the chlorine. But when fine gold is dissolved, the increased rate of dissolution by the KMnO_4/HCl reaction results in total recovery of the Au before the precipitate is formed. While the faster dissolution could be construed as a result of nascent chlorine, it will be shown in Chapter Three that the presence of excess Cl^- ion is the main contributor.

The effect of nascent chlorine was tested primarily by sparging Cl_2 in the presence and absence of light. The results of the experiments showed no general improvement in the dissolution rate of Au in light as compared to darkness. Figures 1-34, 35 and 36 show the comparisons of the dissolution data for various light sources and the corresponding dark experiments. An increase in the dissolution rate of Au by an active $\text{Cl}\cdot$ atom was not observed. But based on the fact that the reaction between Cl_2 and Au is diffusion limited (see Figure 1-19), the only way an increase

would have been possible is in the unlikely event that $\text{Cl}\cdot$ diffuses faster than Cl_2 .

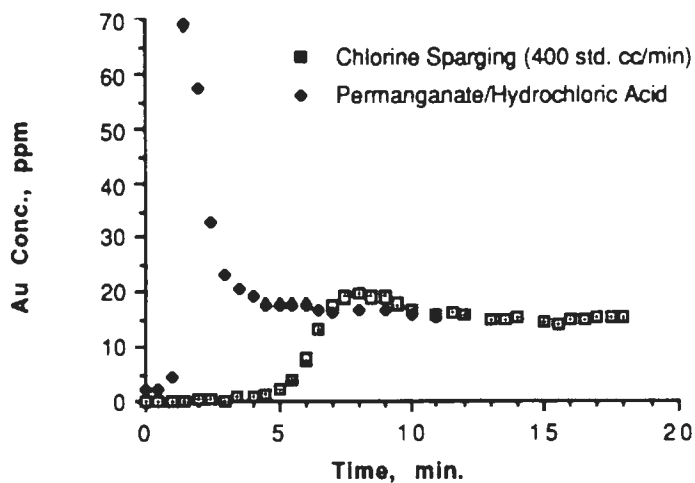


Figure 1-32. Comparison of the chlorination of fine particle Au (-325 Mesh) by sparging with Cl_2 and the generation of Cl_2 by the reaction of KMnO_4 with HCl .

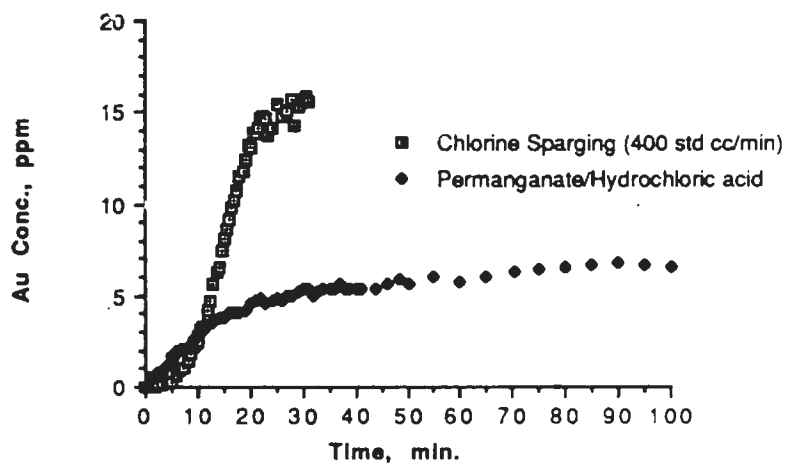


Figure 1-33. Comparison of the chlorination of coarse particle Au (-20 Mesh) by sparging Cl_2 and generation by the reaction of KMnO_4 with HCl .

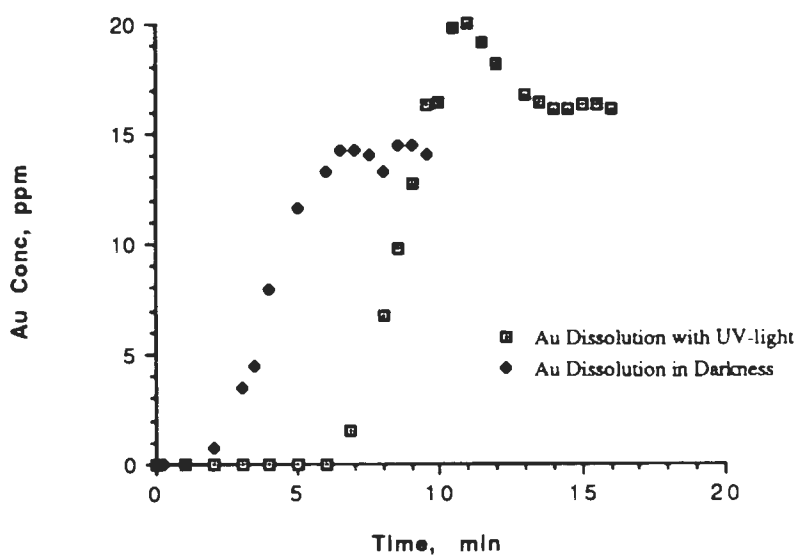


Figure 1-34. Comparison of the dissolution data from Figures 1-9 and 1-10. Both experiments used about 7.5 mg of Au initially in a 0.50-L volume of water (~15 ppm Au is the calculated maximum concentration). The dark experiment used a slightly higher chlorine sparging rate, hence the faster dissolution rate.

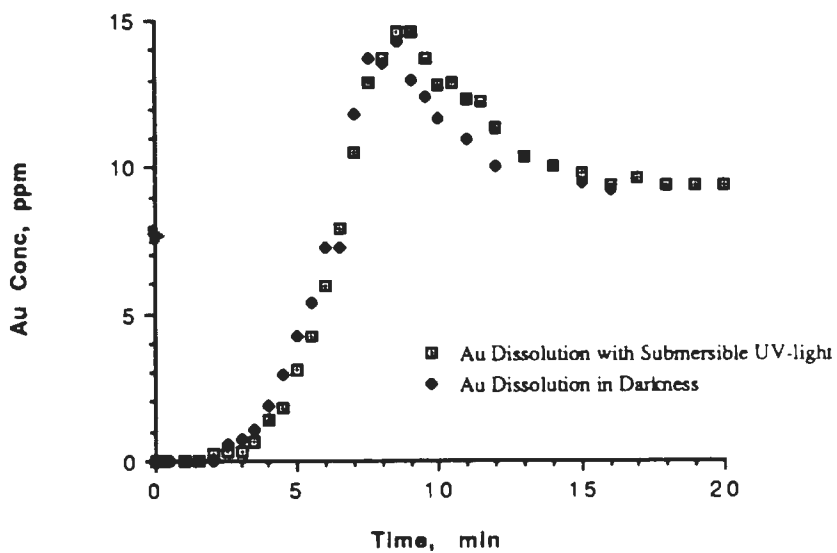


Figure 1-35. Comparison of the dissolution data from Figures 1-11 and 1-12. Both experiments used the same gas flow rate and approximately the same initial conditions (2-L water with 22 mg of the -325 mesh Au for a maximum expected Au concentration of ~11 ppm).

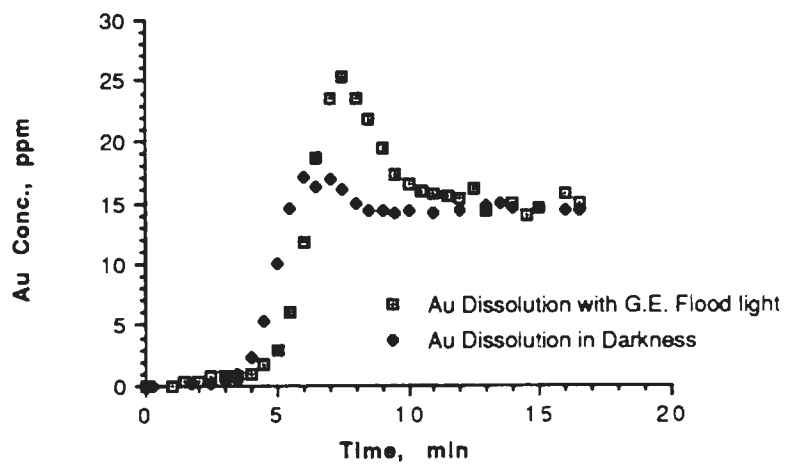


Figure 1-36. Comparison of the dissolution data from Figures 1-13 and 1-14.

Mechanism of the Chlorination of Gold

The identification of the cause of the anomalously high Au concentration peak became a primary goal as the research progressed. Possible contributing factors were systematically eliminated. Possible interference by metal contamination was eliminated when the removal of the stainless steel tubing in the chlorine delivery system didn't lower the peak. Interference by Cl_2 , KMnO_4 , and HCl were eliminated by tests conducted with no gold present. Diffusion was eliminated by two of three experiments which showed complete mixing within 15 seconds (much faster than the 2-3 minute duration of the peak) and when increased stirring didn't lower the peak.

The results of the Au(I) and Au(III) experiments prove that the peak is related to the interferences of the spectra for each ion. However, it would be extremely difficult to quantify these findings. Because of the extremely unstable nature of $[(\text{C}_2\text{H}_5)_4\text{N}]\text{AuCl}_2$, it is difficult to determine the exact amount of the material that is instantly reduced to Au^0 when it comes in contact with water. Therefore, quantification would be difficult.

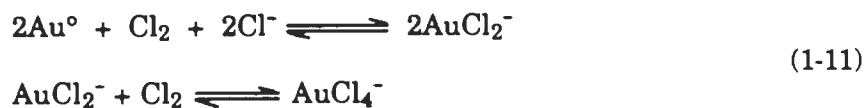
Some tests were attempted to identify the species causing the interference. Early speculation was that the Au(I) spectra was slightly offset from the Au(III) spectra. The AAS would, in essence, double count the two species. But this was immediately discounted. During the synthesis experiments, however, it was observed that elemental Au was formed from the AuCl_2^- complex rapidly. During dissolution, if AuCl_2^- is

formed and injected into the carrier water, the environment would not be suited to its stability. As observed in the synthesis experiments, the result of this change is the instantaneous reduction of Au(I) to Au⁰.

The peak was never eliminated in the tests to maintain AuCl₂⁻ stability in the carrier stream. To explain these results, another look into the stability of AuCl₂⁻ at very low Au concentrations must be taken. At 15 ppm, the region of AuCl₂⁻ complex stability for high chloride ion concentration is limited to a 0 - 10 pH range and an Eh range of 890 - 920 mV. At lower Au concentrations, these ranges may decrease to 0 - 5 for the pH and 1.0 - 1.03 V for the Eh. Therefore an exact pH and Eh within this narrow range must be maintained within the carrier solution. This range could not be achieved with the apparatus used in this study.

In all experiments with the coarse gold powder (-841 μm) no peak was ever observed. An explanation for this comes from the heterogeneous kinetics of the dissolution of a particle. The rate at which a particle dissolves is directly related to the surface area of the particle. For two equal masses of particles--one small diameter, the other large diameter--one would expect the larger particles to dissolve slower in diffusion controlled reactions simply due to the smaller surface area. In chlorination, which is diffusion limited, the slower dissolution of Au would result in slower formation of the AuCl₂⁻ complex which is rapidly oxidized to AuCl₄⁻. This argument explains the observed absence of the anomalous peak in the dissolution of coarse gold.

The proposed mechanism for the reaction of Au with chlorine is mechanism (1-11):



Based on thermodynamic and electrochemical data, the actual species of chlorine which reacts with the gold is most likely Cl_2 , but the presence of Cl^- is important to the overall mechanism.

An attempt to find some consistency relating the height of the peak to experimental parameters was difficult. A larger peak would indicate that the first reaction of mechanism (1-11) would be much faster than the second, or in other words, more AuCl_2^- is produced than is reduced causing a build up of the Au(I) species. In general, the peak was consistently higher in experiments in which KMnO_4 reacting with HCl provided the Cl_2 . From this observation, two generalities relating the peak height can be posed:

- (1) the peak height is related to the rate of dissolution (i.e., the faster dissolutions would result in a higher peak).
- (2) the higher peak is noted in the solutions which are more conducive to the stability of AuCl_2^- (i.e., the higher Cl^- concentrations).

Both of these speculations have some merit based on the relative differences between the solutions encountered in sparging (low Cl^- , slower dissolution) and in KMnO_4/HCl (higher Cl^- , faster dissolution). However, these

arguments break down when attempting to compare the sparging experiments or the permanganate experiments separately. No correlation between light and dark and peak height could be discerned.

This mechanism (1-11) is sensitive to many parameters, including Cl_2 concentration, Au° particle size, and the stir rate. The coarse particles give the impression that Au° oxidizes directly to AuCl_4^- . Figure 1-37 shows the observed effect of particle size on the dissolution kinetics. With the smaller particles, the first reaction is faster than the second, so there is a higher concentration of AuCl_2^- until the second reaction can catch up. But with the larger particles, there is less surface area for the same mass. The first reaction is then slower than the second, hence little AuCl_2^- is observed.

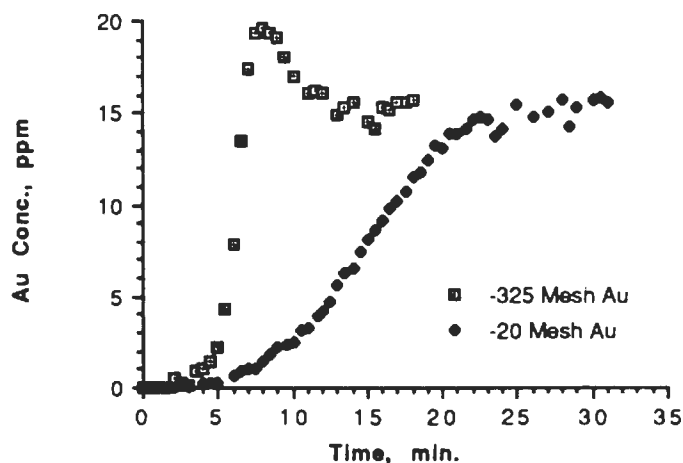


Figure 1-37. The effect of particle size on the chlorination of Au by chlorine sparging.

A possible side reaction is the conproportionation of Au^{+3} with Au° as in equation (1-12):



As discussed above, the surface area difference between the -325 and the -20 mesh particles would play an important role in equation (1-12). But considering the fact that chlorine is such a strong oxidizing agent, this reaction is probably unimportant.

V. Conclusions

The following conclusions may be drawn from the results of the experiments conducted:

- 1) Chlorine sparging and the formation of chlorine *in situ* by the reaction of KMnO_4 and HCl are the two most effective methods for chlorine reacting with gold. The acidification of sodiumhypochlorite produced chlorine too slowly to be a viable method. Chlorine sparging is better overall based on the higher recovery with the larger particle-sized Au.
- 2) Au is dissolved by Cl_2 by the following mechanism:

$$2\text{Au} + \text{Cl}_2 + 2\text{Cl}^- \rightleftharpoons 2\text{AuCl}_2^-$$

$$\text{AuCl}_2^- + \text{Cl}_2 \rightleftharpoons \text{AuCl}_4^-$$
 (The exact species of chlorine (whether Cl_2 or $\text{Cl}\cdot$) that kinetically controlling was indeterminable in these experiments.)
- 3) The ionic species present also have a bearing on the dissolution rate. The presence of excess chloride ions increases the kinetics dramatically, while the presence of hypochlorite ions does not improve the rate.
- 4) The reaction between Au and Cl_2 is diffusion limited.
- 5) A large discrepancy in the detection of gold by AAS was observed. It was determined that the ionic chloride complex of Au(I) reduces to colloidal elemental gold in the carrier stream to the AAS. Although increased chloride concentrations in the carrier was used in an attempt to stabilize the AuCl_2^- , the peak in the gold concentration was never eliminated. However, this conclusion was deemed the cause for the large increase in the observed Au concentration on the basis of thermodynamics.
- 6) Conclusive evidence of the existence of an activated chlorine atom ($\text{Cl}\cdot$) was not observed. The effect of such a species did not improve the dissolution of gold. Nascent chlorine does not improve the reaction rates in dissolving Au.

Chapter Two

The Role of Carbon and Minerals in the Pretreatment of Refractory Gold Ores With Chlorine

I. Introduction

Chlorine Chemistry

The high oxidation potential of the chlorine/chloride couple has been exploited in many processes. The most famous in mineral processing history is the CLEAR Process of Duvall Mining Corporation.⁶⁸ Many others, though less famous, include the treatment of nickel ores at Falconbridge, Canada⁶⁹, the purification of molybdenite concentrates with ferric chloride,⁷⁰ the treatment of complex rare earth titanoniobates⁷¹, and the formation of chromic chloride from ferrochromium pellets.⁷²

A wide range of sulfide minerals have been studied in chlorine/chloride systems.²⁰⁻²³ Strickland and Jackson²² conducted research to investigate the reaction products and the degree of chlorine consumption when sulfide minerals are chlorinated. Woodcock²³ compiled a review article that focused on the effects of mineral structures, particle size, solution composition, temperature and other variables. Most copper sulfide and iron sulfide minerals are readily dissolved by chlorine or concentrated hydrochloric acid solution. In fact, in some processes, the heat evolved by the reactions of the minerals with Cl_2 is so great that the reactors must be cooled. The heats of reaction of copper, zinc, and mercury with chlorine, for instance, range from 50 kcal/mol to over 100 kcal/mol.²¹

The standard free energies of the chlorine/chloride system with the minerals chalcocite, pyrrhotite and pyrite indicate that dissolution is thermodynamically favorable. Using Equation (14) on page 16, values of the change in free energy at room temperature (ΔF°)₂₉₈ may be calculated for mass and charge balanced reactions which assume different product forms of sulfur (elemental sulfur, dissolved H₂S or sulfate) and iron (ferrous or ferric). Table 2-I shows the changes for the mineral/chlorine reactions assuming that the final form of the sulfur is elemental sulfur (S⁰) or dissolved as hydrogen sulfide (H₂S). Table 2-II shows the same reactions for the mineral/chlorine system if the final form of the sulfur is sulfate (SO₄⁻²). The conclusion drawn from these calculations is that the most favorable reactions are between chlorine and the mineral resulting in cationic metal species (with the iron as ferric) and aqueous sulfate anions. Elemental sulfur, aqueous H₂S, ferrous chloride products nor the reaction of chloride ion with the minerals would be expected. However, the results of this thermodynamic approach are not echoed by the experimental results of Strickland and Jackson.²² Their results show that the pyrite and pyrrhotite do dissolve to form ferric ion and sulfate ion, but chalcocite dissolves into the products of cupric chloride and elemental sulfur. From their results it would be concluded that in the dissolution of chalcocite, the mechanism or kinetics affects the reaction in Table 2-I so that S⁰ is the product. Another point of these calculations is that little information is provided about the rate of dissolution of these reactions.

<u>Equation</u>	<u>Free Energy Change</u>
(i) $\text{Cu}_2\text{S}(\text{s}) + 2\text{Cl}_2(\text{aq}) \rightleftharpoons 2\text{CuCl}_2(\text{aq}) + \text{S}^\circ(\text{s})$	$(\Delta F^\circ)_{298} = -97 \text{ kcal}$
$\text{Cu}_2\text{S}(\text{s}) + \text{Cl}_2(\text{aq}) + 2\text{HCl} \rightleftharpoons 2\text{CuCl}_2(\text{aq}) + \text{H}_2\text{S}(\text{aq})$	$(\Delta F^\circ)_{298} = -40 \text{ kcal}$
(ii) a. $\text{FeS}_2(\text{s}) + 3/2\text{Cl}_2(\text{aq}) \rightleftharpoons \text{FeCl}_3(\text{aq}) + 2\text{S}^\circ(\text{s})$	$(\Delta F^\circ)_{298} = -58 \text{ kcal}$
b. $\text{FeS}_2(\text{s}) + \text{Cl}_2(\text{aq}) \rightleftharpoons \text{FeCl}_2(\text{aq}) + 2\text{S}^\circ(\text{s})$	$(\Delta F^\circ)_{298} = -43 \text{ kcal}$
(iii) a. $\text{Fe}_7\text{S}_8(\text{s}) + 21/2\text{Cl}_2(\text{aq}) \rightleftharpoons 7\text{FeCl}_3(\text{aq}) + 8\text{S}^\circ(\text{s})$	$(\Delta F^\circ)_{298} = -505 \text{ kcal}$
$\text{Fe}_7\text{S}_8(\text{s}) + 5/2\text{Cl}_2(\text{aq}) + 16\text{HCl} \rightleftharpoons 7\text{FeCl}_3(\text{aq}) + 8\text{H}_2\text{S}(\text{aq})$	$(\Delta F^\circ)_{298} = -44 \text{ kcal}$
b. $\text{Fe}_7\text{S}_8(\text{s}) + 7\text{Cl}_2(\text{aq}) \rightleftharpoons 7\text{FeCl}_2(\text{aq}) + 8\text{S}^\circ(\text{s})$	$(\Delta F^\circ)_{298} = -404 \text{ kcal}$
c. $\text{FeS}(\text{s}) + 3/2\text{Cl}_2(\text{aq}) \rightleftharpoons \text{FeCl}_3(\text{aq}) + \text{S}^\circ(\text{s})$	$(\Delta F^\circ)_{298} = -73 \text{ kcal}$
$\text{FeS}(\text{s}) + 1/2\text{Cl}_2(\text{aq}) + 2\text{HCl} \rightleftharpoons \text{FeCl}_3(\text{aq}) + \text{H}_2\text{S}(\text{aq})$	$(\Delta F^\circ)_{298} = -16 \text{ kcal}$
d. $\text{FeS}(\text{s}) + \text{Cl}_2(\text{aq}) \rightleftharpoons \text{FeCl}_2(\text{aq}) + \text{S}^\circ(\text{s})$	$(\Delta F^\circ)_{298} = -59 \text{ kcal}$

Table 2-1. Possible reactions of three minerals--(i) chalcocite, (ii) pyrite, and (iii) two forms of pyrrhotite--with chlorine and the associated standard free energies for the reactions.

$$(\Delta F^\circ)_{298} = \sum (\Delta F^\circ)_{298, \text{ products}} - (\Delta F^\circ)_{298, \text{ reactants}}$$

These reactions were derived to compare the free energies of the reactions in which the product form of sulfur is either elemental sulfur or dissolved hydrogen sulfide.

<u>Equations</u>	<u>Free Energy Change</u>
(i) $\text{Cu}_2\text{S} + 5\text{Cl}_2 + 4\text{H}_2\text{O} \rightleftharpoons 2\text{Cu}^{+2} + 8\text{H}^+ + \text{SO}_4^{-2} + 10\text{Cl}^-$	$(\Delta F^\circ)_{298} = -228 \text{ kcal}$
(ii) $\text{FeS}_2 + 15/2\text{Cl}_2 + 8\text{H}_2\text{O} \rightleftharpoons \text{Fe}^{+3} + 16\text{H}^+ + 2\text{SO}_4^{-2} + 15\text{Cl}^-$	$(\Delta F^\circ)_{298} = -349 \text{ kcal}$
(iii) a. $\text{Fe}_7\text{S}_8 + 69/2\text{Cl}_2 + 32\text{H}_2\text{O} \rightleftharpoons 7\text{Fe}^{+3} + 64\text{H}^+ + 8\text{SO}_4^{-2} + 69\text{Cl}^-$	$(\Delta F^\circ)_{298} = -1677 \text{ kcal}$
b. $\text{Fe}_7\text{S}_8 + 9/2\text{Cl}_2 + 4\text{H}_2\text{O} \rightleftharpoons \text{Fe}^{+3} + 8\text{H}^+ + \text{SO}_4^{-2} + 9\text{Cl}^-$	$(\Delta F^\circ)_{298} = -223 \text{ kcal}$

Table 2-II. Possible reactions of three sulfide minerals-- (i) chalcocite, (ii) pyrite and (iii) two forms of pyrrhotite-- with chlorine and the standard free energies for the reactions.

$(\Delta F^\circ)_{298} = \sum (\Delta F^\circ)_{298, \text{ products}} - (\Delta F^\circ)_{298, \text{ reactants}}$

These reactions were derived assuming sulfate was the product form of sulfur.

Flash Chlorination Process Development²⁵⁻³⁰

The patents of several processes using chlorine as a pretreatment for carbonaceous ore are held by the Newmont Mining Company. In the first process, patented in 1971, chlorine is sparged into a slurry of ground ore (80% passing 200 mesh) prior to cyanide leaching (see Figure 1, page 6). The initial lab-scale and pilot plant research was conducted by the U.S. Bureau of Mines Reno Research Center in Reno, Nevada from 1967 to 1969. Then, in 1971, the process was implemented at Carlin, Nevada by Newmont.

Over the next decade, continued research brought changes to the chlorination process. In 1977, "double-oxidation" became the first improvement to the process. High temperatures (90°C) and air sparging prior to chlorination helped to reduce the total amount of chlorine needed to attain the results of the previous process. But due to exorbitant energy costs and excessive equipment wear, the process was abandoned after nearly six years of operation in 1982.

In the mid-80's, a resurgence of research investigated solutions to the following problems:

- 1) reducing reagent costs and improving plant operation,
- 2) questions of the mechanisms and kinetics of the operation, and,
- 3) which constituents were responsible for the gold adsorption.

The immediate result of this research was to modify the process by reducing the time of chlorine sparging while increasing the conditioning time and net concentration of hypochlorite in the solution. The "flash

chlorination" process was implemented in 1987 at the Carlin milling facility in northeastern Nevada (see Figure 2-1).

As the process has changed, so too have the theories explaining the success of the process. Initially, the laboratory research concluded that the Cl_2 and HOCl oxidized the functional groups on the carbon (which was believed to be activated carbon and humic acid). This oxidation rendered the carbon inert to gold cyanide complex adsorption.

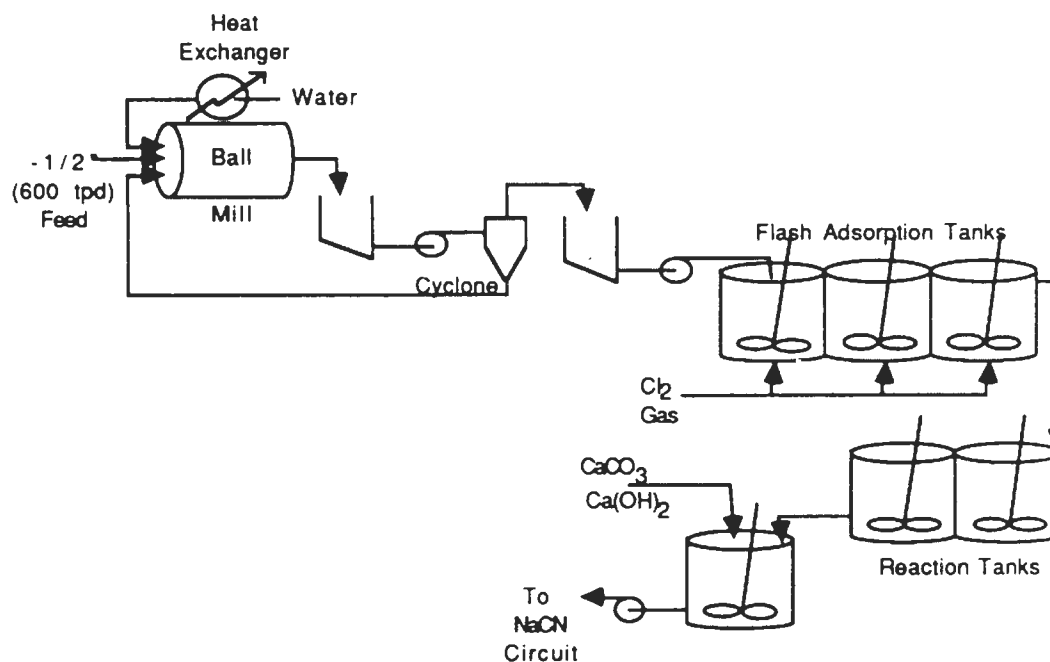


Figure 2-1. Flowsheet of the "flash" chlorination process in operation since 1987²⁹.

However, by the time of the "flash" phase of research this theory had changed. Experiments showed that as much as 85% of the gold was solubilized during flash chlorination. During the attrition time following chlorination, the Eh dropped and the pH rose to levels amenable to Au^0 precipitation. This newly formed Au is more easily recovered by cyanidation according to Brunk and Atwood.²⁹ But no conclusion had been drawn to explain why the carbon is non preg robbing.

The Refractory Ore of Carlin, Nevada

Through the years, numerous studies have dealt with refractory carbon-bearing ore. The potential of gold in the millions of ounces has opened the door for the research of novel methods of recovery. Through the years, lixiviants such as thiourea and thiosulfate have been tested. Competing adsorbers of gold cyanide complex such as commercial resins and carbon, an oxidizing roast and oil additives to bind the carbon have also been tested. But nothing, as yet, has been as attractive as the "flash chlorination" process. But to solve the problems presented by the ore, one must first ascertain the contributing factors to the intractability to cyanidation.

Throughout the history of cyanidation, carbon- and sulfide-bearing ores have been the most difficult to treat economically. The difficulty is compounded because general treatments are not effective since no ores are exactly alike. In general, some of the most common sulfide minerals are pyrite (FeS_2), pyrrhotite (FeS_n), arsenopyrite ($FeAsS$), chalcocite (Cu_2S),

chalcopyrite (CuFeS_2), sphalerite (ZnS), antimony sulfides (such as stibnite and tetrahedrite) and arsenic sulfides (such as orpiment and realgar). These minerals often react much faster with CN^- and to a greater degree of completeness than does gold.⁷³ The cyanide and oxygen robbing character of these minerals has been well documented.⁷³

But the dissimilarity of refractory ores doesn't end with sulfide mineral content. Carbonaceous material may be in the form of graphite, long chain hydrocarbons, or organic acids (like humic acid). Of these, the two most detrimental to cyanidation are graphitic carbon and organic acids. These two have been reported to adsorb $\text{Au}(\text{CN})_2^-$ by many proposed mechanisms.

The mechanism of adsorption by humic acid is under some controversy. Radtke and Scheiner³⁰ proposed that these acids actually chelate the Au(I) from the cyanide complex. Freeman and Baglin⁷⁴ proposed that the benzoic acid derivatives in humic acid may complex Au(III).

The graphitic carbon behaves much like activated carbon used in CIP circuits. However, the interaction of $\text{Au}(\text{CN})_2^-$ with the carbon is also a point of controversy. Cho and Pitt⁷⁵ contended that the interaction is possible because of the relatively large size of the complex. They have shown an increase in adsorption with increased ionic size. But McDougall⁷⁶ has purported that the gold chemisorbs on the surface. His experimental results show that Au has a 0.3 valence state on the surface--somewhere between the 0 valence state of elemental gold, and the expected

1.0 of the $\text{Au}(\text{CN})_2^-$ complex.

Gallagher⁷⁷ has shown that the rate of carbon loading of $\text{Au}(\text{CN})_2^-$, AuCl_4^- , and other gold complexes is directly proportional to the equilibrium capacity of the carbon. This study showed the highest affinity of adsorption for $\text{Au}(\text{SCN})_2^-$ decreasing for $\text{Au}(\text{SC}(\text{NH}_2)_2)_2^+$ and $\text{Au}(\text{CN})_2^-$. By adjusting the potential of the carbon, all of these complexes could be removed from the surface. However, AuCl_4^- was not removed from the carbon even with a large applied positive potential. The conclusion drawn from this was that AuCl_4^- is reduced to Au^0 on the surface of the carbon; the other complexes are adsorbed in the oxidated state. This conclusion has since been corroborated by Hiskey, et al⁷⁸.

These arguments become moot since the form of carbon present in many of the refractory ores investigated has never been satisfactorily identified. Many have felt that the various Carlin-type ores, for instance, contain numerous sulfide minerals and most of the carbonaceous matter was graphitic carbon. However, some have felt that as much as 50% of the total carbon in these ores was humic acid.

While this controversy rages on, it becomes necessary, for the sake of this investigation, to choose sides. With no further scientific explanation beyond "the newest results seem the best", the carbon in Carlin ores will be assumed to be mostly graphitic, or activated carbon. Some unpublished results of Dr. John Nelson⁷⁹ have shown that most of the carbon in samples

<u>Mineral/Component</u>	<u>% by wt. (unless specified)</u>	<u>wt. in 1-L test</u>
FeS ₂	1.8% (Fe)	20.9 g
Cu ₂ S	0.6% (Cu)	0.07 g
C (graphite)	2.0%	13.5 g
Au	.16 oz/t	3.0 mg

Table 2-III. Calculated ore assay based on the analysis of Carlin ore by Dr. J. H. Nelson. The correlated weights used in a 1-L experiment are calculated from these "Heads".

from a relatively new section of the mine is graphitic and not humic. From his analyses, the relative amounts of gold, pyrite, chalcocite and total activated carbon may be calculated so that a synthetic ore could be made to test the effect of chlorination on sulfide minerals and carbon. Table 2-III contains the values which are a composite of Dr. Nelson's results.

In the early days as cyanidation replaced chlorination, one of the purported benefits was the selectivity of cyanide. But based on the present knowledge of carbonaceous ores, perhaps this is a detriment. The relative reactivity of chlorine and chloride with minerals leads to the postulate that the more metal in solution, the more metal that may adsorb on the surface of the carbon. The experimentation in this portion of the research was intent on testing this premise. Favorable results could lead to new means of rendering the carbon inactive under the extremes of pH and ORP that Cl₂ sparging creates.

II. EXPERIMENTAL

Experimental Procedures

a. Mineral Studies

The primary goal of this research was to determine which sulfide minerals, if any, dissolve faster than gold. The dissolution of various sulfide minerals by chlorine was conducted under similar conditions to the gold dissolution experiments discussed in Chapter One. Chlorine sparging and chlorine formation by the permanganate/HCl reaction were both tested on -28 +200 and -200 mesh samples of the minerals.

The initial weight of the minerals were calculated by determining the amounts of the pure minerals needed to produce a concentration of 5 ppm if 100% of the mineral dissolved. The minerals were weighed and placed into the clean, dry 2-L Pyrex reactor vessel. The 1-L of water used in sparging experiments or 0.91-L of water with .36 g of KMnO_4 in the chemical formation tests was added to the vessel and half-speed stirring by the magnetic stirrer was initiated. ORP and pH were monitored until stable, then initial samples were injected into the AAS for analysis. In the gas experiments, the sparger was then placed in the reactor and the ORP and pH were again stabilized before sampling. The timer was started when the gas valve was opened, or when 90 mL conc. HCl was added to the permanganate experiments.

b. Mineral/Gold/Carbon Studies

Two techniques were devised to keep the carbon and minerals separate during the experiments. In the first technique, pouches of carbon were constructed from Spectramesh 710 micron mesh polypropylene filter cloth and stitched closed with Nylon fishing line. In the second technique, a 2 cm glass vial was cut into a cylinder. A piece of the same polypropylene screen was attached to the open end of the vial using electrical lock straps. A small layer of glass wool was placed in the bottom followed by the carbon. More glass wool was placed on the top of the carbon and a final piece of screening was affixed by screwing on the vial's lid which had been cut open. Figure 2-2 shows a cross-section of the vial.

As in the mineral dissolution experiments, the same general procedure of the experiments was followed. The carbon was weighed and loaded into one of the holders described previously. The gold, pyrite and chalcocite were weighed and placed with the carbon apparatus in the clean, dry reactor vessel. The solution volumes (1-L water for sparging, 0.91-L water and permanganate for chemical formation) were added and mixed at half speed and stabilized before sampling. The reactors were run in this manner for periods of 6 to 24 hours to assure complete wetting of the carbon. Then after the sparger was added and the solution again

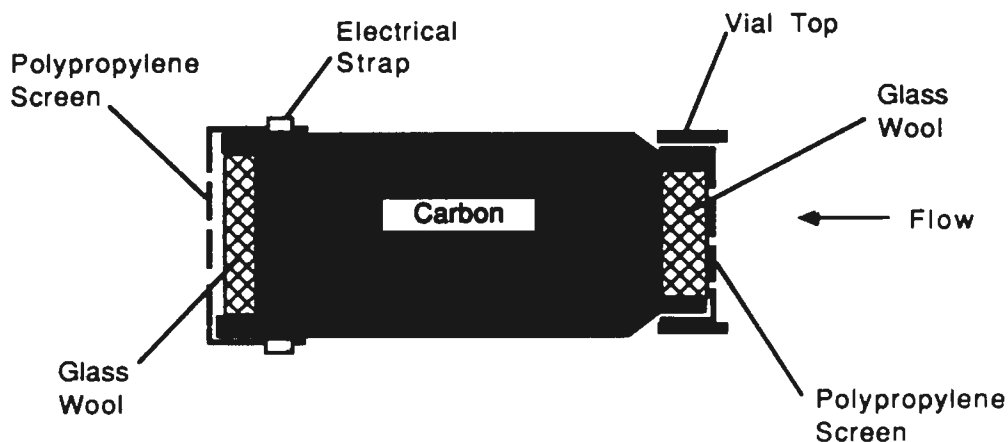


Figure 2-2. Cross-sectional view of a technique devised to secure the carbon in the mineral/carbon/gold experiments.

stabilized, another sample was injected. Then the Cl_2 or HCl was added to begin the dissolution.

Because of the high concentrations of iron and copper in the refractory analysis in Table 2-III, an iron-rich and a copper-rich mineral were needed. Pyrite and chalcocite were chosen based on the common occurrence of both minerals in refractory ores. So that mill operation is more closely represented in these experiments, -200 mesh pyrite and -325 mesh chalcocite and -325 mesh gold were used. The three basic goals of this

phase of the research were as follows:

- (1) Observe overall adsorption of metal species on carbon,
- (2) Determine the adsorption of the various metals with time,
- (3) Determine if pretreating the carbon with Fe^{+3} will hinder Au adsorption.

The first set of experiments used the vial arrangement to hold all of the carbon for an experiment. The carbon was removed and analyzed for metal adsorption. The (2) experiment was conducted using five (5) equal amounts of carbon placed in separate pouches. The pouches were removed at intervals and analyzed for metal adsorption.

In the final set of experiments, the carbon was allowed to mix in the solution. Premeasured volumes of a 1000 ppm standard gold chloride solution were added and the Au concentration was monitored with FIA. Various amounts of $\text{FeCl}_3 \cdot 6\text{H}_2\text{O}$ and $\text{Fe}(\text{NO}_3)_3 \cdot 9\text{H}_2\text{O}$ were added and allowed to condition with carbon for at least 6 hours before the Au solution was added.

Minerals

Chalcocite, chalcopyrite, arsenopyrite, pyrrhotite and pyrite mineral samples were purchased from Wards Mineral Catalog Company and crushed to $-1/2$ inch, pulverized and screened in 10 mesh, 28 mesh, and 200 mesh Tyler screens in series. The $-28 +200$ mesh and the -200 mesh

fractions were collected. The minerals were analyzed by the technique in which the samples underwent acid digestion followed by inductively-coupled plasma (ICP) flame emission spectrophotometric analysis of the dissolved metals. The results of the analyses are provided in Table 2-IV. Although the total metal values measured by the ICP may not be extracted from the mineral, the ICP values of the iron or copper were used to calculate the estimated maximum metal concentration for each mineral test. The initial weight of the sample was multiplied by the ICP analysis value. This value was then plotted in the dissolution results.

Carbon

Based on the identification studies conducted by Dr. Nelson of the Chemistry Department of the University of Nevada, Reno, activated carbon was used to model the carbon found in Carlin-type ores. The specific type of carbon used was Fisher Scientific -16 +20 mesh activated carbon.

Equipment

As with the gold dissolution study described in Chapter One, this phase of the research relied heavily on FIA for sampling. For the entirety of this research, the modified flowchart used in the gold study (see page 28) was used in this phase.

<u>Mineral Sample</u>	<u>ICP Analysis</u>
Arsenopyrite (FeAsS)	Fe - 33.0% As - 26.5%
Pyrite (FeS ₂)	Fe - 46.4%
Pyrrhotite (FeS _n)	Fe - 44.5%
Chalcocite (Cu ₂ S)	Cu - 74.2%
Chalcopyrite (CuFeS ₂)	Cu - 9.3% Fe - 39.3%

Table 2-IV. Results of the analysis of the minerals by the acid digestion and inductively-coupled plasma (ICP) flame emission spectrophotometer.

Analytical Techniques

The same Perkin Elmer model 2380 AAS used in the gold study was employed in conjunction with the FIA for the mineral dissolution experiments. Cathode lamp sources of copper and iron were used. The copper analysis was conducted at 324 nm spectral wavelength and iron was analyzed at 248 nm. Each ion has a linear calibration curve relating concentration to absorbance up to 5 ppm.

The carbon was analyzed for the amount of metal adsorbed on the surface. After the experiment, the carbon was washed with distilled-deionized water to remove residual minerals. The carbon was then dried slowly at a temperature of -80°C . The carbon was placed in a volumetric flask and was mixed with a dilute aqua regia solution. The carbon remained in the aqua regia for at least 24 hours. The solution was then analyzed by AAS for iron, gold and copper.

The aqua regia was prepared from a mixture of concentrated HCl : conc. HNO_3 in a volume ratio of 3 : 1. This stock solution was diluted 1 : 20 with water for the smaller carbon samples (~2.5 g) and 1 : 10 with water for the larger carbon samples (~14 g).

III. Results

Mineral Studies

So that qualitative comparisons of the dissolution rates of the coarse and fine minerals could be made with similarly sized gold particles, four chlorination experiments using no more than 5 mg of gold in 1-L of water were conducted. Two of the chlorination experiments used Cl_2 gas sparging on coarse and fine particle gold. The other tests used the KMnO_4/HCl production method to introduce chlorine to dissolve coarse and fine particle gold. The results of these gold dissolution experiments are referred to repeatedly throughout this section in direct comparisons with the mineral dissolution results. The dissolutions were similar to the experiments of Chapter One in that the peak was observed in all fine experiments, but the length of time before the Au was first detected by the FIA was only 3 minutes--nearly two minutes faster than in the results of the previous chapter. A slightly faster chlorination rate (~450-500 std. cc/min) was used in this research which probably explains the slight increase in dissolution rate.

An estimate of the amount of iron or copper that is recoverable from the mineral samples by chlorination can be calculated by averaging the results from all of the mineral dissolution studies. Assuming that all of the

recoverable metal was extracted in each experiment, the final solution assay (by AAS) divided by the initial weight of metal (ICP value X initial weight of the sample) will give a value of the total metal recovered. A statistical average of all of these values for coarse and fine dissolution experiments will give a good estimate of the total amount of metal that is recoverable from each mineral. A comparison of these values to the ICP values is provided in Table 2-V. In reporting the results of the dissolution experiments, it still is necessary to give a reference composition of the highest expected concentration based on one of these numbers. The ICP values were chosen for this purpose. Because the samples were neither homogeneous nor pure, the calculated value of the recoverable was not deemed a representative basis for comparing the dissolution results.

The final Eh values for the experiments were 900 -1000 mV and the final pH ranged from 1.5 - 2.

<u>Mineral (metal analyzed)</u>	<u>Experimental Avg.</u>	<u>ICP</u>
Arsenopyrite (Fe)	11.9%± 6.5	33.0%
Pyrite (Fe)	24.4%±13.4	46.4%
Pyrrhotite (Fe)	28.8%±11.2	44.5%
Chalcocite (Cu)	48.3%±10.9	74.2%
Chalcopyrite (Cu)	7.3% ± 2.0	9.3%

Table 2-V. Comparison of statistically generated percent of the sample which is recoverable metal (based on initial weight and final metal assay for the dissolution experiments) to the ICP analysis.

a. Pyrite

(i) Chlorine sparging.

The results of chlorine sparging on coarse (-28 +200 mesh) and fine (-200 mesh) pyrite are presented graphically in Figures 2-3 and 2-4, respectively. From both dissolution results, pyrite reacts with chlorine much like gold. Dissolution is detected after about 5 minutes of sparging. Figure 2-5 shows a comparison of coarse pyrite dissolution to coarse gold dissolution under the same conditions. The similarities of slope and concentrations give rise to a qualitative conclusion that coarse pyrite dissolves at about the same rate as coarse gold. Figure 2-6 presents the same comparison for the fine particle sizes. In this comparison the iron concentration lags the gold concentration by about 3 minutes. Also the slope of the gold dissolution is much greater than that for the pyrite dissolution.

(ii) KMnO_4/HCl .

The results of the coarse and fine pyrite particle dissolutions by the KMnO_4/HCl reaction are presented in Figures 2-7 and 2-8, respectively. In both experiments, the iron concentration is detected within 1 minute of the onset. The comparison of Au and pyrite dissolution rates for coarse and fine particles are presented for this method of chlorine addition in Figures

2-9 and 2-10. Coarse pyrite has a similar dissolution to the gold curve. The fine particle pyrite is much slower to react than Au based on the 2 to 3 minutes which pass before iron is detected as compared to the instantaneous detection of Au under the same conditions.

b. Pyrrhotite

(i) Chlorine sparging.

Figures 2-11 and 2-12, respectively, show the graphical results of chlorine sparging on coarse (-28 +200 mesh) and fine (-200 mesh) pyrite. The coarse pyrrhotite dissolution curve resembles the coarse pyrite curve, while the fine particle curve shows the detection of dissolved iron faster. Figure 2-13 shows a comparison of coarse pyrite to coarse gold dissolution. By comparison, the initial slopes and times to first detect dissolved metal is similar for the coarse pyrite as compared to coarse gold. Figure 2-14 presents the same comparison for fine particles which shows nearly the same dissolution rate for both. Admittedly, comparing the fine particle dissolution rates is made difficult by the peak in the gold concentration, but by assuming that complete dissolution of the gold occurs at the peak, then some qualitative estimates may be made.

(ii) KMnO_4/HCl .

The results of the coarse and fine pyrrhotite particle dissolutions by the KMnO_4/HCl reaction are shown in Figures 2-15 and 2-16, respectively. As with coarse particle Au dissolution by this means of Cl_2 addition, Figure 2-15 shows incomplete dissolution of the mineral. But the dissolution of fine pyrrhotite is fast and steady as seen in Figure 2-16. The comparison of Au-pyrrhotite dissolution rates for coarse and fine particles are presented for permanganate generation of chlorine in Figures 2-17 and 2-18. The coarse particle comparison shows that each species is dissolved quickly, but the fine particle comparison shows that gold is dissolved much faster based on the length of time for complete dissolution (less than 5 minutes for gold, but over 20 minutes for pyrrhotite).

c. Chalcocite

(i) Chlorine sparging.

The results of chlorine sparging on coarse (-28 +200 mesh) and fine (-200 mesh) chalcocite are presented graphically in Figures 2-19 and 2-20, respectively. In both dissolutions, the initial detection of dissolved Cu is fairly rapid. Copper is detected within 2 minutes of sparging in both particle sized dissolutions. Figure 2-21 shows that coarse chalcocite

dissolution puts metal into solution slightly faster than coarse gold dissolution under the same conditions. Figure 2-22 presents the same comparison for the fine particle sizes. Again, the gold peak makes comparing the two dissolutions difficult, but both have the same time required to detect metal, and a similar initial slope to the curves.

(ii) KMnO_4/HCl .

The results of the coarse and fine pyrite particle dissolutions by the KMnO_4/HCl reaction are presented in Figures 2-23 and 2-24, respectively. As noted in the other mineral dissolutions by this method, copper is detected almost instantly after the experiment is started. Coarse chalcocite appears to not dissolve as completely as the fine mineral. The comparison of Au and chalcocite dissolution rates for coarse and fine particles are presented for permanganate generation of chlorine in Figures 2-25 and 2-26. As in the sparging experiment, the coarse particle dissolution curves are very similar for both chalcocite and gold chlorination. Each have a short time before the first metal is detected and similar initial dissolution rates. The fine particle dissolutions are again difficult to compare, but both seem to dissolve at a similar rate.

d. Chalcopyrite

(i) Chlorine sparging.

The results of chlorine sparging on coarse (-28 +200 mesh) and fine (-200 mesh) chalcopyrite are presented graphically in Figures 2-27 and 2-28, respectively. In both sized dissolutions, copper is detected early in the experiments. Figures 2-29 and 2-30 show the comparisons of coarse and fine particle dissolutions of chalcopyrite and gold under the same conditions. Coarse particle chalcopyrite puts metal into solution at about the same initial rate as is noted in coarse particle gold dissolution. The fine particle curves are similar, except for the peak in gold concentration.

(ii) KMnO_4/HCl .

The results of the coarse and fine chalcopyrite particle dissolutions by the KMnO_4/HCl reaction are presented in Figures 2-31 and 2-32, respectively. Both sizes of chalcopyrite react quickly to put copper into solution within the first few minutes of the experiment. Also, the copper concentration rises steadily in each, but at a slightly faster rate in the fine particle dissolution. The comparison of Au-chalcopyrite dissolution rates for coarse and fine particles are presented for permanganate generation of chlorine in Figures 2-33 and 2-34. In comparing both coarse and fine chalcopyrite dissolution, the time before metal is detected is similar to gold,

but the rate of gold dissolution is slightly faster for the gold based on the initial slope of the curves.

e. Arsenopyrite

(i) Chlorine sparging.

The results on coarse (-28 +200 mesh) are presented graphically in Figures 2-35. The dissolution of this mineral was very slow and incomplete. The final amount of iron detected in solution was only about 10% of the calculated maximum concentration. The fine (-200 mesh) arsenopyrite dissolution is shown in Figure 2-36, and shows different results. Initial detection of iron occurs 1 minute after sparging is initiated. Also, the steep slope of the dissolution curve may suggest rapid kinetics. Figure 2-37 shows a comparison of coarse arsenopyrite dissolution to coarse gold dissolution under the same conditions. Both curves are slow to rise initially, but the gold concentration increases steadily while the iron level stays low. Figure 2-38 presents the fine particle comparison. The initial slope and rapid increase would suggest that fine arsenopyrite dissolves faster than gold.

(ii) KMnO_4/HCl .

The results of the coarse and fine arsenopyrite dissolutions by chlorine formation are presented in Figures 2-39 and 2-40, respectively. As noted in the sparging experiment of arsenopyrite, the coarse particle mineral does not react completely. But detection of iron comes much earlier than in the previous tests. Likewise, fine arsenopyrite dissolves very quickly initially. The iron concentration curve levels within 5 minutes of the initiation of the KMnO_4/HCl reaction. The comparison of Au-arsenopyrite dissolution rates for coarse and fine particles are presented in Figures 2-41 and 2-42. Both coarse particles dissolve at about the same rate as shown by the comparison in Figure 2-41. Likewise, the rate of the fine arsenopyrite and gold are quite similar.

Carbon Studies

(a) Pyrite/Chalcocite/Gold Dissolution with Carbon

The final leach solution of the test in which 13.5 g of carbon was placed in a dissolution of chalcocite, pyrite and gold by sparged Cl_2 was analyzed by AAS with the following results:

Au	2.7 ppm	
Cu	24.5 ppm	(pH = 1.1; Eh = 740 mV)
Fe	1468.0 ppm	

The final solution from the carbon analysis resulted in the following metal concentrations:

Au	0.3 ppm
Cu	1.4 ppm
Fe	8.7 ppm

These values may be converted directly to the total amount of metal adsorbed (mg). The AAS error factors were $\pm 2\%$ for Au, $\pm 4\%$ for Cu and $\pm 2\%$ for Fe in both analyses. A mass balance accounted for about 80% of the initial Au weight.

A graph of the Au concentration as a function of time for this experiment is provided in Figure 2-43. The plot shows that the concentration steadily increases as the chlorination progresses. However, it should be immediately noted that even though fine particle gold was used, no peak in Au concentration was observed.

Sample Time	Wt., g	Carbon Analysis		
		Au(mg)	Cu(mg)	Fe(mg)
1 min.	2.6131	0.060	0.33	5.23
5.5 min	2.6374	0.096	1.06	5.88
10 min	2.6306	0.056	1.41	5.16
15 min	2.5358	0.046	1.03	2.95
40 min	2.6928	0.002	0.51	7.95

Table 2-VI. Results of the timed removal of carbon during the chlorination of pyrite, chalcocite, and gold.

The results of the timed removal of carbon are shown in Table VI. The results of Table VI are graphed in Figure 2-44 to show the relative times that each metal adsorbed on the carbon. Iron adsorbs relatively fast and increases as the chlorination proceeded. Copper adsorption followed a bell-shaped curve with the peak concentration occurring at 10 minutes. In the meantime, Au adsorption began early, but decreased as the experiment proceeded. The final leach solution for this test analyzed as follows:

Au	2 ppm	
Cu	25 ppm	(pH = 1.3; Eh = 820 mV)
Fe	1385 ppm	

by AAS analysis. A mass balance of the Au in solution and on the carbon accounts for nearly 83% of the initial weight of the gold. A similar balance on the iron and copper show that only 14.6% of the pyrite was dissolved and that nearly 57% of the chalcocite dissolved over the course of the test.

(b) Adsorption of Au on Carbon

The results of the pretreatment of carbon with various metals before addition of gold are presented as graphs of Au concentration over a period of time. For baseline comparisons, Au was added to the carbon slurry directly. The concentration of Au in solution as a function of time is plotted in Figure 2-45. As can be seen in this figure, Au concentration peaked early, but decreased to a final concentration of about 0.25 ppm. Next a test was conducted in which the carbon slurry was sparged with Cl_2 for nine minutes and conditioned for 30 minutes before the Au was added. The results of this test are provided in Figure 2-46 and show that the gold concentration followed the same pattern as that in Figure 2-45. Immediately upon addition of Au, the concentration rose, but fell to a level below 0.2 ppm within a few minutes.

The effect of pretreating the carbon in a solution of 1.8 g/L Fe^{+3} was examined with two salts--ferric chloride and ferric nitrate. The Au concentration after a ferric chloride pretreatment of the carbon is shown in Figure 2-47; the ferric nitrate pretreatment results are shown in Figure 2-48. As can be seen in these figures, neither method succeeded in keeping the Au concentration high, but the final concentration of Au was slightly higher than the previous experiments with no pretreatment or Cl_2 sparging. In the last experiment, ferric chloride and chlorine are added to

the solution with the carbon, then conditioned for 20 minutes prior to Au addition. The results are shown in Figure 2-49. The Au adsorption was considerably slowed as can be seen by the peak at which the concentration of Au in solution was nearly 50% of the initial step concentration (25 to 29 minutes after the sparging was initiated). The Eh and pH of this experiment are plotted for the duration of the experiment in Figure 2-50. In the time period of 25 to 29 minutes in the experiment, the pH and Eh of the experiment were below 9 and above 1.1 V, respectively.

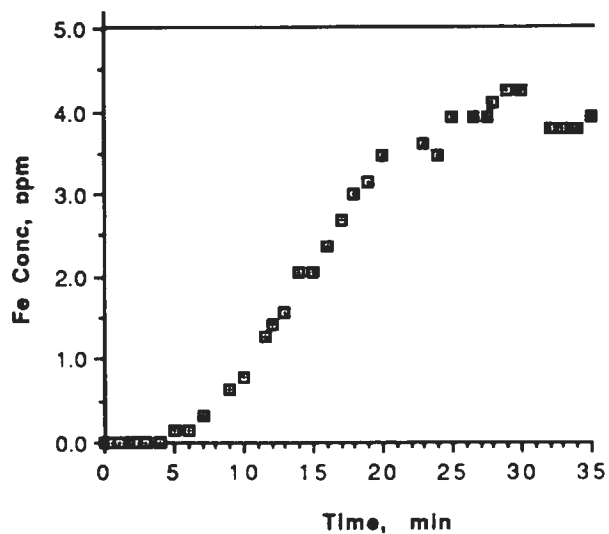


Figure 2-3. Dissolution of coarse (-28 +200 mesh) pyrite by sparging chlorine gas. The line at 5.0 ppm represents the maximum iron concentration calculated by multiplying the initial weight of pyrite by the ICP value of total Fe present.

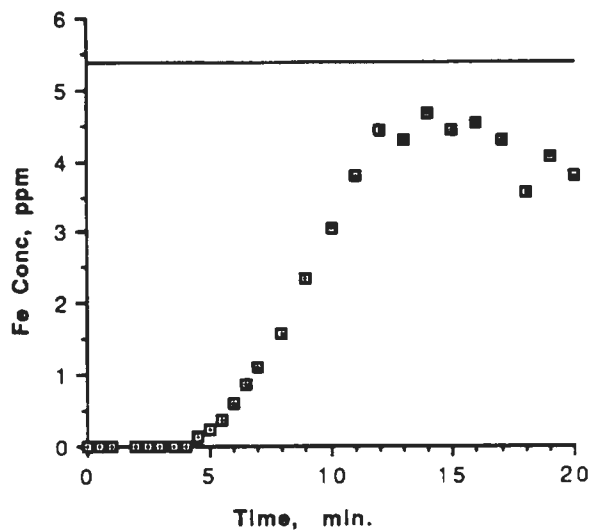


Figure 2-4. Fine (-200 mesh) pyrite dissolution with chlorine gas. The line at 5.3 ppm represents the maximum iron concentration calculated by multiplying the initial weight of pyrite by the ICP value of total Fe present.

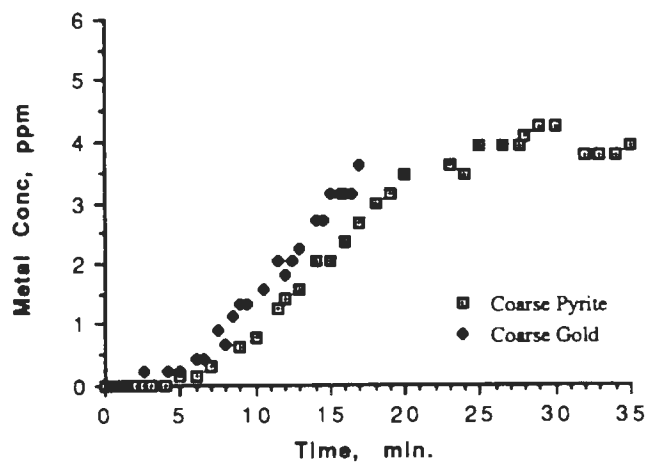


Figure 2-5. Comparison of the dissolution of coarse Au to coarse (-28 +200 mesh) pyrite by sparging chlorine gas.

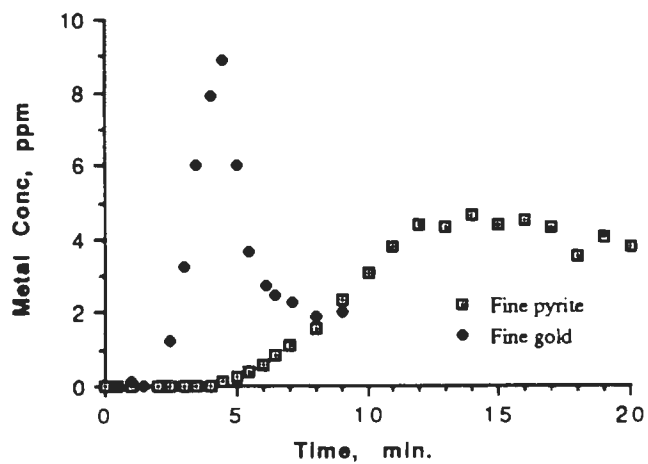


Figure 2-6. Comparison of fine particle Au and pyrite dissolution by chlorine sparging.

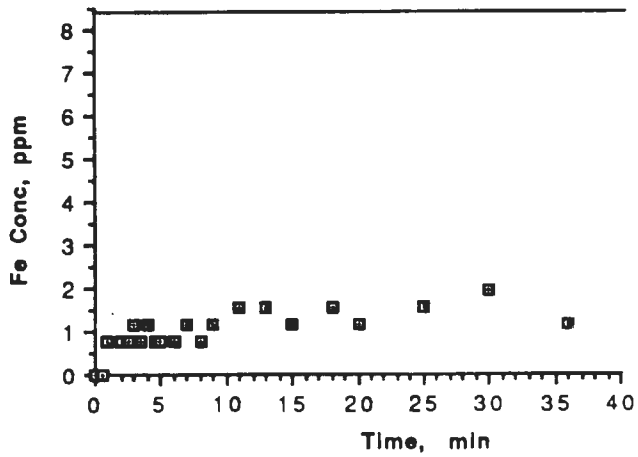


Figure 2-7. Coarse (-28 +200) pyrite dissolution by the permanganate acidification reaction. The line at 8.4 ppm represents the maximum iron concentration calculated by multiplying the initial weight of pyrite by the ICP value of total Fe present.

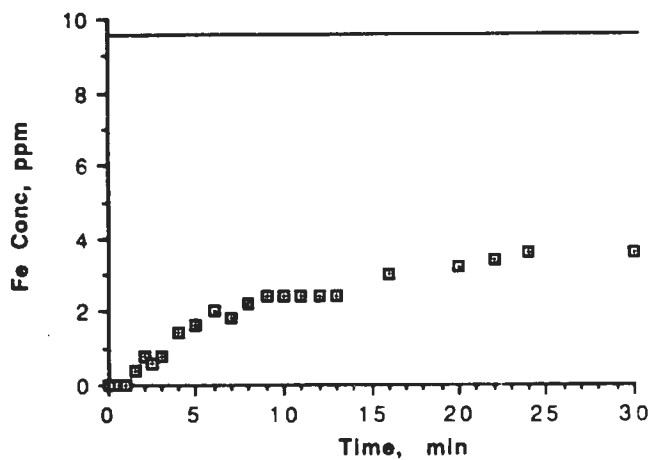


Figure 2-8. Fine particle (-200 mesh) pyrite dissolution by KMnO_4/HCl reaction. The line at 9.5 ppm represents the maximum iron concentration calculated by multiplying the initial weight of pyrite by the ICP value of total Fe present.

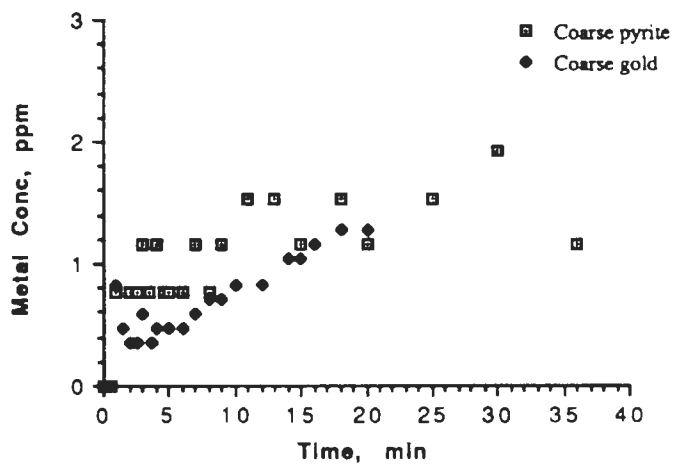


Figure 2-9. Comparison of the dissolutions of coarse particle Au and pyrite by the acidification of KMnO_4 .

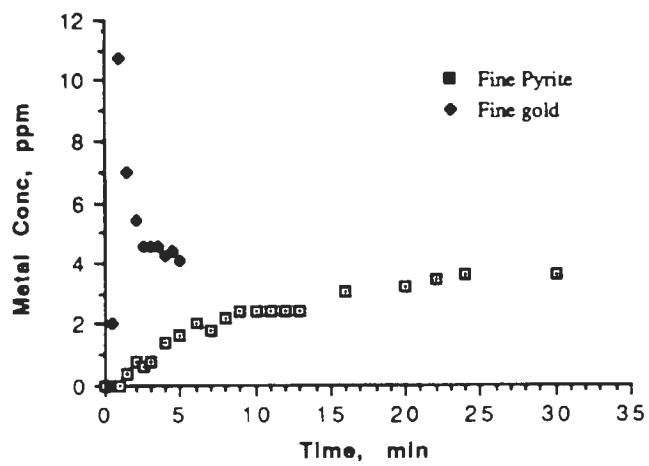


Figure 2-10. Comparison of the permanganate acidification reaction dissolution of fine particle Au and pyrite.

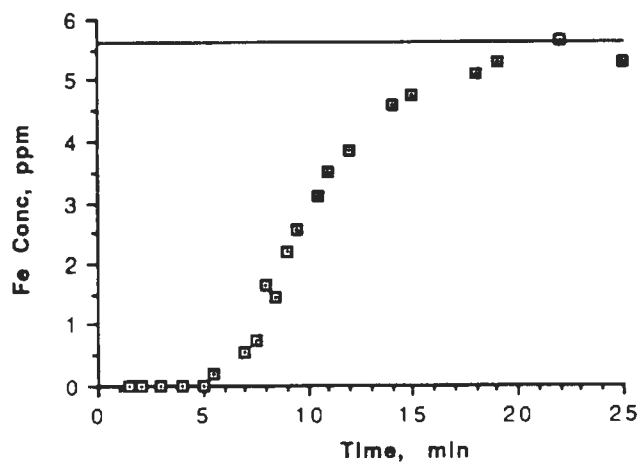


Figure 2-11. Sparged chlorine dissolution of coarse (-28 +200 mesh) pyrrhotite. The line at 5.6 ppm represents the maximum iron concentration calculated by multiplying the initial weight of pyrrhotite by the ICP value of total Fe present.

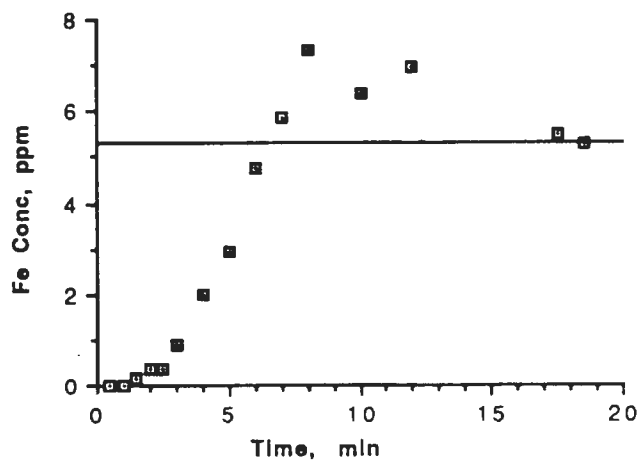


Figure 2-12. Sparged chlorine dissolution of fine (-200 mesh) pyrrhotite. The line at 5.6 ppm represents the maximum iron concentration calculated by multiplying the initial weight of pyrrhotite by the ICP value of total Fe present.

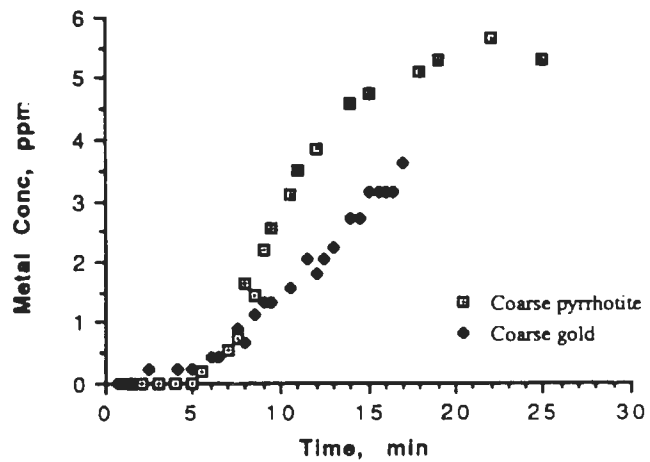


Figure 2-13. Coarse particle Au and pyrrhotite dissolution comparison for sparging chlorine gas.

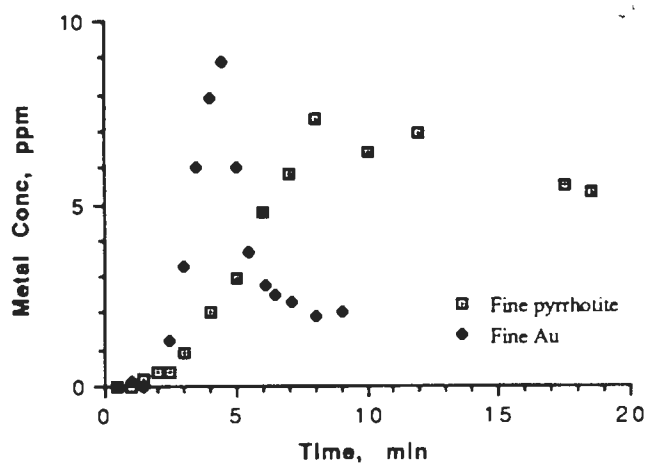


Figure 2-14. Comparison of the dissolution of fine particle Au and pyrrhotite by sparging chlorine gas.

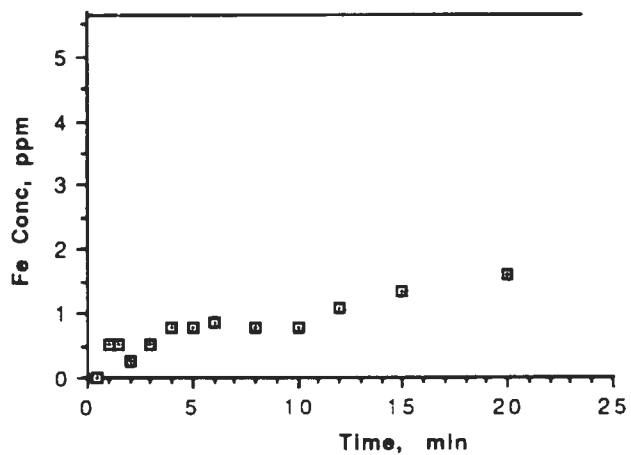


Figure 2-15. KMnO_4 acidification of coarse (-28 +200 mesh) pyrrhotite. The line at 5.6 ppm represents the maximum iron concentration calculated by multiplying the initial weight of pyrrhotite by the ICP value of total Fe present.

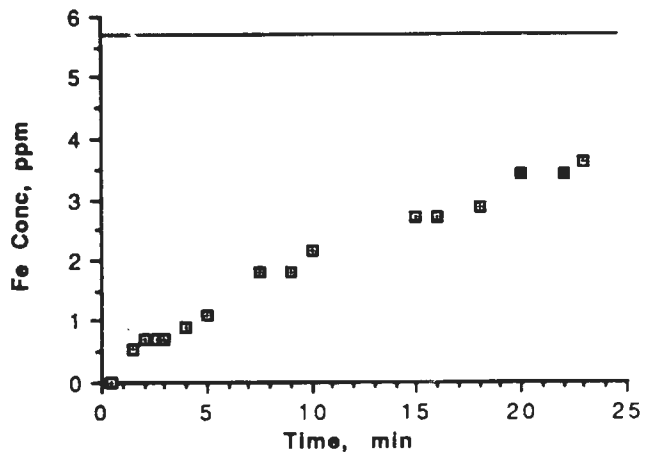


Figure 2-16. KMnO_4 acidification of fine (-200 mesh) pyrrhotite. The line at 5.7 ppm represents the maximum iron concentration calculated by multiplying the initial weight of pyrrhotite by the ICP value of total Fe present.

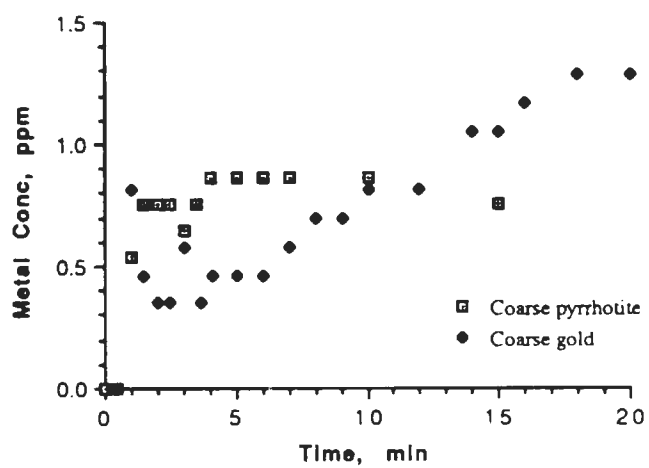


Figure 2-17. Comparison of the dissolution of coarse Au and pyrrhotite by the KMnO_4/HCl reaction.

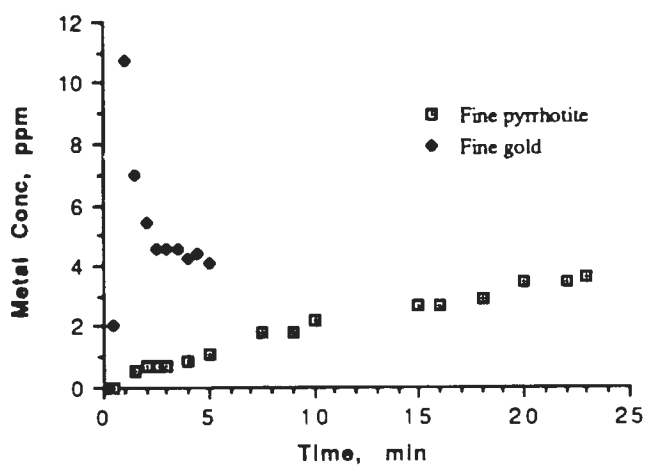


Figure 2-18. Comparison of the dissolution by KMnO_4/HCl of fine particle Au and pyrrhotite.

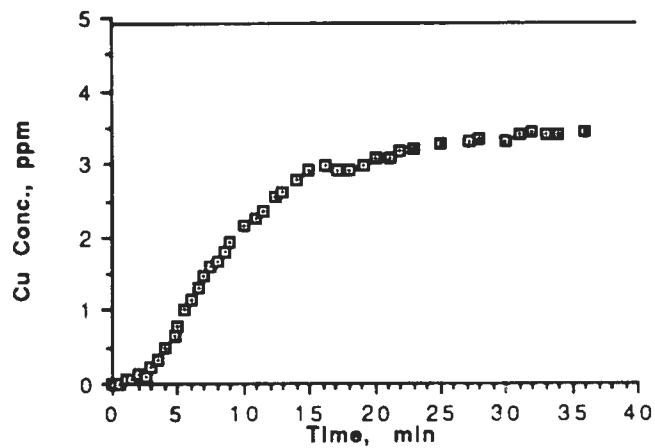


Figure 2-19. Coarse particle (-28 +200 mesh) chalcocite dissolution by gas sparging. The line at 4.9 ppm represents the maximum copper concentration calculated by multiplying the initial weight of chalcocite by the ICP value of total Cu present.

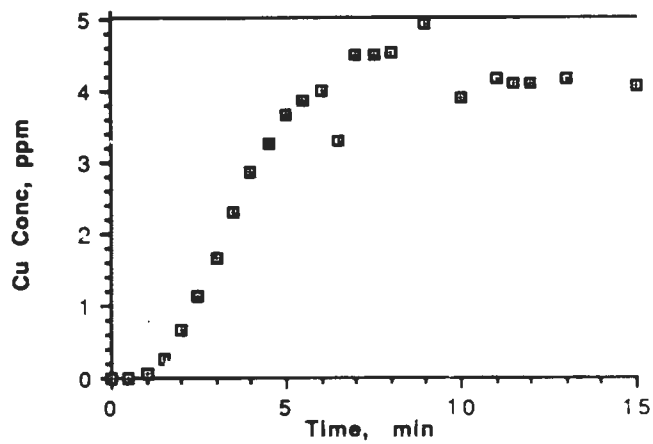


Figure 2-20. Fine particle (-200 mesh) chalcocite dissolution by gas sparging. The line at 5.0 ppm represents the maximum copper concentration calculated by multiplying the initial weight of chalcocite by the ICP value of total Cu present.

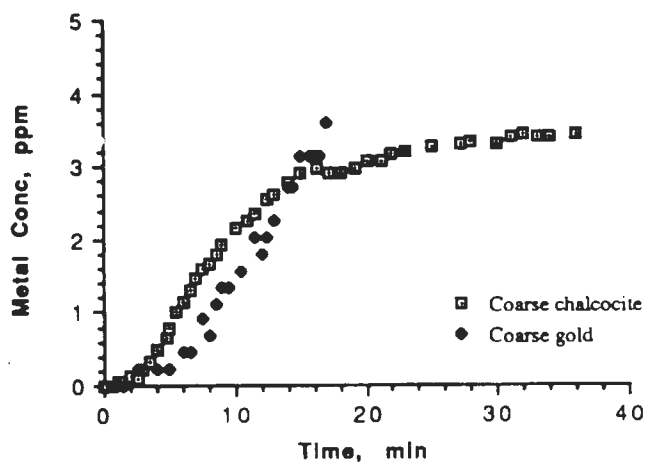


Figure 2-21. Comparison of the dissolution by sparging Cl_2 on coarse particles of Au and chalcocite.

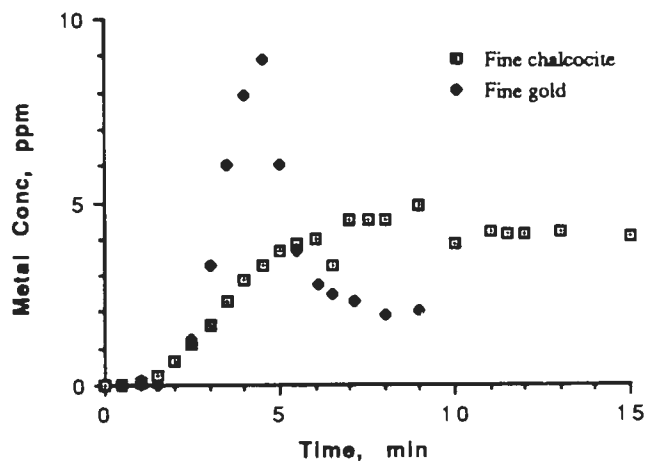


Figure 2-22. Comparison of fine particle Au and chalcocite dissolution by sparging.

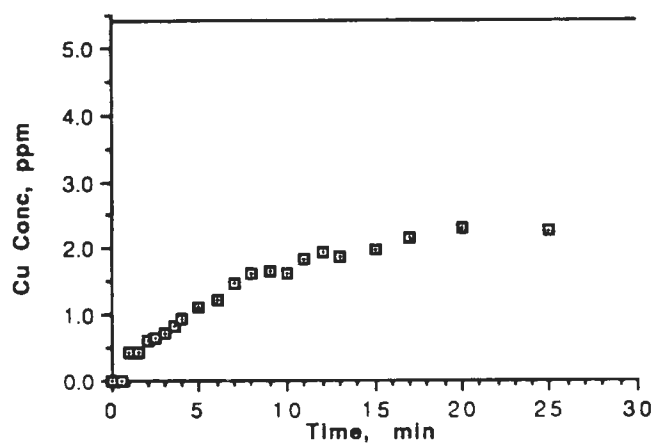


Figure 2-23. KMnO_4/HCl reaction dissolution of coarse (-28 +200 mesh) chalcocite. The line at 5.4 ppm represents the maximum copper concentration calculated by multiplying the initial weight of chalcocite by the ICP value of total Cu present.

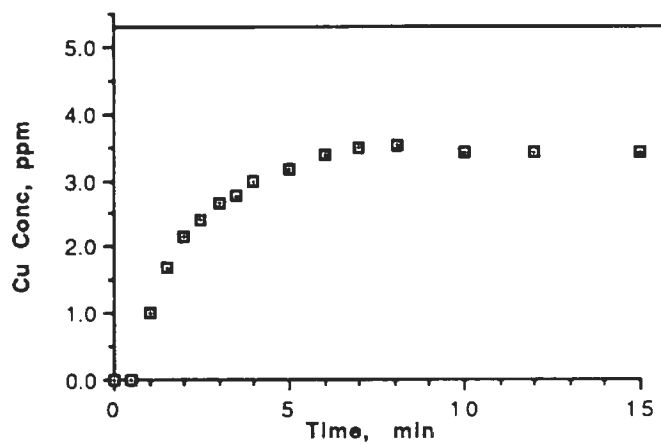


Figure 2-24. KMnO_4/HCl reaction dissolution of fine (-200 mesh) chalcocite. The line at 5.3 ppm represents the maximum copper concentration calculated by multiplying the initial weight of chalcocite by the ICP value of total Cu present.

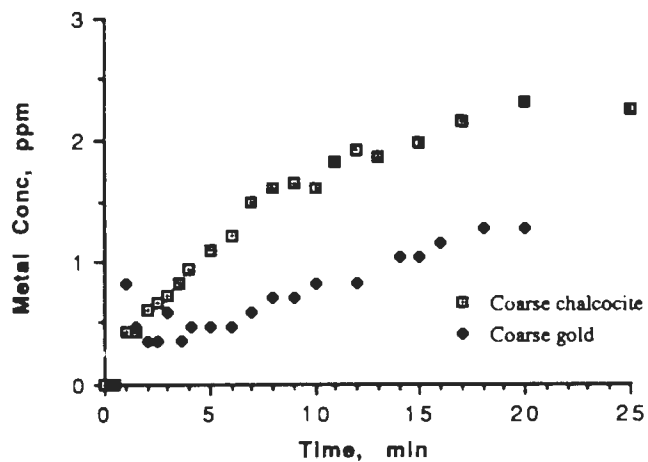


Figure 2-25. Coarse particle dissolution comparison for Au and chalcocite in the acidification of potassium permanganate.

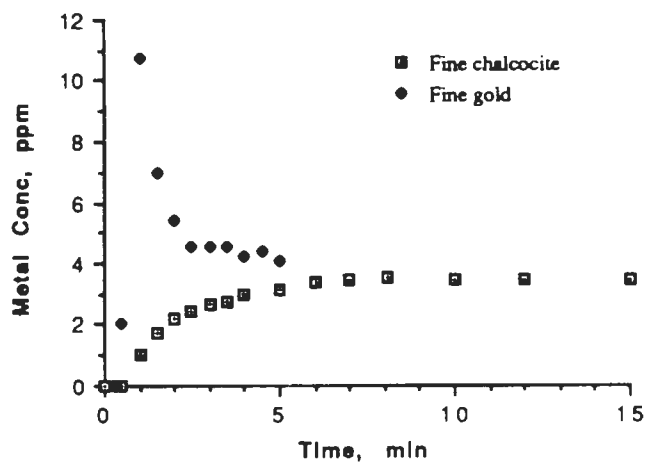


Figure 2-26. Fine particle Au and chalcocite dissolution comparison by the KMnO_4/HCl reaction.

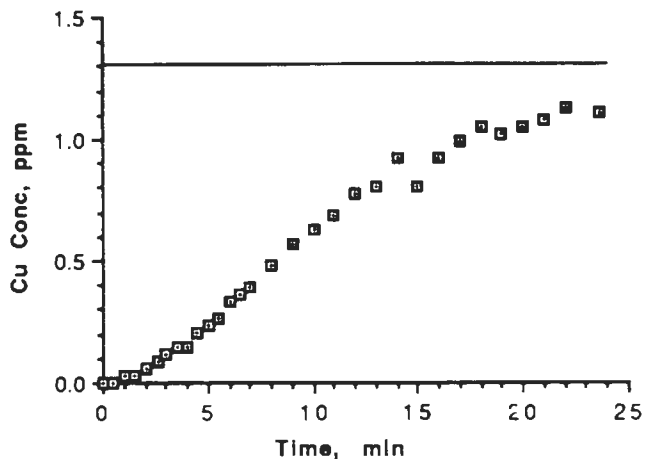


Figure 2-27. Results of the dissolution of coarse (-28 +200 mesh) chalcopyrite by Cl_2 sparging. The line at 1.3 ppm represents the maximum copper concentration calculated by multiplying the initial weight of chalcopyrite by the ICP value of total Cu present.

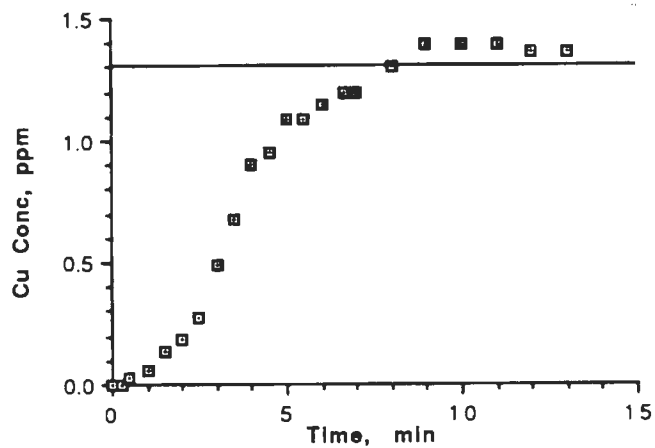


Figure 2-28. Results of the dissolution of fine (-200 mesh) chalcopyrite by Cl_2 sparging. The line at 1.3 ppm represents the maximum copper concentration calculated by multiplying the initial weight of chalcopyrite by the ICP value of total Cu present.

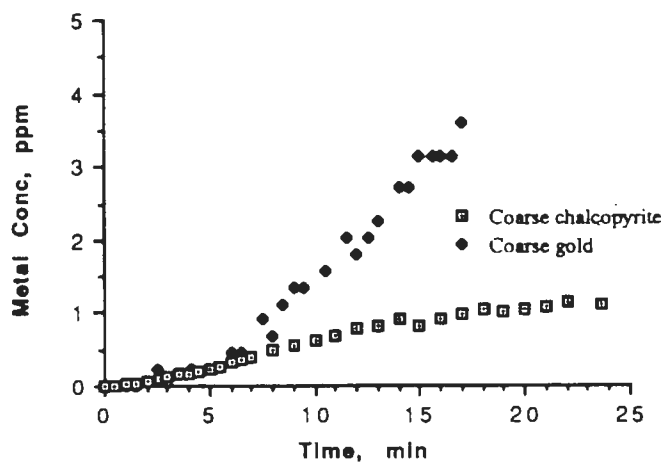


Figure 2-29. Coarse Au and chalcopyrite dissolution comparison by sparging Cl_2 gas.

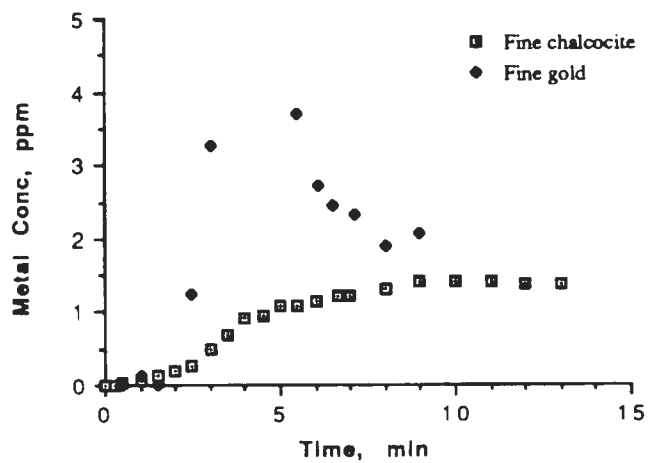


Figure 2-30. Comparison of the dissolution by sparging of fine particle Au and chalcopyrite.

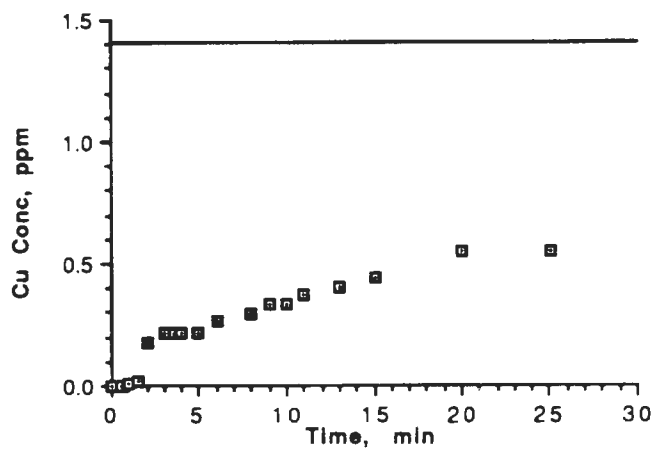


Figure 2-31. Permanganate dissolution of coarse (-28 +200 mesh) chalcopyrite. The line at 1.4 ppm represents the maximum copper concentration calculated by multiplying the initial weight of chalcopyrite by the ICP value of total Cu present.

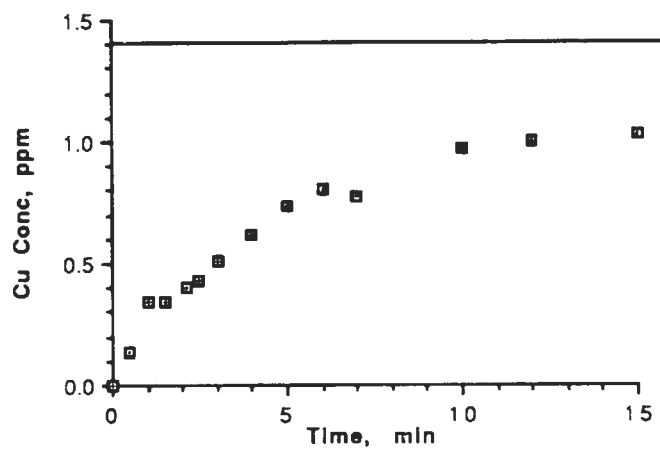


Figure 2-32. Permanganate dissolution of fine (-200 mesh) chalcopyrite. The line at 1.4 ppm represents the maximum copper concentration calculated by multiplying the initial weight of chalcopyrite by the ICP value of total Cu present.

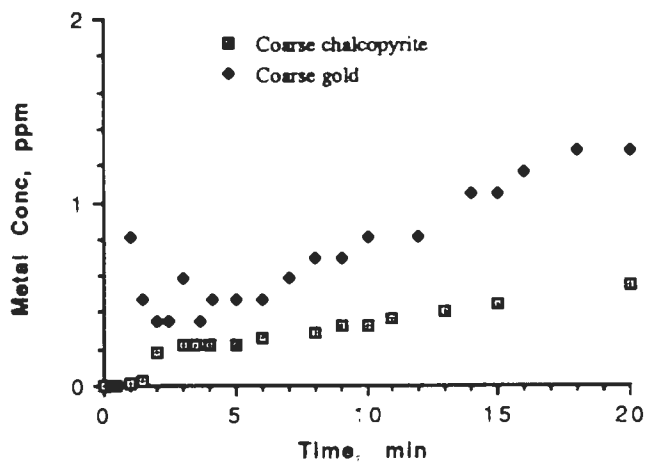


Figure 2-33. Comparison of the dissolution of coarse particle Au and chalcopyrite by the KMnO_4/HCl reaction.

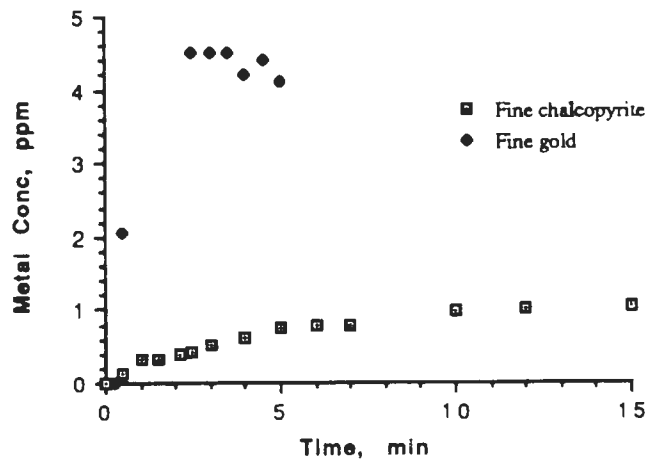


Figure 2-34. Comparison of the dissolution of fine chalcopyrite and Au by the permanganate method.

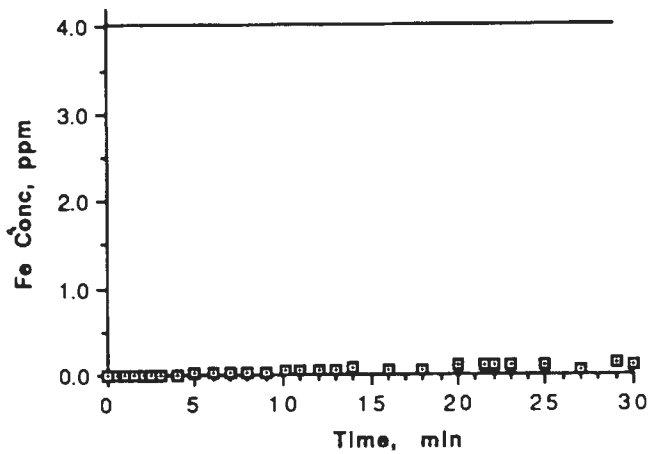


Figure 2-35. Dissolution of coarse particle (-28 +200 mesh) arsenopyrite by sparging chlorine gas. The line at 4.0 ppm represents the maximum iron concentration calculated by multiplying the initial weight of arsenopyrite by the ICP value of total Fe present.

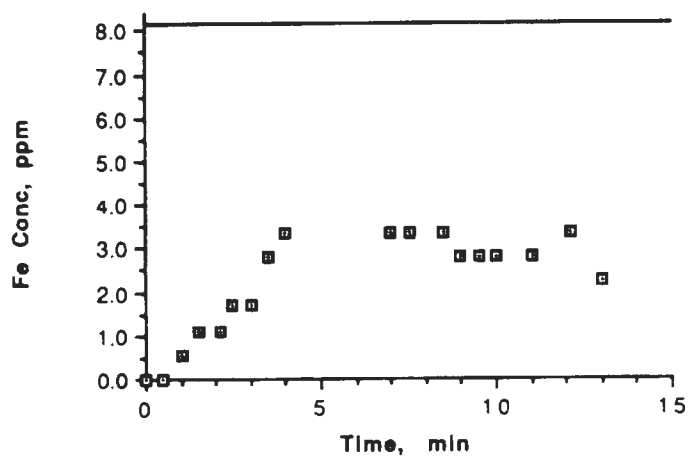


Figure 2-36. Dissolution of fine particle (-200 mesh) arsenopyrite by sparging chlorine gas. The line at 8.1 ppm represents the maximum iron concentration calculated by multiplying the initial weight of arsenopyrite by the ICP value of total Fe present.

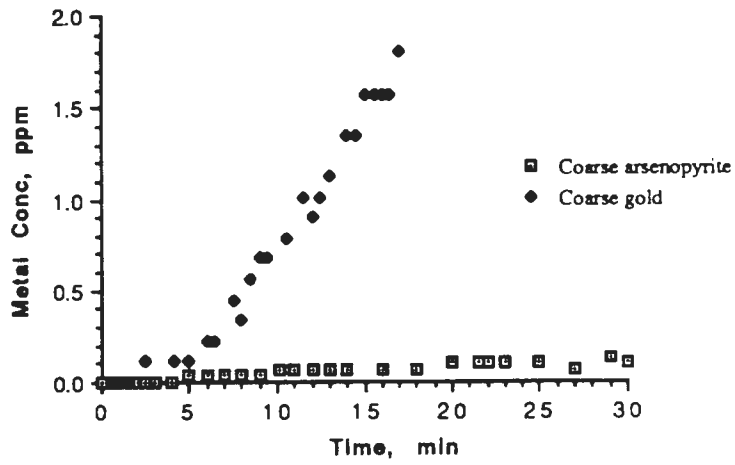


Figure 2-37. Comparison of coarse particle dissolution of Au and arsenopyrite by Cl_2 gas.

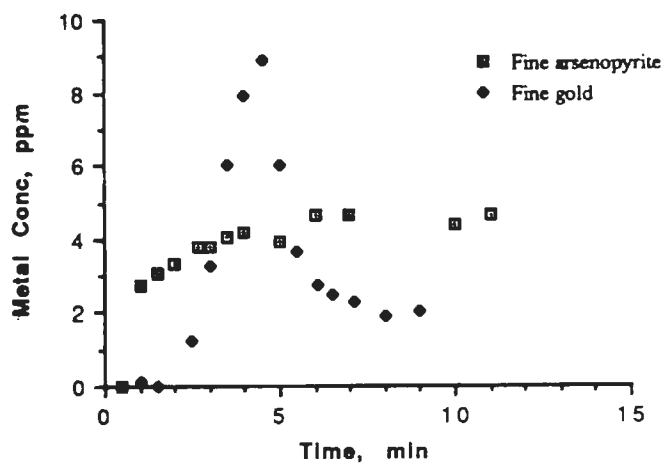


Figure 2-38. Fine particle dissolution comparison for Au and arsenopyrite by gas sparging.

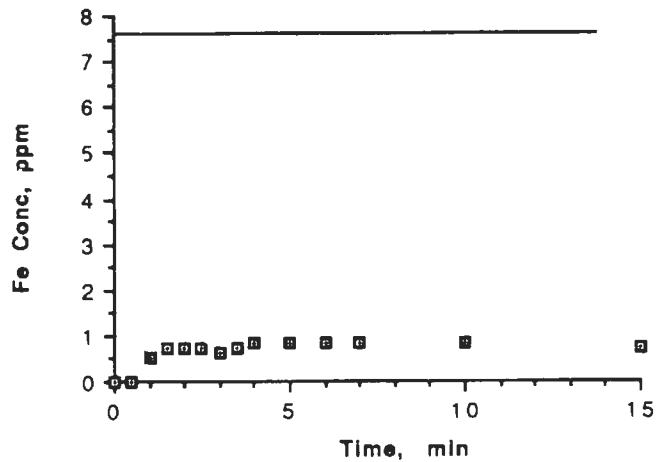


Figure 2-39. Dissolution of coarse particle (-28 +200 mesh) arsenopyrite by acidifying KMnO_4 . The line at 7.6 ppm represents the maximum iron concentration calculated by multiplying the initial weight of arsenopyrite by the ICP value of total Fe present.

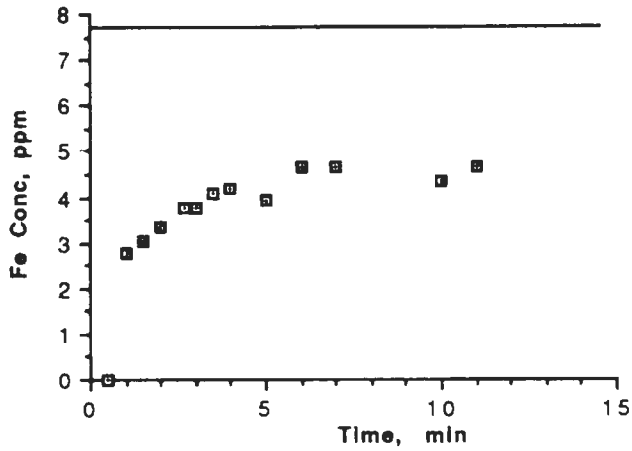


Figure 2-40. Dissolution of fine particle (-200 mesh) arsenopyrite by acidifying KMnO_4 . The line at 7.7 ppm represents the maximum iron concentration calculated by multiplying the initial weight of arsenopyrite by the ICP value of total Fe present.

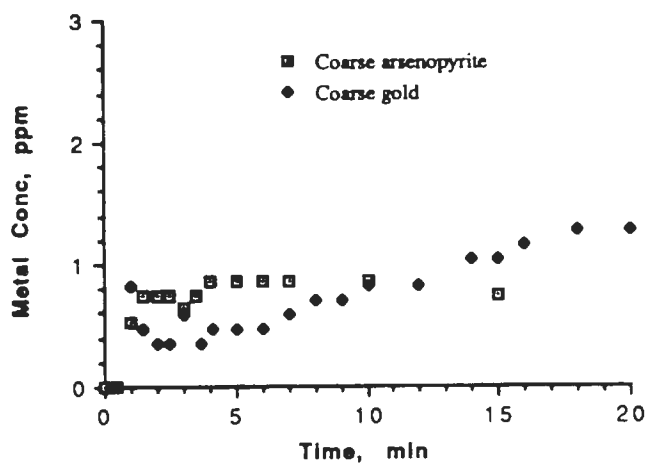


Figure 2-41. Comparison of the dissolution of coarse particle Au and arsenopyrite by chlorine formed chemically by the reaction of KMnO_4 with HCl .

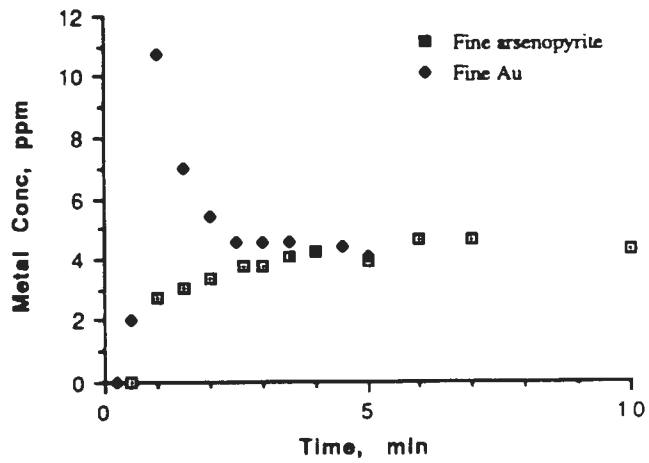


Figure 2-42. Dissolution comparison for fine Au and arsenopyrite for the permanganate method of adding chlorine.

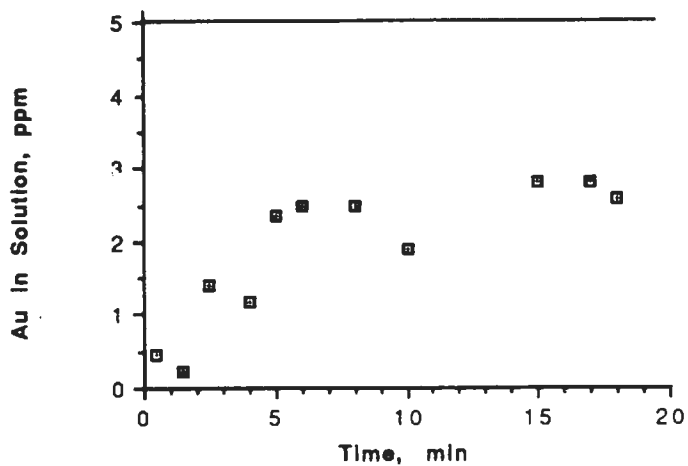


Figure 2-43. Results of the dissolution of Au during the sparging of chlorine in a slurry of pyrite, chalcocite, Au with carbon in a vial apparatus. The line at 5.0 ppm represents the calculated maximum Au concentration if 100% dissolution of the initial Au added is assumed.

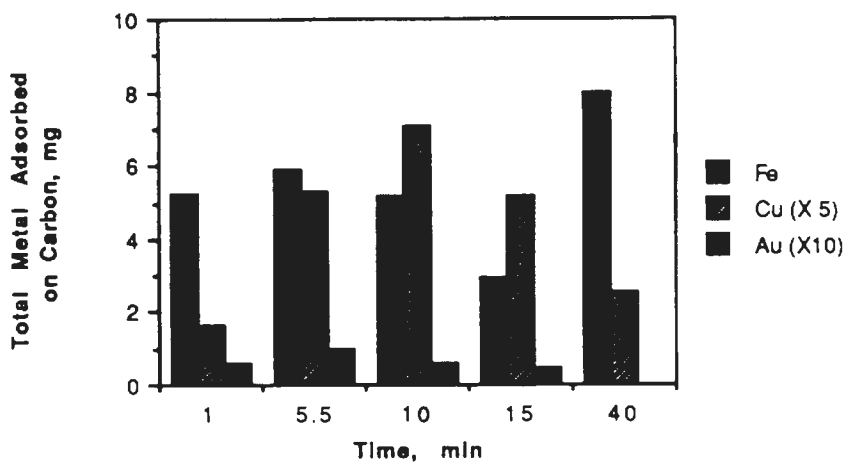


Figure 2-44. Results of the experiment in which equal amounts of carbon (~2.7g) were removed at intervals to show the adsorption character of Fe, Cu and Au as a function of time. (The actual amounts of Cu were 1/5 those graphed; the concentration of Au was actually 1/10 of the values shown.)

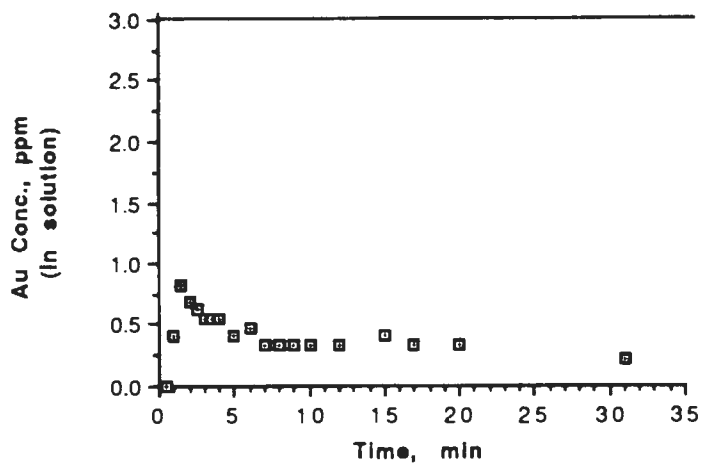


Figure 2-45. Au adsorption on carbon with no pretreatment. Three mL of the 1000 ppm gold standard was added at time 0. This concentration is represented by the line.

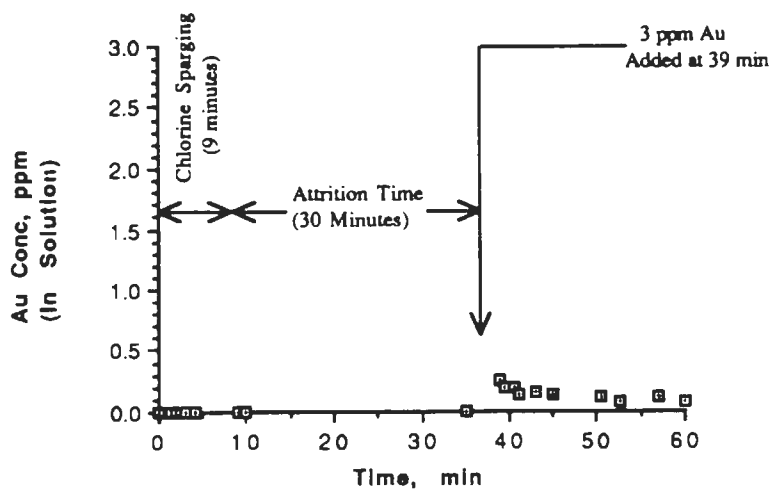


Figure 2-46. Au adsorption on carbon pretreated with sparged Cl_2 . Three mL of the 1000 ppm gold standard was added at time = 39 minutes. The maximum concentration of Au possible is represented by the the right arrow and line.

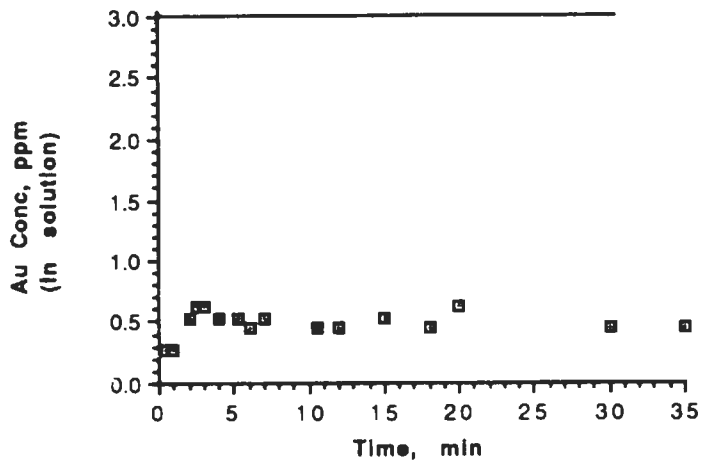


Figure 2-47. Effect of 1.8 g/L Fe^{+3} ($\text{FeCl}_3 \cdot 6\text{H}_2\text{O}$) pretreatment of carbon in hindering the adsorption of dissolved Au. Three mL of the 1000 ppm gold standard was added at time 0. This concentration is represented by the line.

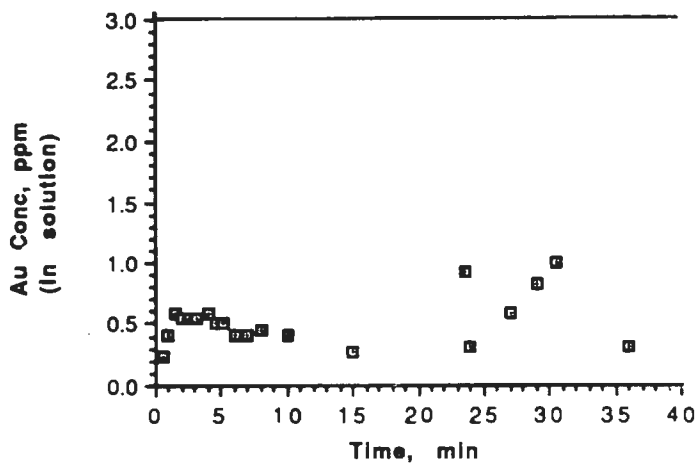


Figure 2-48. Effect of 1.8 g/L Fe^{+3} ($\text{Fe}(\text{NO}_3)_3 \cdot 9\text{H}_2\text{O}$) pretreatment of carbon in hindering the adsorption of dissolved Au. Three mL of the 1000 ppm gold standard was added at time 0. This concentration is represented by the line.

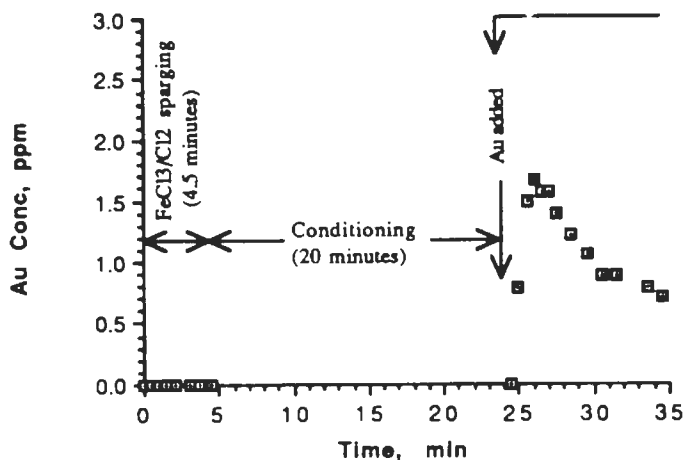


Figure 2-49. Effect of 1.8 g/L Fe^{+3} ($\text{FeCl}_3 \cdot 6\text{H}_2\text{O}$) and chlorine sparging pretreatment of carbon in hindering the adsorption of dissolved Au. Three mL of the 1000 ppm gold standard was added at time after 24 minutes. The maximum concentration for this portion of the experiment is represented by the line at 3 ppm.

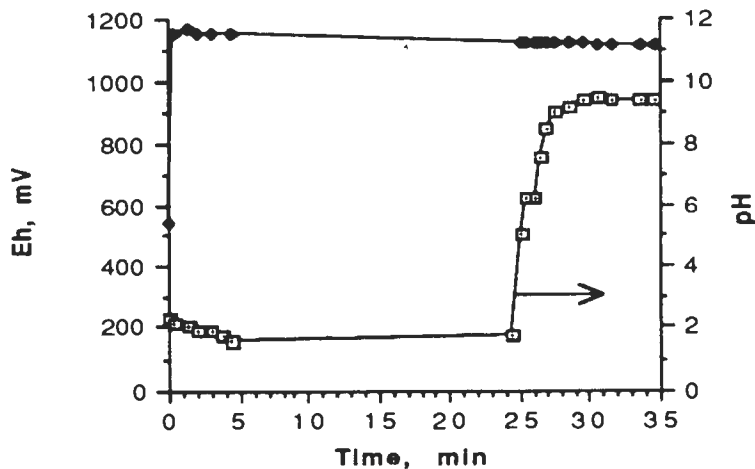


Figure 2-50. The pH and Eh of the experiment using a ferric chloride and Cl_2 pretreatment of carbon prior to Au addition. Chlorine sparging with the ferric chloride was performed for the first 4.5 minutes followed by 20 minutes of conditioning, then three ppm Au was added at 24.5 minutes.

IV. Discussion

Mineral Studies

The results of this research can be investigated by two avenues--the rate of dissolution (initial slope of the dissolution curves) and the time prior to detection of the metal. Figure 2-51 is provided as a qualitative comparison of all the coarse sulfide mineral dissolutions by chlorine sparging. Figure 2-52 is the same comparison of the fine particle mineral dissolution by Cl_2 sparging. Figures 2-53 and 2-54 are the same comparisons for coarse and fine particle mineral dissolution by the permanganate method of introducing chlorine. These comparisons show that chalcocite is consistently one of the faster minerals to dissolve, while pyrite and chalcopyrite are usually the slowest based on the initial slope of the respective dissolution curves, and the time required after initiation of the experiment before the dissolved metal is observed.

The dissolution of coarse particle arsenopyrite by chlorine sparging was considerably slower than all other minerals in both methods of chlorine addition. Although Jackson and Strickland²² observed a decrease in the dissolution rate constant for coarse particle arsenopyrite, the observed dissolution in this study is orders of magnitude smaller. This result does not follow with the other results and was considered a result of the nonhomogeneous nature of the samples used.

Introduction of chlorine by the permanganate reaction with HCl had similar results for the mineral dissolution as in the gold dissolution experiments. Coarse particles are dissolved faster initially, but are not

completely dissolved. Likewise, fine particles are dissolved faster and more completely as compared to gas sparging.

The time before metal is first detected increases in the order arsenopyrite, chalcocite, pyrrhotite, chalcopyrite followed by pyrite. This order agrees with the findings of Jackson and Strickland²². The differences in the dissolution rates of the copper bearing minerals, chalcocite and chalcopyrite, was expected. From the mineral structures, the Cu-S bond would be considerably weaker than the Cu-Fe bonds giving credibility to the observation of Cu_2S dissolving faster than CuFeS_2 .

To explain why the pyrrhotite was observed to dissolve faster than pyrite, a look at the crystal structure of the two minerals is necessary. Pyrite is primarily a cubic structured mineral; pyrrhotite is most commonly a tabular mineral. These structures behave differently in dissolution. In a tabular structure, combinations of ionic and covalent bonds can occur within the plane, but weak van der Waal forces hold the planes together. However, the cubic structure is more rigidly held together by ionic, covalent, and even metallic bonds. Jackson and Strickland²² and Woodcock²³ reported that pyrite dissolution is limited to specific sites on the mineral. Most likely these sites are lattice dislocations or substitutions on the surface. Pyrrhotite dissolved uniformly across the surface. This observation would indicate the effect of crystal structure on the disparity in the rates of dissolution of pyrrhotite and pyrite.

Arsenopyrite is a rather peculiar mineral. Mineralogy texts describe it as a combination of $\text{FeS}_2\cdot\text{FeAs}_2$ and FeAsS crystals. Jackson and

Strickland²² observed in their dissolution experiments with chlorine that although little chlorine is consumed the mineral dissolved rapidly in the initial stages of the experiment. They speculated that the mineral surface was partially oxidized prior to testing. But pyrrhotite will oxidize in air fairly rapidly, also, yet the same dissolution observation was not observed. It follows that the Fe-As bond must be easier to break than the Fe-S bond when As is a lattice substitute in pyrite. Arsenopyrite would then dissolve faster than pyrrhotite, as was observed.

In general, the comparisons of the mineral dissolutions to the Au dissolutions, chalcocite and arsenopyrite will dissolve faster than Au. Chalcopyrite and pyrrhotite dissolve at about the same rate. As in cyanidation, copper minerals and arsenopyrite are a detriment in the recovery of gold by chlorination. Interestingly, the pyrite is apparently less refractory toward chlorination than toward cyanidation.

Typically, iron and copper are the most prevalent metals found in ores, but arsenic, lead, antimony and many others are present in quantities orders of magnitude higher than the 0.5-1.0 oz of gold per ton of ore. One would expect a wide range of metal species to be present in large concentrations in the solution during flash chlorination. The results of this research lends credence to the premise that metal ions may already start adsorbing on the surface of the carbon as the gold is just dissolving. One can look at the hindrance of gold adsorption by the adsorption of other metals as a sort of race. The first ones in solution would be the first to adsorb. Chalcocite and arsenopyrite have demonstrated that copper and

iron are in solution before gold under the same conditions of chlorination. This observation was noted for other minerals in coarser particle sizes.

In viewing the results of this study, one should keep in mind that the tests were conducted with an attempt to have nearly the same final concentration of each metal at the end of each experiment so that comparisons of the dissolutions could be made. But in actual ores, the iron and copper are often present in amounts nearly 4000 times greater than gold.

Carbon Studies

(a) Pyrite, Chalcocite and Au with Carbon.

In the experiment in which all the carbon remained in the vessel until the end, the results showed that iron and copper adsorb on the carbon in much larger amounts than the Au. But this fact is easily understood if one considers the relative amounts of pyrite and chalcocite present at the onset of chlorination.

In the experiment in which portions of the carbon were removed, the results show that the gold begins to adsorb within the first 5 to 6 minutes of the dissolution, but is apparently replaced by the iron and copper as the dissolution of the pyrite and chalcocite proceeds. Some of the earlier discussion⁷⁷⁻⁷⁸ of the adsorption of gold on carbon had suggested that only Au(III) reduces on the carbon. This theory of adsorption is questioned by these results. Recall from Chapter One that the Au(I) concentration was highest in the 5-7 minute range of dissolution. Figure 2-55 shows the Au

adsorption results from Table VI plotted with an earlier Au dissolution experiment (Figure 1-16). This graph shows that the highest level of Au adsorption on carbon correlates to the anomalous peak of the dissolution experiment. The anomalous peak corresponds to the highest concentration of AuCl_2^- . This would indicate that Au(I) will adsorb early in the dissolution, and be replaced later by the more prevalent metals--Cu and Fe.

The results of Gallagher⁷⁷ and Hiskey, et al.⁷⁸ have shown that when AuCl_4^- adsorbs on carbon it is reduced to Au° on the surface. In both sets of experiments, solutions containing various amounts of AuCl_4^- were prepared. Carbon was subjected to these solutions under various conditions and the reduction of AuCl_4^- to Au° was concluded. However, neither study considered the dynamic change of gold valence states during dissolution by chlorine. The results of this study show that Au(I) adsorbs readily on the carbon. Based on the fact that Au(I) reduces to Au° with relative ease, it can be concluded that Au(I) will be reduced on the surface of the carbon as well. As the ferric chloride concentration increases, and more iron is adsorbed, the gold is redissolved. In this case, the ferric chloride may play an important role in the dissolution of the adsorbed Au° , but the exact role will have to be left for further study, as these experiments were not equipped for such a task. Ferric chloride seems to affect the adsorption of copper in much the same way, except that copper chloride is probably not reduced on the surface of the carbon.

(b) Au with Carbon

Many conclusions could be drawn from the results of this adsorption study. First, the test in which sparging of chlorine was the only carbon pretreatment prior to addition of the dissolved Au complex, shows rather conclusively that chlorine alone will not hinder the adsorption of Au on the carbon. By the same token, carbon pretreated by ferric chloride or ferric nitrate will not decrease Au adsorption. Only with a combined ferric chloride and chlorine pretreatments did any discernable reduction in gold adsorption occur. In the initial stages of this experiment, the Au concentration in solution remained fairly high (see Figure 2-49). The conditions in the vessel at this time were high Eh (~1.12 V) and low pH (< 9). The amount and source of ferric ion seemed not to matter, but the relatively high Eh and low pH were key to hindering the adsorbance of gold.

The last conclusion drawn from this study is that the most predominant metal species present--iron--is the most likely reason for the success of the flash chlorination process. As the chlorination proceeds, the levels of ferric ion increase, and replace the adsorbed Au on the surface of the carbon. Pretreating the ore with ferric chloride prior to chlorination should greatly improve the process by providing ferric ion for adsorption earlier than is seen by the dissolution of the minerals pyrite, pyrrhotite, chalcopyrite or any other iron containing sulfide. An increase in the dissolved Au concentration would be expected.

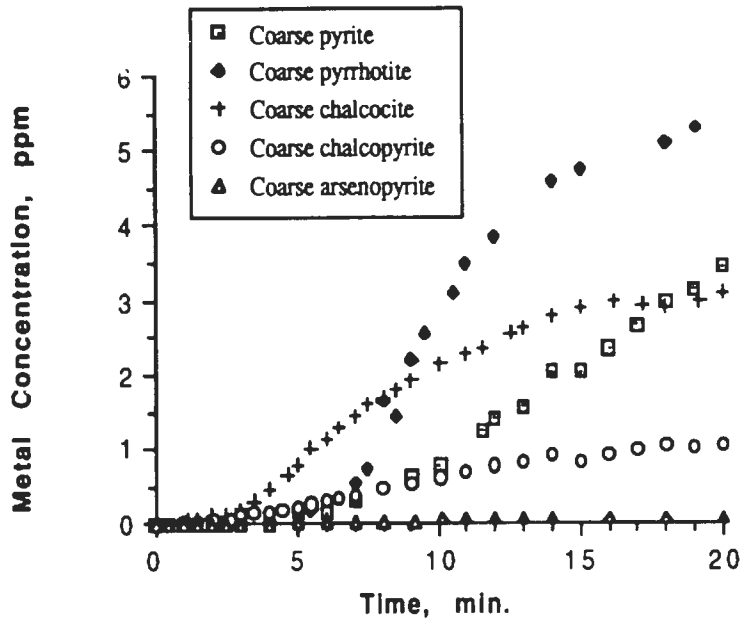


Figure 2-51. Comparison of the dissolution curves of the coarse (-28 +200 mesh) minerals by sparging chlorine.

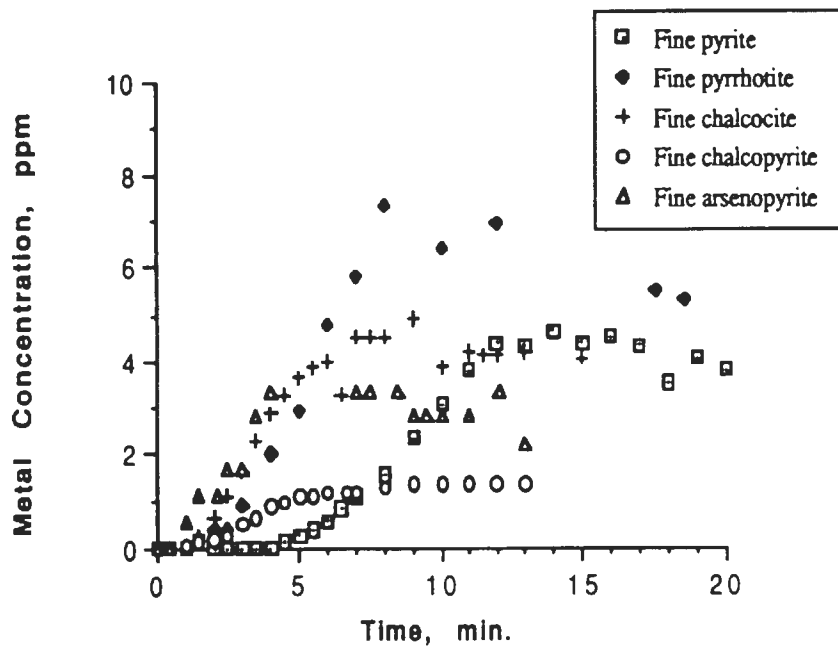


Figure 2-52. Comparison of the dissolution of fine (-200 mesh) sulfide minerals by sparged chlorine.

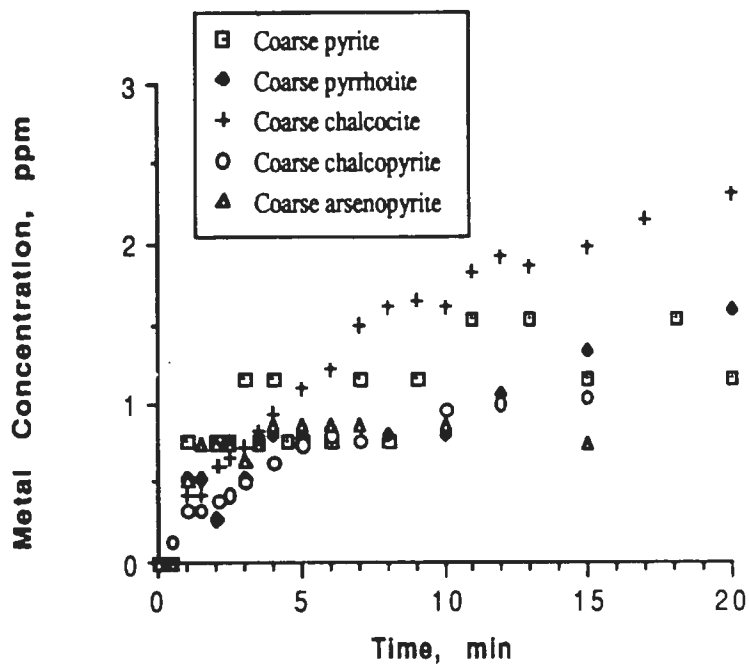


Figure 2-53. Comparison of the dissolution of coarse (-28 +200 mesh) minerals by chlorine produced *in situ* by the KMnO_4/HCl reaction.

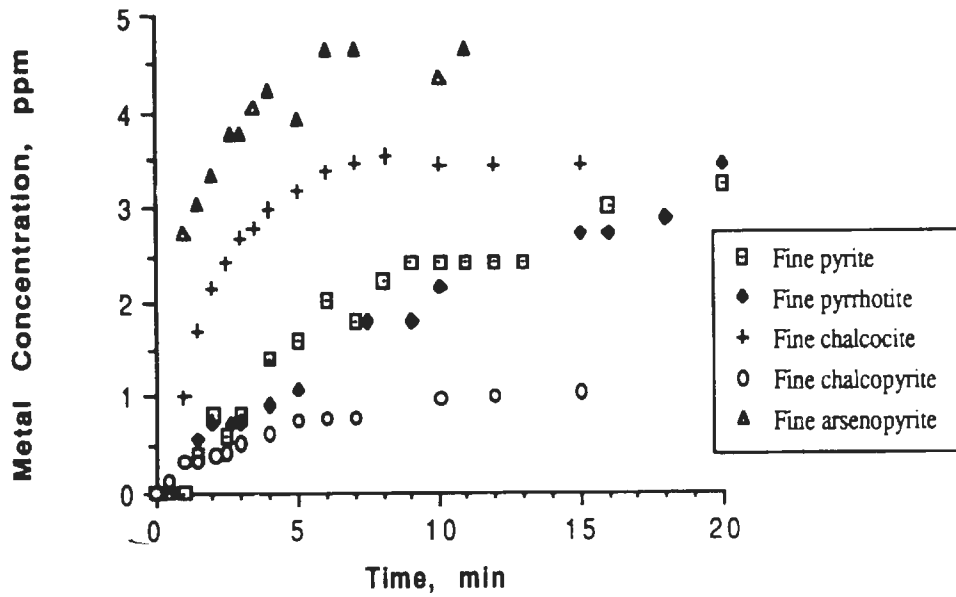


Figure 2-54. Comparison of the dissolution of fine (-200 mesh) sulfide minerals by chlorine produced *in situ* by the KMnO_4/HCl reaction.

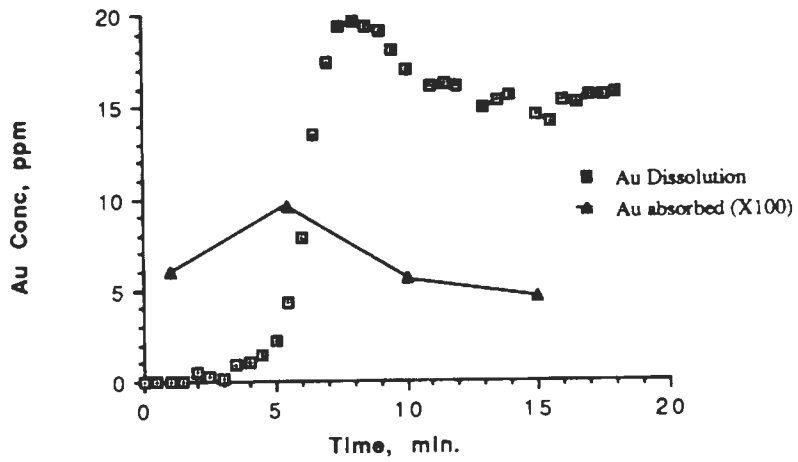


Figure 2-55. Comparison of the dissolution of Au^0 by sparging and the adsorption of Au on carbon during sparging.

V. Conclusions

The conclusions drawn from the mineral and carbon studies are as follows:

- 1) In general, the time required for sulfide minerals to put metal species into solution during chlorination increases in the following order:
arsenopyrite, chalcocite, pyrrhotite, chalcopyrite, pyrite. This holds for both dissolution by chlorine sparging and chemical formation of Cl_2 by the reaction of KMnO_4 with HCl .
- 2) The individual rates of dissolution decrease with an increase in particle size of the minerals.
- 3) Fine particle arsenopyrite will dissolve faster than fine Au when chlorine is introduced by sparging. Chalcocite, pyrrhotite and chalcopyrite will dissolve at about the same rate as Au for both methods of adding Cl_2 . Pyrite dissolves much faster than Au.
- 4) AuCl_2^- and AuCl_4^- rapidly adsorb by reducing to Au^0 on the surface of activated carbon.
- 5) Pyrite and chalcocite present during chlorination of carbonaceous ores will reduce the Au adsorption on the carbon. The Fe^{+3} and Cu^{+2} chloride species will replace adsorbed Au on the surface of the carbon.
- 6) A high oxidation potential and low pH are necessary for Fe^{+3} to replace Au on activated carbon. If chlorine is the lixiviant used for Au recovery, pretreatment of the ore with ferric chloride will reduce the amount of adsorption of Au as long as the conditions of high Eh and low pH are maintained.

Chapter Three

The Effect of Multivalent Chloride Salts in the Chlorination of Gold Ores

I. Introduction

Chloride Salts

Peters⁸⁰ noted that chloride salts in high concentrations enhanced the activity of HCl. He also predicted that multivalent salts would be more effective than the monovalent salts. Amadiantehrani⁸¹ also showed that the dissolution of galena by ferric chloride was enhanced by the addition of multivalent salts.

In a study reported in 1944, Putnam¹⁹ showed that the rate of dissolution of gold leaf increased with increasing chloride ion concentration. However, increased concentrations of other ions (such as NO_3^- and SO_4^{-2}) had no effect. From this work, Figure 3-1 was generated to show what effect increased ionic strength by chloride salt addition has on gold dissolution by chlorine. An interesting mathematical relationship exists for several chlorine concentrations. The study concluded by merely generalizing that chloride salt addition increases the dissolution rate. But more specifics can be gained from the data presented in Figure 3-1.

The effect of an increase in the activity of chloride ion (a_{Cl^-}) is easily shown thermodynamically. For the sake of comparison, both $\text{Au}^\circ \rightarrow \text{Au(I)}$ and $\text{Au}^\circ \rightarrow \text{Au(III)}$ will be considered.

Equation (3-1) is the mass and charge balanced equation for the $\text{Au}^\circ \rightarrow \text{Au(I)}$ chloride mechanism.

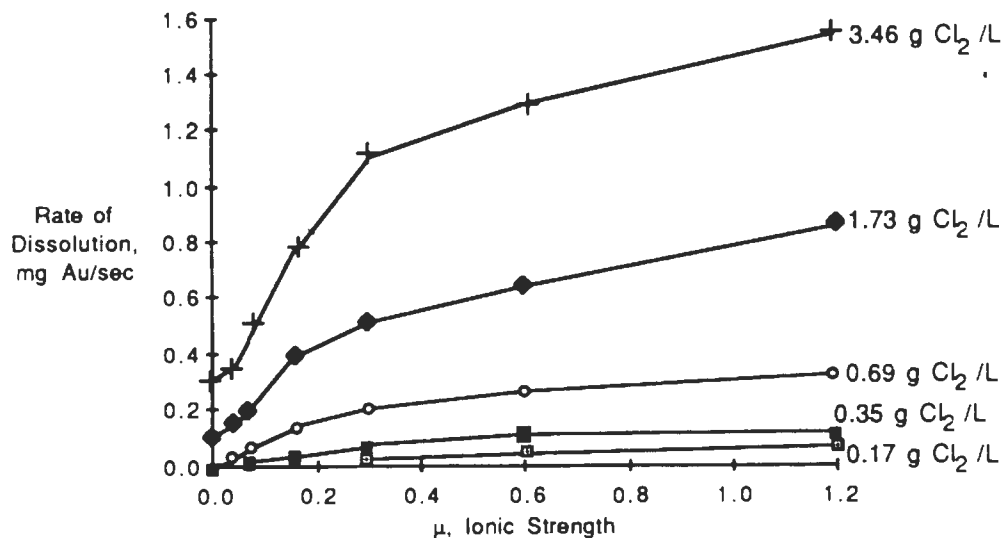


Figure 3-1. Effect of various ionic strengths of the solution of chloride ion on the rate of dissolution of gold for various chlorine concentrations. The data were calculated from the results of Putnam.¹⁹



In electrochemical notation, for a $2e^{-}$ transfer, this can be written by equation (3-2):

$$E = E^{\circ} - 0.0295 \log \left(\frac{[\text{AuCl}_2^{-}]^2}{[\text{Cl}^{-}]^2[\text{Cl}_2]} \right) \quad (3-2)$$

Likewise, equations (3-3) and (3-4) can be written for an $\text{Au}^{\circ} \rightarrow \text{Au(III)}$ mechanism:



$$E = E^{\circ} - 0.0098 \log \left(\frac{[\text{AuCl}_4^{-}]}{[\text{Cl}^{-}]^2[\text{Cl}_2]} \right) \quad (3-4)$$

Analysis of equations (3-2) and (3-4) shows that for an increase in $[\text{Cl}^{-}]$ the log term in each equation becomes more positive and the overall E of the

reaction increases. Even though the overall solubility of $\text{Cl}_2(\text{g})$ in water decreases with increasing salt concentration,⁸² the net change in $[\text{Cl}_2(\text{aq})]$ is much smaller than the net increase in $[\text{Cl}^-]$, so the overall effect is that the denominator of the log term increases as $[\text{Cl}^-]$ increases. Since $\Delta F = -n\mathcal{F}E$, as E increases, ΔF decreases and the reaction becomes thermodynamically more favorable. Markus⁸³ describes a relation between the increased rate of electron-transfer to a net change in the kinetic rate. In general, since the probability of e^- -transfer is greater in solutions of high ionic strength, the result should be observed in an increased rate of transfer which relates to faster dissolution of Au^0 .

Chlorine Activity

Several methods exist for estimating the activity of chloride ions as a function of the ionic strength of the solution. The Extended Debye-Hückel equation⁸⁴ determines the activity coefficient (γ) for ions in solutions with an ionic strength greater than $10^{-2.3}$ M (0.005M). Also, Meisner and Tester⁸⁵⁻⁸⁶ have derived a family of graphs which may be used to estimate the γ_{\pm} for any ionic strength. Both methods will be used for comparison purposes.

(a) Extended Debye-Hückel

The Extended Debye-Hückel (EDH) Equation is as follows:

$$-\log(\gamma_i) = \frac{Az_i^2\sqrt{I}}{(1 + Ba\sqrt{I})} \quad (3-5)$$

where: A, B are constants based on the Temperature
 a = constant inherent to the ion i
 I = ionic strength of the solution = $[0.5\sum[C](z)^2]$
 [C] = the concentration of the species i
 z_i = ionic charge of i.

For Cl⁻ at 25°C,⁸⁴ A = 0.5085
 B = 0.3281
 a = 3.0
 z = -1.

So, equation (3-5) becomes:

$$-\log_{10}(\gamma_i) = \frac{0.5085\sqrt{I}}{(1 + 0.9843\sqrt{I})}$$

or,

$$(\gamma_i) = 10^{-\left(\frac{0.5085\sqrt{I}}{(1 + 0.9843\sqrt{I})}\right)} \quad (3-6)$$

(b) Meisner and Tester⁸⁵⁻⁸⁶ Plots

The basis for this method is a family of curves that were generated from experimental data for numerous salts in aqueous solutions at 25°C. A new variable (Γ) is defined in which:

$$\Gamma = \gamma^{(1/Z_+Z_-)} \quad (3-7)$$

where γ = the activity coefficient
 Z₊ = charge of the cationic component
 Z₋ = charge of the anionic component.

From the manipulation of experimental γ values, the plots relating Γ to the ionic strength (μ) were generated for many different salts. When the

experimental values of Γ were attained and the $\log_{10}\Gamma$ is plotted against ionic strength (μ), a functionality was noticed. As more results for different salts were plotted, some redundancy of information was noted. Meisner and Tester then compiled all of the different curves and ascertained that all salts will behave similarly to those of the experiments. These plots are provided in Figures 3-2 and 3-3. These functions can be used to determine values of $\log_{10}\Gamma$ for any ionic strength by interpolating values from a known point. For a known value of γ at a specific μ , the point is located on the plots as $(\log_{10}\Gamma, \mu)$. Any value of $\log_{10}\Gamma$ can be determined for any other μ by following the lines on the plots in Figures 3-2 or 3-3 to the new $\log_{10}\Gamma$ value. The activity coefficient is then calculated using equation (3-8) with the value of Γ determined graphically:

$$\gamma = \Gamma^{(Z_+Z_-)} \quad (3-8).$$

The variables are the same as defined in equation (3-7).

(c) Comparison of Debye-Hückel and Meisner and Tester Methods

Since the main objective of this study was to determine the effect of using multivalent chloride salts on the dissolution of Au with chlorine gas, several salts were investigated. To compare the two methods of estimating Cl^- activity, NaCl, HCl, $\text{CaCl}_2 \cdot 2\text{H}_2\text{O}$, $\text{NiCl}_2 \cdot 6\text{H}_2\text{O}$ and $\text{FeCl}_3 \cdot 6\text{H}_2\text{O}$ were chosen. Cl^- concentration was chosen as the variable to base the

experimental parameters. The values chosen for the comparison are 0.05 M Cl⁻, 0.1 M Cl⁻, 0.5 M Cl⁻ and 1.0 M Cl⁻. Using these values and the two methods of estimating the activity (a_{Cl^-}), Table 3-I was generated for the [Cl⁻] and salts chosen.

Cl ⁻ Source	[Cl ⁻], mol/L	(μ. M)	(E.D.H.)		(M.T.)	
			γ_{Cl^-}	a_{Cl^-}	γ_{Cl^-}	a_{Cl^-}
HCl	0.05	0.05	0.81	0.04	0.85	0.04
	0.10	0.10	0.75	0.08	0.81	0.08
	0.50	0.50	0.61	0.34	0.75	0.38
	1.00	1.00	0.55	0.55	0.80	0.80
NaCl	0.05	0.05	0.81	0.04	0.83	0.04
	0.10	0.10	0.75	0.08	0.78	0.08
	0.50	0.50	0.61	0.34	0.69	0.34
	1.00	1.00	0.55	0.55	0.66	0.66
CaCl ₂ ·2H ₂ O	0.05	0.075	0.78	0.04	0.63	0.03
	0.10	0.15	0.72	0.07	0.58	0.06
	0.50	0.75	0.58	0.29	0.45	0.22
	1.00	1.50	0.52	0.52	0.44	0.44
NiCl ₂ ·6H ₂ O	0.05	0.075	0.78	0.04	0.63	0.03
	0.10	0.15	0.72	0.07	0.58	0.06
	0.50	0.75	0.58	0.29	0.46	0.23
	1.00	1.50	0.52	0.52	0.46	0.46
FeCl ₃ ·6H ₂ O	0.05	0.10	0.75	0.04	0.47	0.02
	0.10	0.30	0.66	0.07	0.30	0.03
	0.50	1.00	0.55	0.28	0.29	0.15
	1.00	3.00	0.47	0.47	0.25	0.25

Table 3-I. Comparison of the activity coefficients as calculated from the Extended Debye-Hückel equation (E.D.H.) and by the Meisner and Tester (M.T.) graphical analysis technique.

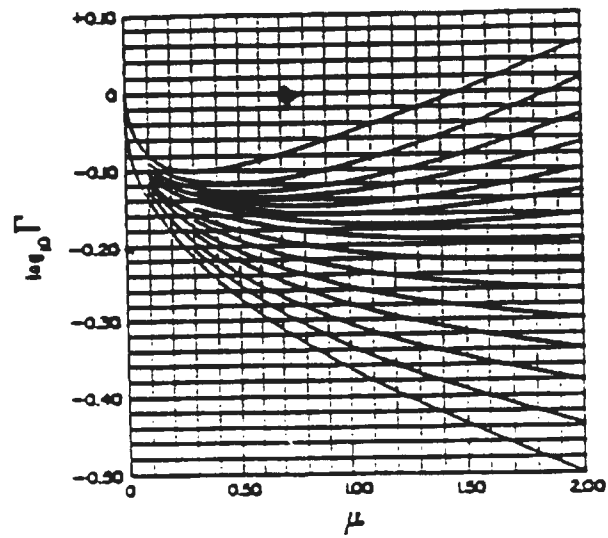


Figure 3-2. Plots of Meisner and Tester⁸⁵ for μ (ionic strength) of 0 to 2.0M

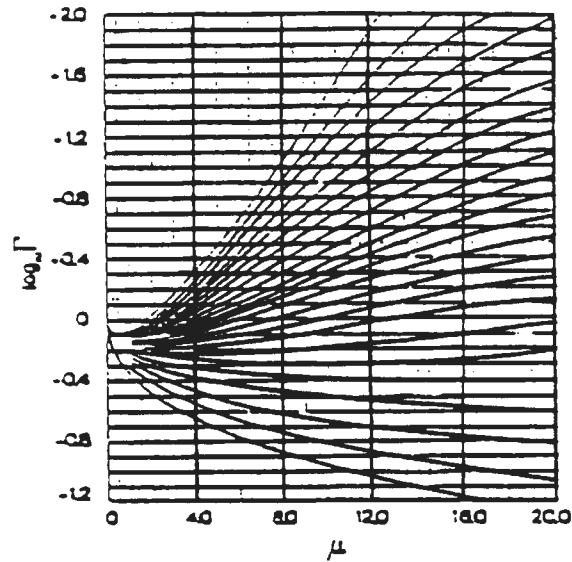


Figure 3-3. Family of plots from Meisner and Tester⁸⁵ for high ionic strengths

II. Experimental

Procedure

The solution to be tested was prepared in a 2-L volumetric flask. One liter of this solution was added to a preweighed amount of fine particle (-325 mesh, -44 μ m) gold powder in the reactor vessel. The remainder of the solution was used as the carrier solution to the AAS.

The ORP and pH were monitored and an initial sample from the reactor sample loop was injected and analyzed for Au dissolution prior to sparging. The chlorine sparger was then placed in the vessel, and the pH and ORP were allowed to stabilize before another sample injection was analyzed. Then, the Cl₂ sparging was begun and the timing initiated.

Equipment

The bulk of the analytical data was obtained with FIA as before. Likewise, a 2-L Pyrex reactor vessel was used for the reaction with magnetic stirring. ORP and pH measurements were constantly monitored throughout the gold dissolution experiments.

The FIA flow circuit was the same as shown in Figure 1-4 with one exception. Because some of the salts used in the tests had an effect on the absorbance, a portion of the reaction solution replaced the water carrier stream to the AAS. This provided a base-line absorbance for the AAS in measuring Au concentrations.

The mass flow meter used to monitor the gas addition was also an important element of the equipment. Prior to each experiment the

chlorine flow rate was set to between 400 and 500 std. cc/min. A typical flow rate was near 460 std. cc/min.

Reagents

Deionized-distilled water was used throughout the experimentation. Reagent grade reagents used were acquired from Fisher Scientific or VWR. The -325 mesh gold powder from Aldrich was used throughout this research.

III Results

No Salt

For the sake of comparison, a gold dissolution experiment was conducted in which no salt was added. The results of this test are shown in Figure 3-4 and are similar to the dissolution curves seen in Chapter One. The dissolution was detected slightly earlier than normal, but the chlorine flow rate in this experiment was larger than those in Chapter One.

Monovalent Cationic Chloride Sources

(a) HCl

Hydrochloric acid was added in four (4) separate experiments to provide chloride ion concentrations of 0.05M, 0.1M, 0.5M and 1.0M. The results of Au dissolution under these conditions are given in Figures 3-5, 3-6, 3-7 and 3-8, respectively. Again, the anomalous gold concentration peak was noted in all of these experiments. The height and duration of the peak

varied in no discernible pattern with the chloride ion concentration. The peak varied in relative height over the final concentrations from $6\bar{r}$ ppm for the 0.05 M Cl^- experiment to only 15 ppm for the 1.0 M test. The duration of the peak varied from about 3 minutes with the lowest HCl concentration to nearly 8 minutes with the highest HCl concentration, while the peaks at the intermediate concentrations lasted about 2.5 minutes for the 0.1M HCl test and about 3 minutes for the 0.5M test.

(b) NaCl

As with HCl, sodium chloride was used to provide chloride concentrations of 0.05M, 0.1M, 0.5M and 1.0M. The results of each of these experiments are given in Figures 3-9, 3-10, 3-11 and 3-12, respectively. For these tests a similar variation in the anomalous gold peak was observed. The relative height of the peak as compared to the final concentrations increased with increasing chloride concentrations to 0.5 M Cl^- , but was smallest for the highest concentration of NaCl. However, as the chloride ion concentration increased, the time before Au detection was first observed decreased. The rate of chlorine sparging was constant for the three experiments with the lowest concentrations of Cl^- . However, the chlorine bubbles in the high concentration solution were much finer and more dispersed in this experiment as compared to the other three tests.

The ionic strengths of HCl and NaCl solutions containing 0.05M, 0.1M,

0.5M and 1.0M chloride ion concentrations are 0.05M, 0.1M, 0.5M and 1.0M.

Divalent Cationic Chloride Sources

(a) $\text{CaCl}_2 \cdot 2\text{H}_2\text{O}$

Calcium chloride dihydrate was added to experiments so that the same four Cl^- concentrations as in the monovalent salt experiments were achieved--0.05M, 0.1M, 0.5M and 1.0M. The results of the chlorination of gold in these solutions are presented in Figures 3-13, 3-14, 3-15 and 3-16, respectively. The anomalous gold concentration peaks in these four experiments varied in height and width with no apparent relation to the concentration of Cl^- . The length of time before dissolved Au was initially detected decreased with increasing chloride ion concentration. As observed in the monovalent experiments in which the chloride ion concentration was 1.0M, the chlorine bubbles were smaller and more dispersed with the high CaCl_2 concentration. The reaction solutions appeared to effervesce during these experiments.

(b) $\text{NiCl}_2 \cdot 6\text{H}_2\text{O}$

Nickel chloride hexahydrate was added in experiments as a source of Cl^- . Au dissolutions were conducted in solutions containing chloride ion concentrations of 0.05M, 0.1M and 0.5M. The results are given in Figures 3-17, 3-18 and 3-19, respectively. The gold peak heights for the 0.05M and 0.1M tests were about the same relative height (~10 ppm); however, the

0.5M test had a peak nearly 25 ppm higher than the final concentration. As seen in the earlier experiments, Au was detected earlier with increased Cl^- concentrations.

The ionic strengths of the various solutions of these salts were calculated for the concentrations tested. For the 0.05M Cl^- tests, μ was 0.075M; for the 0.1M, 0.5M and 1.0M experiments, the ionic strength was 0.15M, 0.75M and 1.5M, respectively.

Trivalent Cationic Chloride Sources

(a) $\text{FeCl}_3 \cdot 6\text{H}_2\text{O}$

Ferric chloride hexahydrate was used as a trivalent cationic source for chloride ion. Because of the hazardous nature and decreased solubility at room temperature, only 0.05M Cl^- and 0.1M Cl^- concentrations were tested. These solutions have an ionic strength of 0.1M and 0.3M, respectively. The results of dissolutions conducted in these solutions are presented in Figures 3-20 and 21. These results are similar to the previous results--no relation of peak shapes to Cl^- concentrations and faster detection of Au after sparging was initiated.

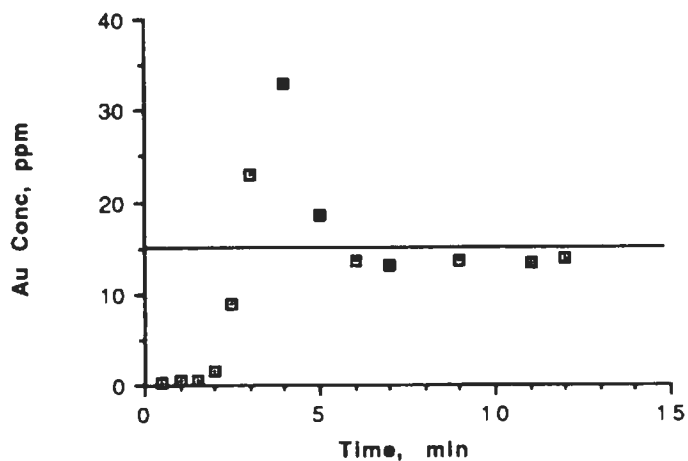


Figure 3-4. Au dissolution by sparging Cl_2 (~400 std.cc/min) with no salt added. The calculated maximum gold concentration for this experiment was 15 ppm based on total dissolution of the original weight of gold in 1-L of water.

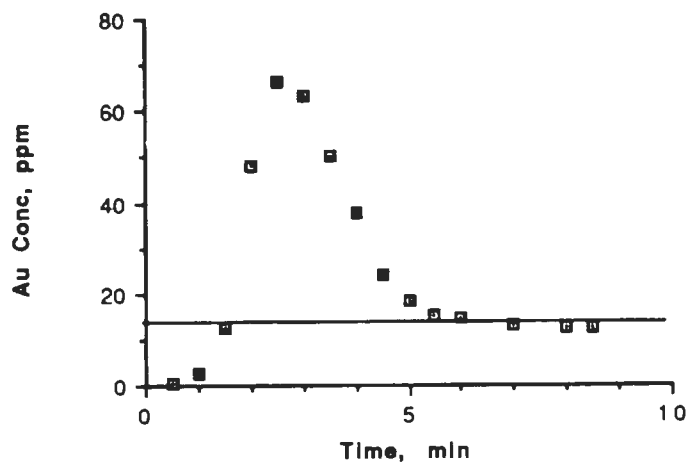


Figure 3-5. Au dissolution by sparging Cl_2 (~400 std. cc./min) with 0.05M chloride ion concentration from HCl. The calculated maximum gold concentration for this experiment was 136 ppm based on total dissolution of the original weight of gold in 1-L of water.

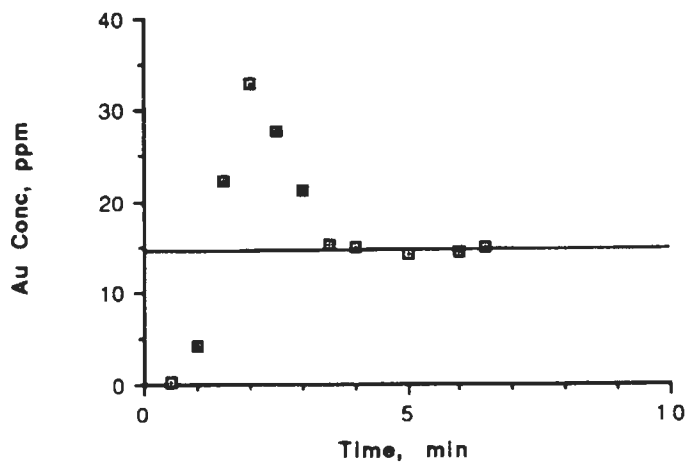


Figure 3-6. Au dissolution by sparging Cl_2 (~400 std. cc./min) with 0.1M $[\text{Cl}^-]$ from HCl. The calculated maximum gold concentration for this experiment was 14.6 ppm based on total dissolution of the original weight of gold in 1-L of water.

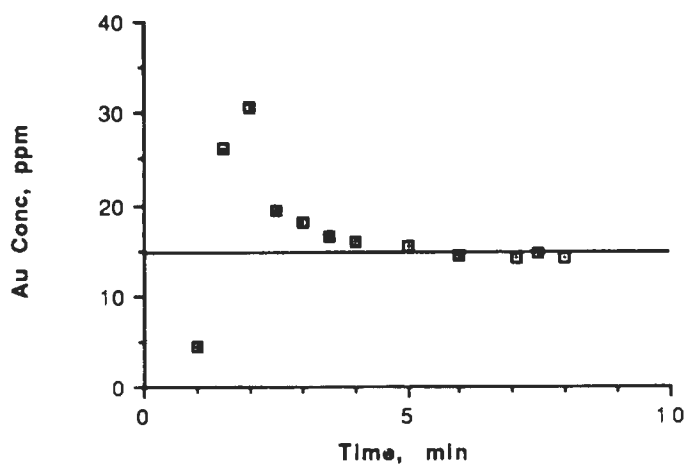


Figure 3-7. Au dissolution by sparging Cl_2 (~400 std. cc./min) with 0.5M $[\text{Cl}^-]$ from HCl. The calculated maximum gold concentration for this experiment was 14.6 ppm based on total dissolution of the original weight of gold in 1-L of water.

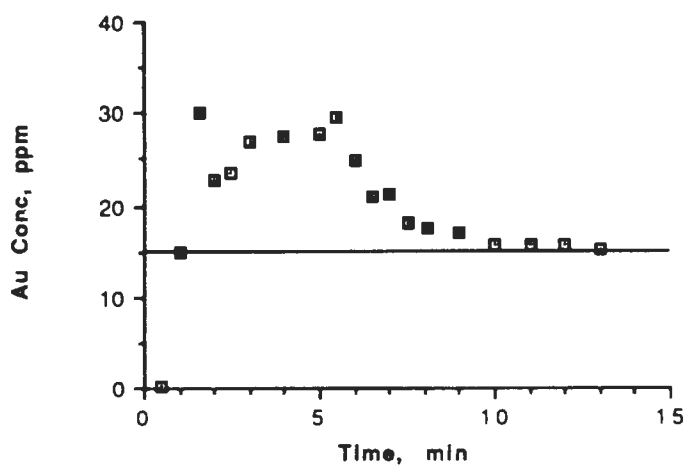


Figure 3-8. Au dissolution by sparging Cl₂ (~400 std. cc./min) with 1.0M [Cl⁻] from HCl. The calculated maximum gold concentration for this experiment was 15 ppm based on total dissolution of the original weight of gold in 1-L of water.

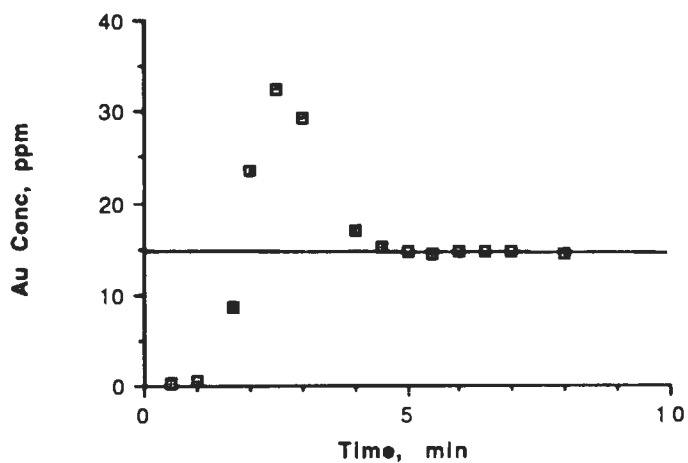


Figure 3-9. Au dissolution by sparging Cl_2 (~400 std. cc./min) with 0.05M $[\text{Cl}^-]$ from NaCl. The calculated maximum gold concentration for this experiment was 14.8 ppm based on total dissolution of the original weight of gold in 1-L of water.

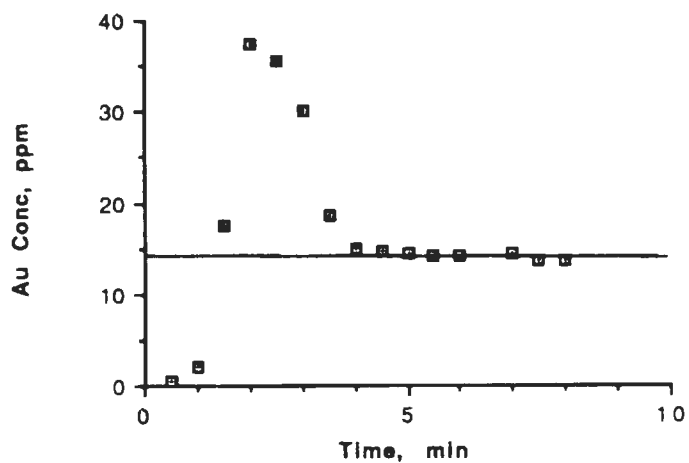


Figure 3-10. Au dissolution by sparging Cl_2 (~400 std. cc./min) with 0.1M $[\text{Cl}^-]$ from NaCl. The calculated maximum gold concentration for this experiment was 13.6 ppm based on total dissolution of the original weight of gold in 1-L of water.

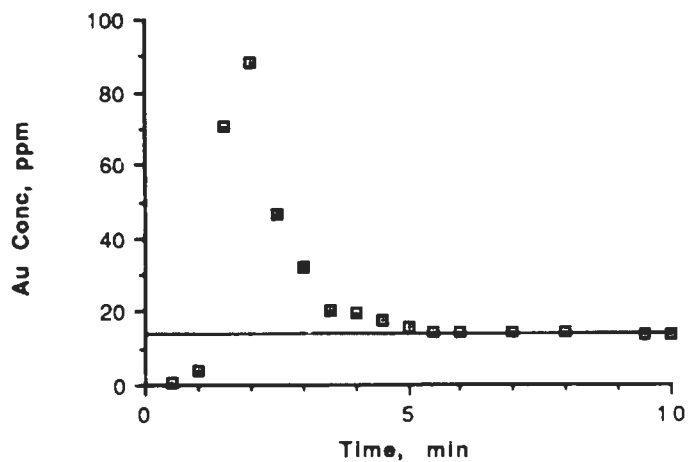


Figure 3-11. Au dissolution by sparging Cl_2 (~400 std. cc./min) with 0.5M $[\text{Cl}^-]$ from NaCl. The calculated maximum gold concentration for this experiment was 14.3 ppm based on total dissolution of the original weight of gold in 1-L of water.

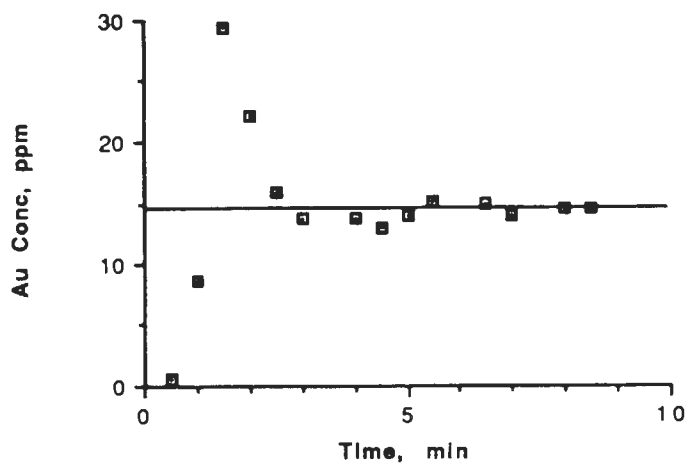


Figure 3-12. Au dissolution by sparging Cl_2 (~400 std. cc./min) with 1.0M $[\text{Cl}^-]$ from NaCl. The calculated maximum gold concentration for this experiment was 14.5 ppm based on total dissolution of the original weight of gold in 1-L of water.

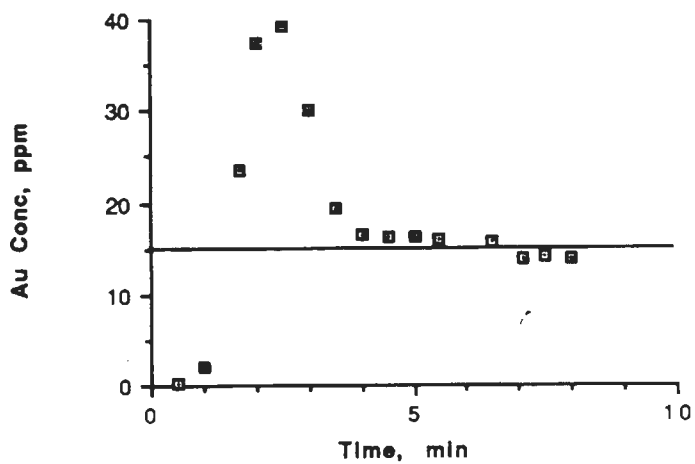


Figure 3-13. Au dissolution by sparging Cl_2 (~400 std. cc./min) with 0.05M $[\text{Cl}^-]$ from $\text{CaCl}_2 \cdot 2\text{H}_2\text{O}$. The calculated maximum gold concentration for this experiment was 14.6 ppm based on total dissolution of the original weight of gold in 1-L of water.

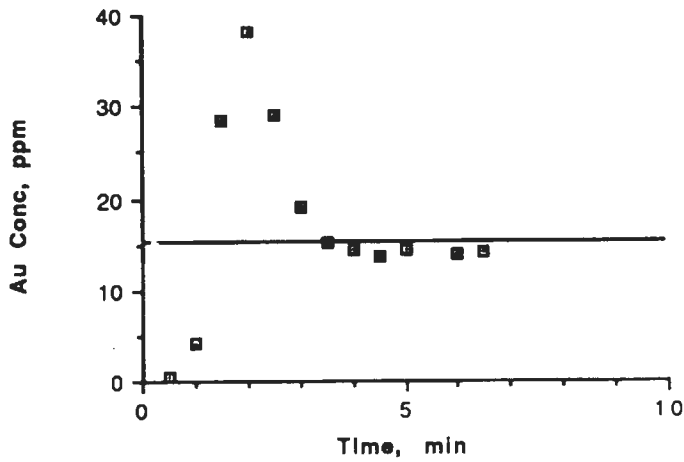


Figure 3-14. Au dissolution by sparging Cl_2 (~400 std. cc./min) with 0.1M $[\text{Cl}^-]$ from $\text{CaCl}_2 \cdot 2\text{H}_2\text{O}$. The calculated maximum gold concentration for this experiment was 15.2 ppm based on total dissolution of the original weight of gold in 1-L of water.

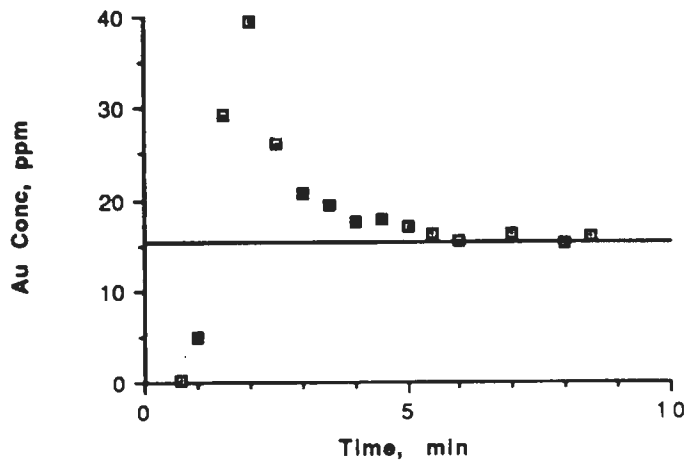


Figure 3-15. Au dissolution by sparging Cl_2 (~400 std. cc./min) with 0.5M $[\text{Cl}^-]$ from $\text{CaCl}_2 \cdot 2\text{H}_2\text{O}$. The calculated maximum gold concentration for this experiment was 15.2 ppm based on total dissolution of the original weight of gold in 1-L of water.

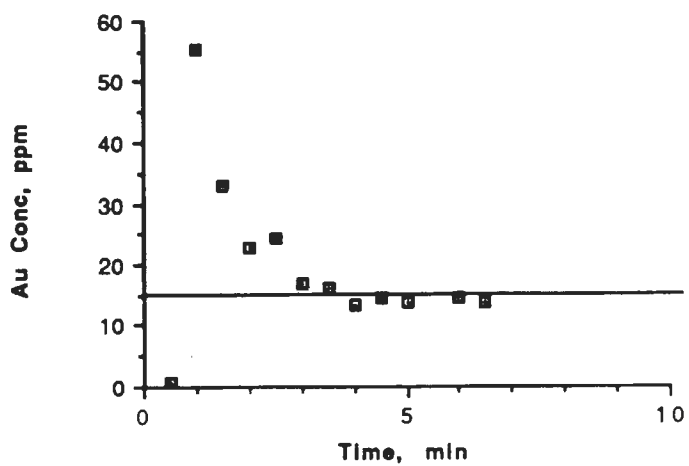


Figure 3-16. Au dissolution by sparging Cl_2 (~400 std. cc./min) with 1.0M $[\text{Cl}^-]$ from $\text{CaCl}_2 \cdot 2\text{H}_2\text{O}$. The calculated maximum gold concentration for this experiment was 14.7 ppm based on total dissolution of the original weight of gold in 1-L of water.

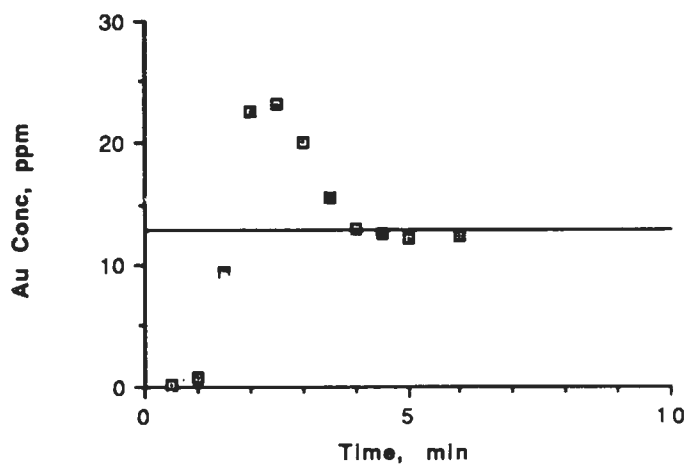


Figure 3-17. Au dissolution by sparging Cl_2 (~400 std. cc./min) with 0.05M $[\text{Cl}^-]$ from $\text{NiCl}_2 \cdot 6\text{H}_2\text{O}$. The calculated maximum gold concentration for this experiment was 13.6 ppm based on total dissolution of the original weight of gold in 1-L of water.

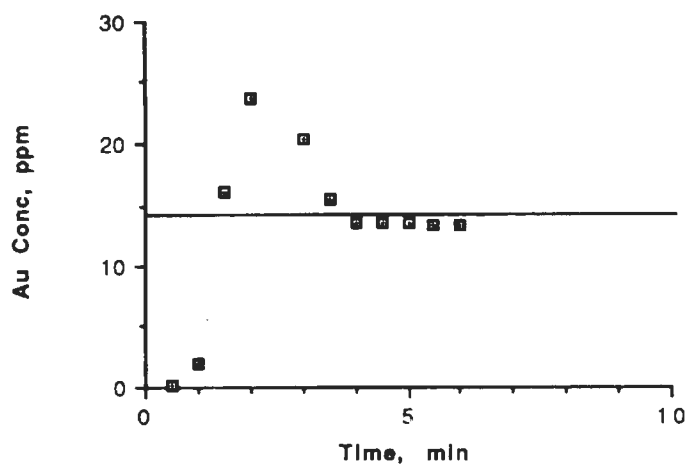


Figure 3-18. Au dissolution by sparging Cl_2 (~400 std. cc./min) with 0.1M $[\text{Cl}^-]$ from $\text{NiCl}_2 \cdot 6\text{H}_2\text{O}$. The calculated maximum gold concentration for this experiment was 14.5 ppm based on total dissolution of the original weight of gold in 1-L of water.

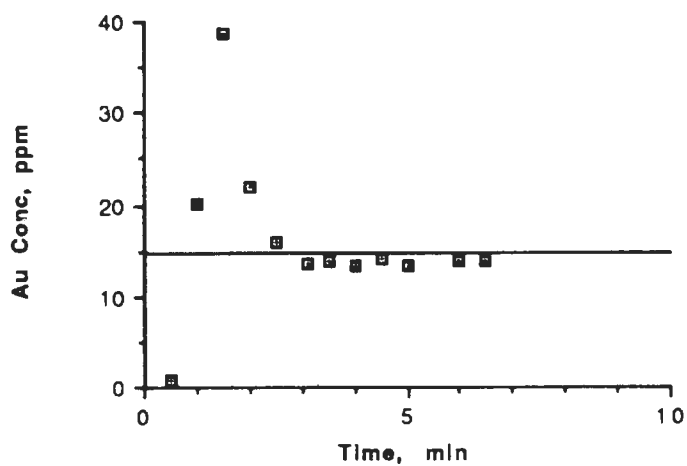


Figure 3-19. Au dissolution by sparging Cl_2 (~400 std. cc./min) with 0.5M $[\text{Cl}^-]$ from $\text{NiCl}_2 \cdot 6\text{H}_2\text{O}$. The calculated maximum gold concentration for this experiment was 14.5 ppm based on total dissolution of the original weight of gold in 1-L of water.

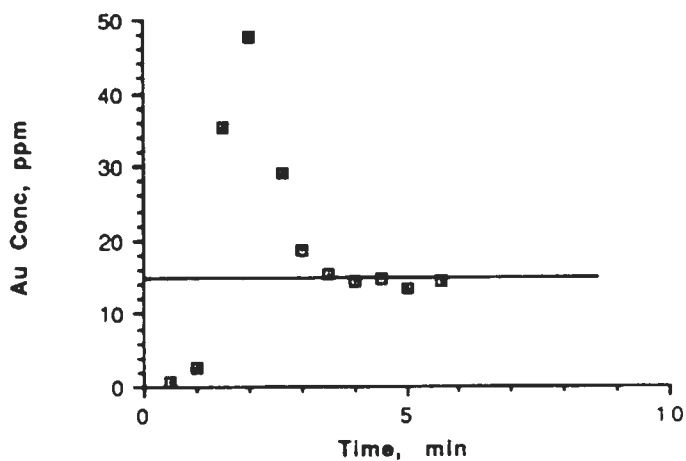


Figure 3-20. Au dissolution by sparging Cl_2 (~400 std. cc./min) with 0.05M $[\text{Cl}^-]$ from $\text{FeCl}_3 \cdot 6\text{H}_2\text{O}$. The calculated maximum gold concentration for this experiment was 14.4 ppm based on total dissolution of the original weight of gold in 1-L of water.

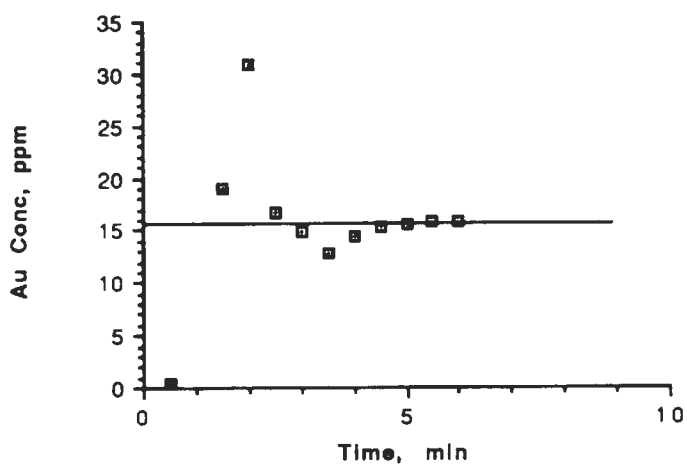


Figure 3-21. Au dissolution by sparging Cl_2 (~400 std. cc./min) with 0.1M $[\text{Cl}^-]$ from $\text{FeCl}_3 \cdot 6\text{H}_2\text{O}$. The calculated maximum gold concentration for this experiment was 15.5 ppm based on total dissolution of the original weight of gold in 1-L of water.

IV. Discussion

The direct comparisons of the gold dissolution profiles with various concentrations of Cl^- from the different sources are presented in Figure 3-22 for HCl, Figure 3-23 for NaCl, Figure 3-24 for CaCl_2 , and Figures 3-25 and 3-26 for the NiCl_2 and FeCl_3 , respectively. From these plots, the effect of increased Cl^- concentration is directly seen. However, the effect of increased ionic strength from the various cationic species is better shown by comparing the dissolution rate of gold at the same Cl^- concentrations. The plots of Au dissolution are provided in Figures 3-27, 3-28, 3-29, and 3-30 for $[\text{Cl}^-]$ of 0.05 M, 0.1 M, 0.5 M and 1.0 M respectively.

In using these plots, two points should be focused upon--(1) the slopes of the dissolution curves, and (2) the relative time after the start of sparging at which Au is first detected. In all of the comparisons given in Figures 3-22 through 3-26, the time required before dissolved Au was detected decreased with an increase in $[\text{Cl}^-]$. The relative rates of dissolution (slopes) are difficult to generalize, but the rates tend to increase with chloride ion concentration.

From Figures 3-27 through 3-30, the slopes and the initial times prior to Au detection are very similar for the same $[\text{Cl}^-]$ from each salt. But comparing the results is made more difficult by the presence of the gold concentration peak.

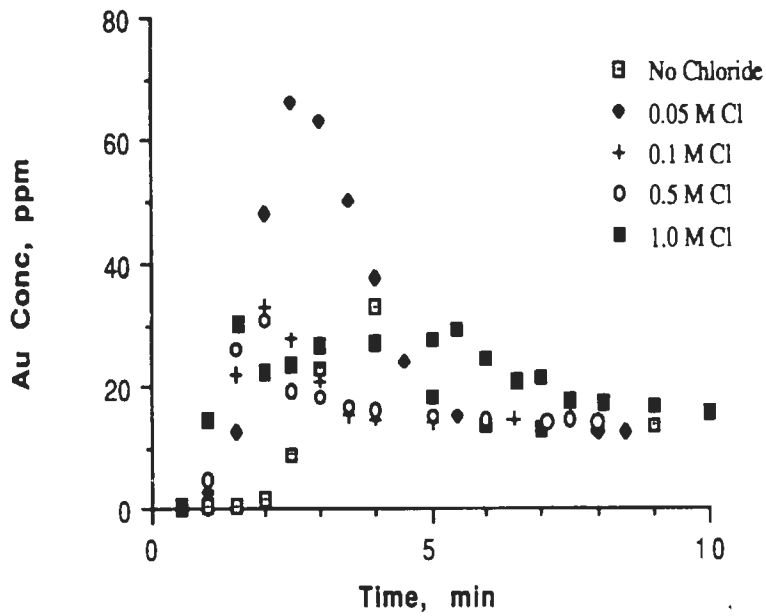


Figure 3-22. Comparison of the dissolution experiments for various Cl^- concentrations from HCl addition and no salt addition.

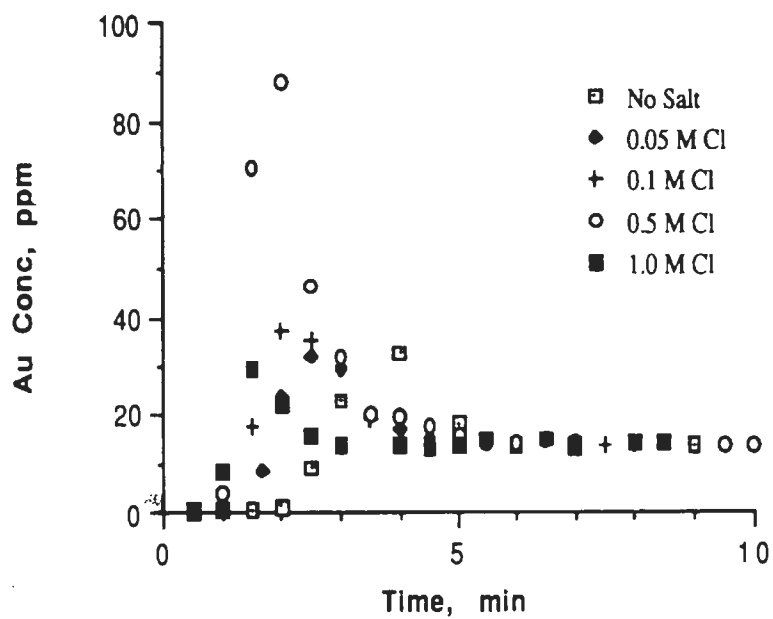


Figure 3-23. Comparison of the dissolution experiments for various Cl⁻ concentrations from NaCl addition and no salt addition.

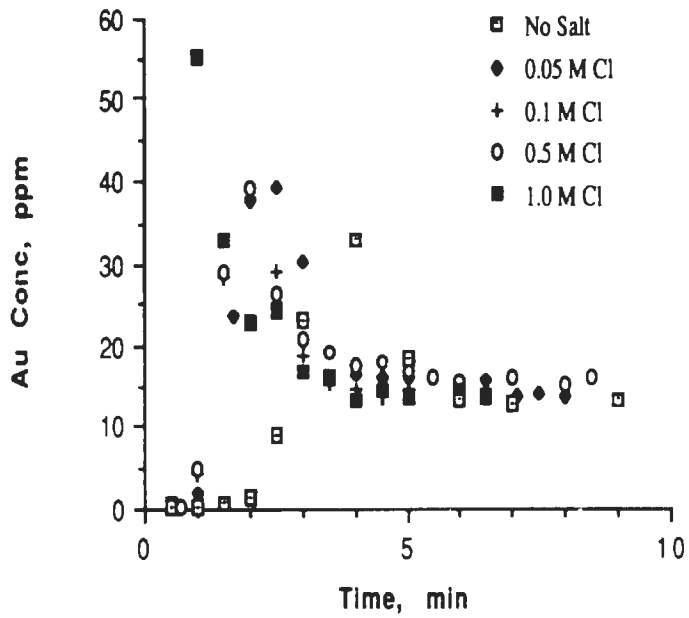


Figure 3-24. Comparison of the dissolution experiments for various Cl^- concentrations from $\text{CaCl}_2 \cdot 2\text{H}_2\text{O}$ addition and no salt addition.

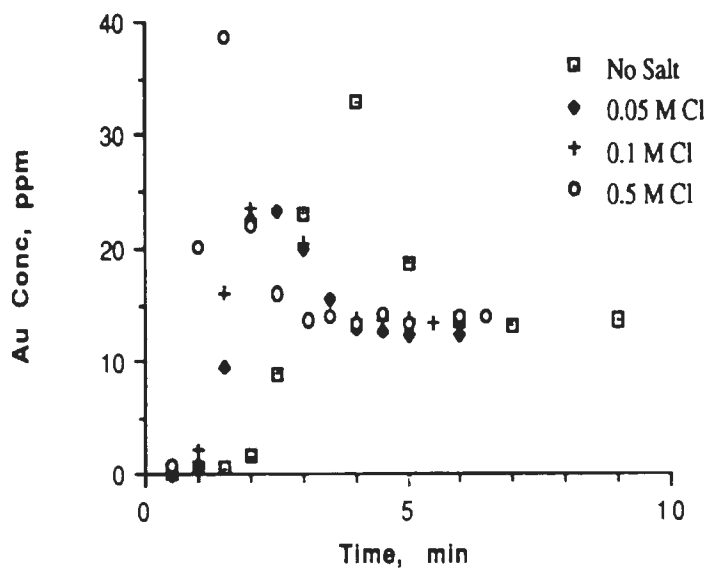


Figure 3-25. Comparison of the dissolution experiments for various Cl^- concentrations from $\text{NiCl}_2 \cdot 6\text{H}_2\text{O}$ addition and no salt addition.

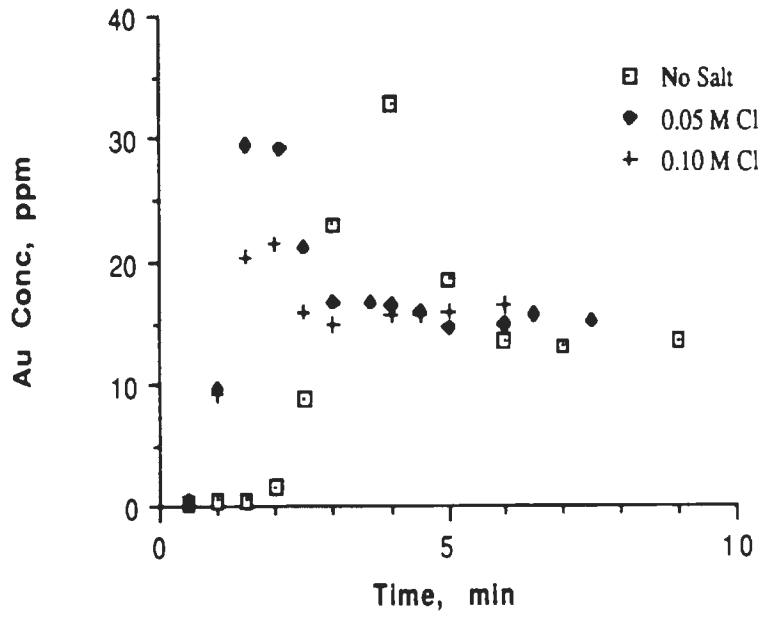


Figure 3-26. Comparison of the dissolution experiments for various Cl^- concentrations from $\text{FeCl}_3 \cdot 6\text{H}_2\text{O}$ addition and no salt addition.

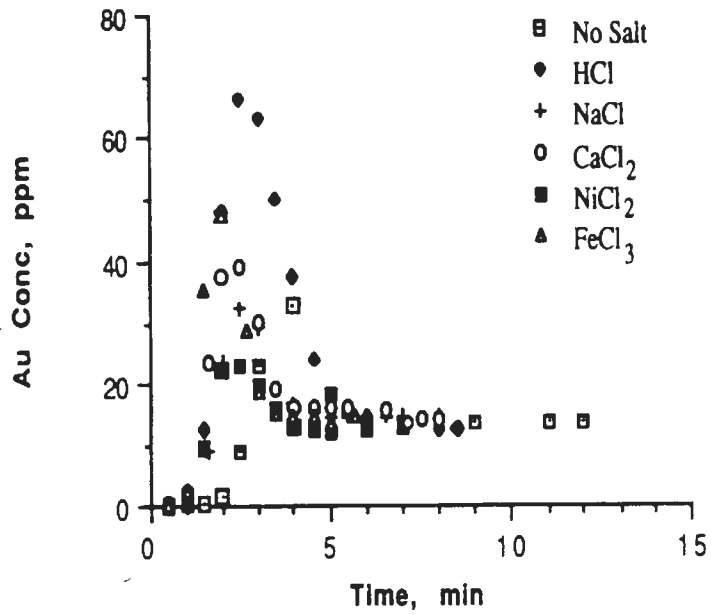


Figure 3-27. Comparison of gold dissolution in which the concentration of Cl⁻ was 0.05M.

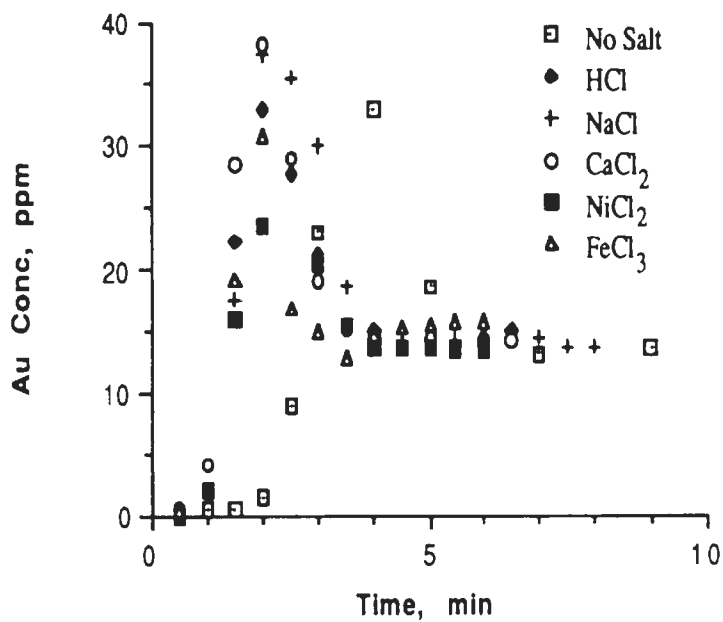


Figure 3-28. Comparison of gold dissolution in which the concentration of Cl⁻ was 0.1M.

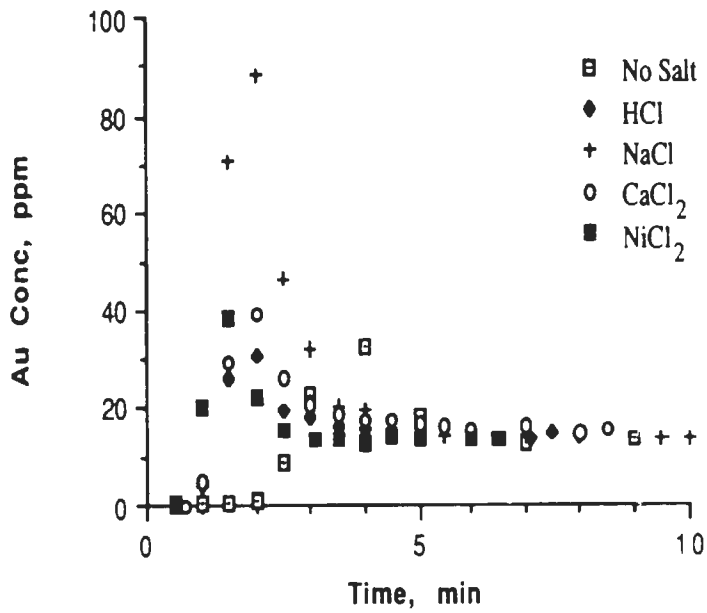


Figure 3-29. Comparison of gold dissolution in which the concentration of Cl⁻ was 0.5M.

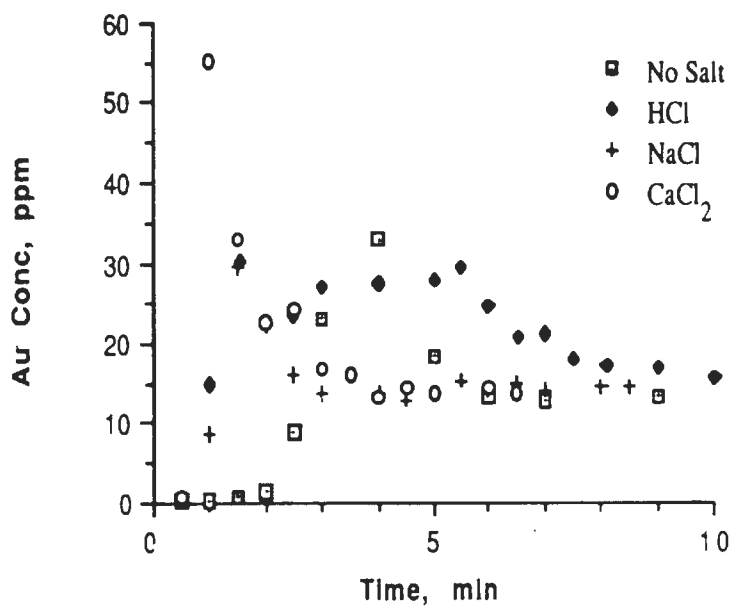
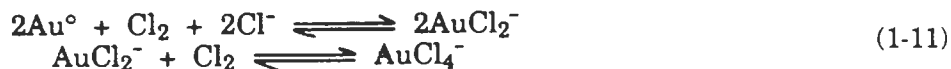


Figure 3-30. Comparison of gold dissolution in which the concentration of Cl⁻ was 1.0M.

For the sake of argument, a typical gold concentration profile from a fine gold dissolution experiment is provided in Figure 3-31 and labelled for further discussion. Also for reference, the mechanism (1-11) is given:



Region I represents the time in which the first reaction of mechanism (1-11) predominates. At point P, the concentration of AuCl_2^- is at its maximum, hence the interference is at a peak. Initially, the relative rate of Au° dissolution to form AuCl_2^- is much faster than the oxidation of AuCl_2^- to AuCl_4^- . As the amount of Au° goes to zero, the production of AuCl_2^- slows. As a result, the rate of disappearance of AuCl_2^- by the second reaction is now faster than the first reaction, as represented by Region II. So as a good approximation, point P also represents the point that nearly all of the Au° is dissolved. Using this approximation, an average dissolution

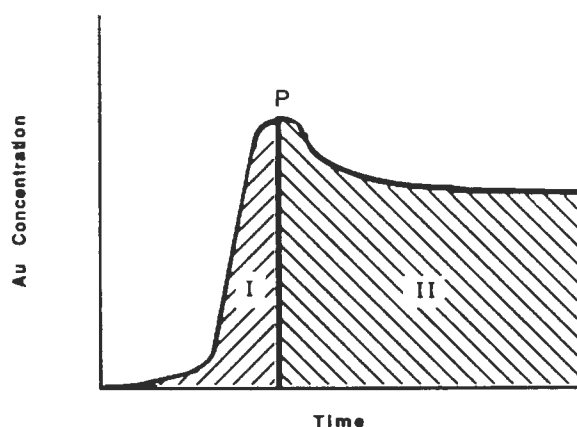


Figure 3-31. Typical dissolution profile for fine particle Au dissolved by Cl_2 sparging.

Salt	Chloride Ion Concentration			
	0.05 M	0.1M	0.5 M	1.0M
HCl	5.4	7.3	7.3	9.7
NaCl	5.9	6.8	7.2	10.4
CaCl ₂ ·2H ₂ O	5.8	7.6	7.6	14.7
NiCl ₂ ·6H ₂ O	5.4	6.9	9.7	-
FeCl ₃ ·6H ₂ O	7.2	7.8	-	-
No Salt	4.2			

Table 3-II. Average dissolution rate (mg/min) calculated from the various dissolution experiments.

rate may be calculated for the time to dissolve the fine Au⁰, that is, the time to reach the peak in the dissolution experiments. The results of this calculation for each experiment are compiled in Table 3-II. From the table, it can be concluded that the dissolution rate increases with increasing chloride concentration.

As another and more useful means of comparing the data, Table 3-III was generated to show the same average dissolution rates as a function of the ionic strength of solution. Ionic strengths above 1.0M resulted in an

Salt	Ionic Strength (μ . M)								
	0.05	.075	0.10	0.15	0.3	0.5	0.75	1.0	1.5
HCl	5.4	-	7.3	-	-	7.3	-	9.7	-
NaCl	5.9	-	6.8	-	-	7.2	-	10.4	-
CaCl ₂ ·2H ₂ O	-	5.8	-	7.6	-	-	7.6	-	14.7
NiCl ₂ ·6H ₂ O	-	5.4	-	6.9	-	-	9.7	-	-
FeCl ₃ ·6H ₂ O	-	-	7.2	-	7.8	-	-	-	-
No Salt	4.2								

Table 3-III. Comparison of the dissolution rate of Au (mg/min) for chlorine sparging (~400 std. cc/min) at various ionic strengths (μ).

average dissolution of over 10 mg/min. To ~~achieve that~~ μ , more than 1.0M NaCl or HCl is needed, 0.33 M CaCl₂ or NiCl₂, or only 0.17M FeCl₃. A plot of the data presented in Table 3-III is presented in Figure 3-32 and shows a similar relationship of gold dissolution rate to ionic strength as was calculated from Putnam's research (Figure 3-1).

In the experiments in which the Cl⁻ concentration was ~1M, the Cl₂ bubbles were smaller and more easily dispersed in the solution than at lower concentrations. This effect was determined to be directly related to an increase in the surface tension of the solutions with increasing salt concentrations. Any effect that the finer bubbles had on the observed increased dissolution rate could not be determined but was assumed to be negligible.

The two methods of calculating the chloride ion activity compare favorably. Figure 3-33 is a plot of the chloride ion activities calculated by the two methods in Table 3-I and the average gold dissolution rates observed in the experiments as functions of the ionic strength. The two methods follow the dissolution rate increase with increasing ionic strength. Marcus predicted that the increase in the overall reaction rate constant is directly proportional to the rate constant of electron transfer (k_{el}). The probability of transfer relates to the salt concentration and would represent an increase in the value of k_{el} which directly relates to an increase in the rate of dissolution. This fact is seen in Figure 3-33.

With regard to Austin's observation of "greater energy" in Chapter One, the observation is more easily credited to the increase in the ionic strength of the solution, and not attributed to "new-born" chlorine. As a proof, similar dissolution rates are observed between the dissolution experiment conducted at 1.0 M NaCl (Figure 3-12) with sparged Cl_2 and the experiment in which HCl was added to KMnO_4 in the Chapter One (Figure 1-22). The average dissolution rate for the permanganate experiment was 10.9 mg/min; the rate calculated from the 1M NaCl experiment was 10.4 mg/min.

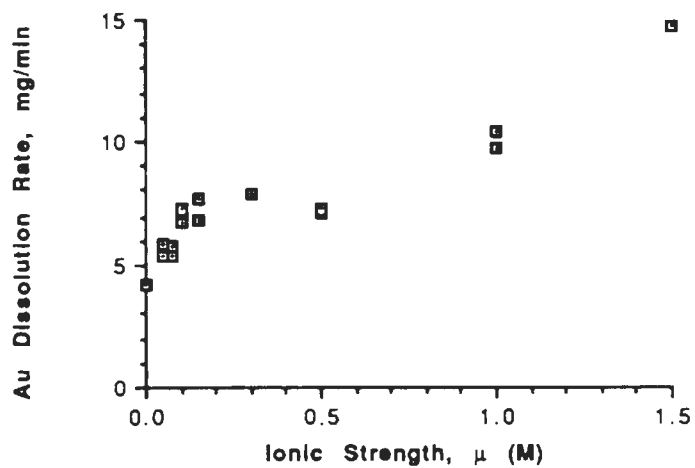


Figure 3-32. Graphical representation of the data presented in Table 3-III showing the net effect of ionic strength on the average dissolution rate of Au for the same chlorine sparging rate.

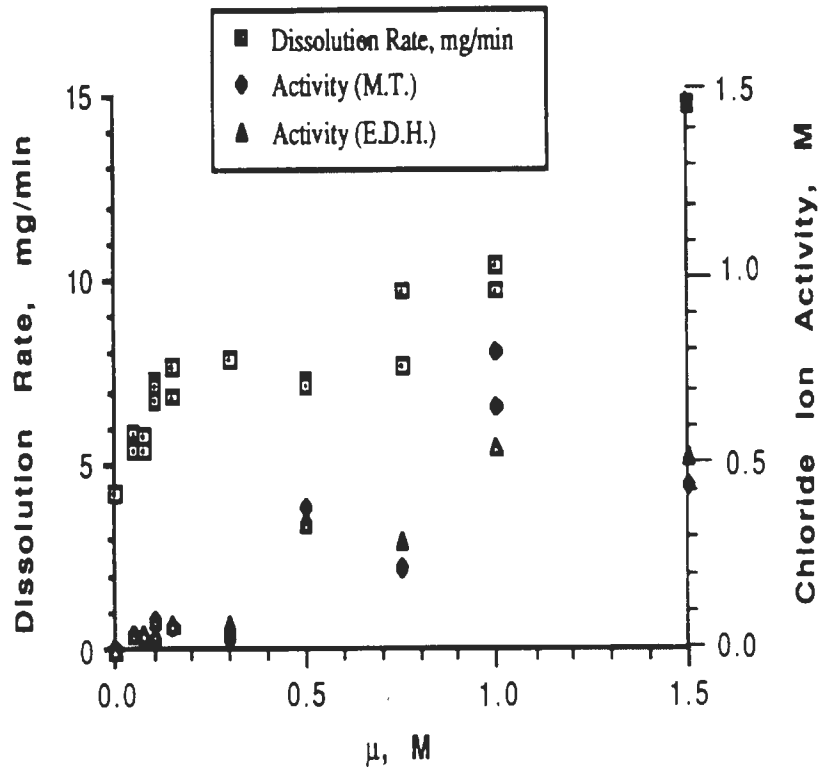


Figure 2-33. Graphical representation of the activity of chloride ion as calculated from the extended Debye-Hückel equation (E.D.H.) and the Meisner and Tester (M.T.) plots and the average Au dissolution rate (mg/min) from the chlorine sparging experiments.

V. Conclusions

The following conclusions were drawn as a result of the research conducted on the effect of multivalent cation chloride salt addition on the dissolution of Au by sparging Cl_2 :

- 1) The rate at which Au is dissolved by gaseous chlorine may be increased by adding chloride salts.
- 2) The rate of dissolution of Au increases with an increase in the ionic strength of solution. The rate of dissolution of Au in a 0.1M ionic strength solution is twice that in a solution with no salt added. This ionic strength can be achieved by the addition of 0.1 M HCl or NaCl, 0.04 M CaCl_2 or NiCl_2 , or 0.017 M FeCl_3 . A 150% increase in the Au dissolution may be reached with an ionic strength of 1.0 M (1.0M HCl or NaCl, 0.4M CaCl_2 or NiCl_2 , or 0.17 M FeCl_3).
- 3) An increase in Au dissolution is noted with an increase in the valence of the cationic species present in the chloride source. The valence affects the ionic strength which in turn affects the rate of dissolution. For instance, at a Cl^- concentration of 0.05M, a solution of ferric chloride will have an ionic strength of 0.1M and had an average Au dissolution rate of about 7.2 mg/min, while the same for sodium chloride will be 0.05 M and had an average dissolution rate of about 5.4 mg/min.
- 4) The rate of dissolution of gold increases with increasing chloride ion activity. The dissolution rate increased from 5.4 mg/min to over 10 mg/min with the corresponding increase of a_{Cl^-} of ~ 0.04 M to ~ 0.66 M.
- 5) Values of chloride activity derived by the extended Debye-Hückel equation and by graphical estimation by the Meisner and Tester plots are equally useful for determining the activity of chloride ion.
- 6) The "greater energy upon the gold" as claimed by Austin⁴ is attributed to the increased ionic strength gained when excess Cl^- (as HCl or NaCl) is present in the *in situ* chemical formation of chlorine during Au dissolution.

Chapter Four

Summary of Study

Chlorine possesses all of the characteristics desired for a lixiviant of gold. It reacts faster than cyanide, will dissolve coarse and fine particle gold, and is more tolerated for release to the environment in water (EPA regulations allow up to 330 ppm Cl_2 and up to 10 ppm CN^-). But cyanide is still preferred. It is much less reactive, especially with sulfide minerals and plant equipment than chlorine. Chlorination's return in hydrometallurgical operations is an uphill battle. The results of this three-phase study suggest some reasons for inclusion of chlorine in gold processing.

Chlorine will react to dissolve Au nearly ten times faster than cyanide. The rates of this reaction can be doubled with a minimal addition of a soluble trivalent or divalent cationic chloride salt ($<0.1\text{M}$). Although the concentration of Cl_2 is important in the rate of dissolution, a large excess isn't necessary for rapid gold recovery. History would bear witness to chlorine's ability to the recovery of fine gold with solutions well below chlorine saturation concentrations. The only problem with low Cl_2 concentrations is that most sulfide minerals, as well as the process equipment itself, will consume the reagent rapidly. Low grade ores with a wide variety of mineral compositions are being exploited by cyanide heap leaching; the future of chlorine as a sole lixiviant of gold in ores of this nature is bleak.

The future of chlorine remains in the area of pretreating

carbonaceous ores. The success of chlorine in this capacity has been attributed to any number of things--oxidation of the carbon surface groups, oxidation of humic acid components, and the ability of gold chloride to be precipitated for easy recovery by cyanide. But the property of chlorine that most reduces its chances at replacing cyanide is the reason for its success with carbon--high reactivity with sulfide minerals. Since chlorine reacts with pyrite, chalcocite, pyrrhotite and chalcopyrite, the solution during flash chlorination is abundant with dissolved gold, iron and copper. But because the sulfide minerals are present in the ore in amounts ranging from 0.1-2 weight percent and Au is only present in the 0.01 wt. % range, the solution may be as much as 500 times richer in iron and copper than gold. The iron and copper will saturate the graphitic carbon present in the ore and keep the Au in solution. Changing the pH and oxidation potential of the solution in preparation for cyanidation should reduce the dissolved gold to elemental gold. This gold is redissolved by cyanide later in the process. In the meantime, the carbon is now non-preg robbing because of the excess of metals present on the surface, and not from reactions with chlorine. Prior to cyanidation, the pulp is mixed with lime to raise the pH to over 10. The increased pH would initiate the formation of colloidal hydroxide precipitates on the carbon which would also hinder the adsorption of $\text{Au}(\text{CN})_2^-$ complex.

Two proposed changes to the flash chlorination process may be advanced based on the results of this study. First, conditioning the ore with ferric chloride solution and subsequent treatment with chlorine would

serve two benefits. Dissolved iron would be available to adsorb on the surface of the carbon before gold is dissolved. The increased ionic strength of the solution from the ferric chloride will significantly increase the rate of gold dissolution. The chlorine provides the environment (low pH and high Eh) necessary for hindering Au adsorbance by ferric chloride. The other proposed change to the process would be to add a step to recover the gold prior to cyanidation. The pretreatment with ferric chloride and chlorine should increase the concentration of Au in the solution, and a decantation step would allow for recovery of this gold. The best possible results of these changes to the process would be the elimination of the cyanidation step.

Economically, the cost of building a new facility to use chlorine in the recovery of gold would be prohibitively expensive. Teflon and titanium construction is a necessity in chlorine or ferric chloride processes. Although the potential for eliminating the cyanidation step may be alluring, in the long run, the cyanide process is a cheap process to construct and operate. So the relative cost effectiveness of introducing ferric chloride would have to include the comparison of the cost of specialty materials that are "chlorine proof", such as Teflon and titanium to the savings from the elimination of a very inexpensive, effective process.

Also the environmental impacts of each process must be considered. Although the EPA allows up to 330 ppm Cl_2 in waste water and only 10 ppm of CN^- , much more stringent restrictions are placed on the heavy metals leached by chlorine during the process, not to mention the direct addition of ferric ion in the process. Cyanide releases much less metals into the water,

and may actually be less environmentally hazardous than chlorine.

No hydrometallurgical study is complete without consulting at least one Pourbaix diagram. The diagram is a great tool to determine the ultimate speciation of reactions. But the diagram has some shortcomings. For instance, during the course of research of the mechanism of gold dissolution by chlorine, the diagram suggested that AuCl_2^- was not stable under the conditions tested. This diagram slowed the process of determining the cause of the anomalous gold peak because the presence of AuCl_2^- as an intermediate was not anticipated. The Eh-pH diagram of the Au-Cl-H₂O system showed that AuCl_2^- complex would not appear under the conditions of the experiment.

The Pourbaix diagrams are inherently biased by the term "equilibrium". Since most hydrometallurgical processes were developed with the primary goal of the timely recovery of metals, the diagrams are not definitive by themselves because neither the rates nor the mechanisms of reactions are considered. Many of the stable species reported in Eh-pH diagrams may not reach "equilibrium" for minutes or hours. The recovery of the stable dissolved species may take too long to be feasible for process considerations.

Bibliography

1. O'Driscoll, F., Notes on the Treatment of Gold Ore, Offices of "Engineering", London, 1889.
2. Küstel, G., Nevada and California Processes of Silver and Gold Extraction, Frank D. Carlton, San Francisco, 1863.
3. Austin, L.S., The Metallurgy of the Common Metals: Gold, Silver, Iron, Copper, Lead, and Zinc, 1st Ed., Mining and Scientific Press, San Francisco, 1907.
4. Austin, L.S., ibid, 3rd Ed., Mining and Scientific Press, San Francisco, 1911.
5. Austin, L.S., ibid, 6th Ed., Mining and Scientific Press, San Francisco, 1926.
6. Rose, T.K., The Metallurgy of Gold, 1st Ed., Charles Griffin & Company, Ltd., London, 1894.
7. Rose, T.K., ibid, 2nd Ed., Charles Griffin & Company, Ltd., London, 1896.
8. Rose, T.K., ibid, 3rd Ed., Charles Griffin & Company, Ltd., London, 1898.
9. Rose, T.K., ibid, 4th Ed., Charles Griffin & Company, Ltd., London, 1902.
10. Rose, T.K., ibid, 5th Ed., Charles Griffin & Company, Ltd., London, 1906.
11. Rose, T.K., ibid, 6th Ed., Charles Griffin & Company, Ltd., London, 1915.
12. Rose, T.K., ibid, 7th Ed., Charles Griffin & Company, Ltd., London, 1937.
13. Liddell, D.M., Handbook of Non-ferrous Metallurgy, McGraw-Hill Book Company, Inc., New York, 1926.
14. Eissler, M., The Metallurgy of Gold, 2nd Ed., Crosby Lockwood & Son, London, 1889.

15. Phillips, J.A., The Mining and Metallurgy of Gold and Silver, E. & F.N. Spon, Ltd, London, 1867.
16. Johnson, J.C.F., Getting Gold: A Treatise for Prospectors, Miners, and Students, 2nd Ed., Charles Griffin & Company, LTD, London, 1889.
17. Louis, H., A Handbook of Gold Milling, 2nd Ed., MacMillan and Company, Ltd, London, 1899.
18. Lock, C.G.W., Gold Milling: Principles and Practice, E. & F.N. Spon, Ltd., London, 1901.
19. Putnam, G., "Chlorine as a Solvent in Gold Hydrometallurgy", Engineering and Mining Journal, 145(1), pp. 70-73, 1944.
20. Walker, G.A., Australasia Institute of Mining and Metallurgy Proceedings, 21, 1956.
21. Nagy, I., Mrkusic, P., and McCulloch, H.W., "Chemical Treatment of Refractory Gold Ores: A Literature Survey", National Institute of Metallurgy, Report No. 38, 1966.
22. Jackson, K.J. and Strickland, J.D.H., "The Dissolution of Sulfide Ores in Acid Chlorine Solutions; A Study of the More Common Sulfide Minerals", Transactions of TMS of AIME, 212, June, 1958, pp. 373-379.
23. Woodcock, J.T., "Some Aspects of the Oxidation of Sulphide Minerals in Aqueous Suspensions", Proceedings the Aus. I. M. M., 198, pp. 47-85, 1961.
24. Hiskey, J.B., and Atluri, V.P., "Dissolution Chemistry of Gold and Silver in Different Lixiviants", Mineral Processing and Extractive Metallurgy Review, 1988, Vol. 4, Gordon and Breach, Science Publishers, Inc., Great Britain, pp. 94-134, 1988.
25. Scheiner, B.J., Lindstrom, R.E., and Henrie, T.A., "Oxidation Process for Improving Gold Recovery From Carbon-bearing Gold Ores", Report of Investigations 7573, U.S. Bureau of Mines, 1971.
26. Scheiner, B.J., Lindstrom, R.E., and Henrie, T.A., "Processing Refractory Carbonaceous Ores for Gold Recovery", Journal of Metals, 23, pp. 37-40, March, 1971.
27. Scheiner, B.J., et al., "Extraction of Gold from Carbonaceous Ores: Pilot Plant Studies", Report of Investigations 7597, U.S. Bureau of Mines, 1972.

28. Guay, W.J. and Peterson, D.G., "Recovery of Gold from Carbonaceous Ores at Carlin Nevada", Transactions of SME of AIME, **254**, pp. 102-104, 1973.
29. Brunk, K.A. and Atwood, R.L., "Practical Aspects of Cyanidation of Carbonaceous Ores", AIME-SME Preprint, 87-165, Presented the Annual AIME Meeting, Denver, Colorado, 1987.
30. Radtke, A.S. and Scheiner, B.J., "Studies of Hydrothermal Gold Deposition(1). Carlin Gold Deposit, Nevada: The Role of Carbonaceous Materials in Gold Deposition", Economic Geology, **65**(2), pp. 87-102, March-April, 1970.
31. Ružička, J. and Hansen, E.H., "Flow Injection Analysis. Part I. A New Concept of Fast Continuous Flow Analysis," Anal. Chim. Acta, **78**, pg. 145, 1974. [Danish Patent Application No. 4846/74 (1974); U.S. Patent No. 4,022,575.]
32. Ružička, J. and Stewart, J.W.B., "Flow Injection Analysis. Part II. Ultrafast Determination of Phosphorous in Plant Material by Continuous Flow Spectrophotometry," Anal. Chim. Acta, **79**, pg. 79, 1975.
33. Stewart, J.W.B., Ružička, J., Bergamin F^o, H., and Zagatto, E.A.G., "Flow Injection Analysis. Part III. Comparison of Continuous Flow Spectrophotometry and Potentiometry for the Rapid Determination of the Total Nitrogen Content in Plant Digests", Anal. Chim. Acta, **81**, pg. 371, 1976.
34. Stewart, J.W.B., Ružička, J., and Zagatto, E.A.G. "Flow Injection Analysis. Part IV. Stream Sample Splitting and Its Application to the Continuous Spectrophotometric Determination of Chloride in Brackish Waters", Anal. Chim. Acta, **81**, pg. 387, 1976.
35. Stewart, J.W.B. and Ružička, J., "Flow Injection Analysis. Part V. Simultaneous Determination of Nitrogen and Phosphorous in Acid Digests of Plant Material with a Single Spectrophotometer", Anal. Chim. Acta, **82**, pg. 137 Chloride in Blood Serum by Dialysis and Sample Dilution", Anal. Chim. Acta, **87**, pg. 353, 1976.
36. Ružička, J. and Hansen, E.H., "Flow Injection Analysis. Part IV. The Determination of Phosphate and Chloride in Blood Serum by Dialysis and Sample Dilution," Anal. Chim. Acta, **87**, pg. 353, 1974.
37. Betteridge, D. and Ružička, J., "The Determination of Glycerol in Water by Flow Injection Analysis--A Novel Way of Measuring Viscosity", Talanta, **23**, pg. 409, 1976.

38. Ružička, J., Hansen, E.H., and Zagatto, E.A.G. "Flow Injection Analysis. Part VII. Use of Ion-Selective Electrodes for Rapid Analysis of Soil Extracts and Blood Serum. Determination of Potassium, Sodium, and Nitrate", Anal. Chim. Acta, **88**, pg.1, 1977.
39. Hansen, E.H., Ružička, J. and Rietz, B., "Flow Injection Analysis. Part VIII. Determination of Glucose in Blood Serum with Glucose Dehydrogenase", Anal. Chim. Acta, **89**, pg.241, 1977.
40. Ružička, J., Hansen, E.H., and Mosbæk, H., "Flow Injection Analysis. Part IX. A New Approach to Continuous Flow Titrations", Anal. Chim. Acta, **92**, pg. 235, 1977.
41. Ružička, J. and Hansen, E.H., Flow Injection Analysis, 2^{ed} Ed., John Wiley & Sons, New York, 1985.
42. Gallagher, N.P., Hendrix, J.L., Milosavljević, E.B., and Nelson, J.H., "The Affinity of Carbon for Gold Complexes: Dissolution of finely Disseminated Gold Using a Flow Electrochemical Cell", Journal of the Electrochemical Society, **136**, 9, pg. 2546, September, 1989.
43. Nord, L. and Karlberg, B., "Extraction Based on the Flow Injection Principle. Part 5. Assessment with a Membrane Phase Separator for Different Organic Solvents", Anal. Chim. Acta, **118**, pg. 285, 1980.
44. Ramsing, A., Ružička, J., and Hansen, E.H., "A New Approach to Enzymatic Assay Based on Flow Injection Spectrophotometry with Acid-Base Indicators", Anal. Chim. Acta, **114**, pg. 165, 1980.
45. Landis, J.B., "Rapid Determination of Corticosteroids in Pharmaceuticals by Flow Injection Analysis", Anal. Chim. Acta, **114**, pg. 155, 1980.
46. Madsen, B.C., "Utilization of Flow Injection with Hydrazine Reduction and Photometric Detection for the Determination of Nitrate in Rain-Water", Anal. Chim. Acta, **124**, pg. 437, 1981.
47. Hansen, E.H. and Ružička, J., "The Principles of Flow Injection Analysis as Demonstrated by Three Lab Exercises", Journal of the Chemical Educator, **56**, pg. 677, 1979.
48. Christian, G.D. and Ružička, J., "Analysis Technique. Allows Online Control", Chemical Engineering, pg. 57, March 28, 1988.

49. Kuroda, R. and Mochizuki, T., "Continuous Spectrophotometric Determination of Copper, Nickel and Zinc in Copper-Base Alloys by Flow Injection Analysis", Talanta, **28**, pg. 389, 1981.
50. Karlberg, B., "Liquid-Liquid Extractions in Flow Injection Analysis", FI Astar Newsletter, **2**, pg. 1, 1985.
51. Ramasamy, S.M. and Mottola, H.A., "Repetitive Determination of Sulfur Dioxide Gas in Air Samples by Flow Injection and Chemical Reaction at a Gas-Liquid Interface", Anal. Chim. Acta, **54**, pg. 283, 1982.
52. Ramasamy, S.M., Jabbar, M.S.A., and Mottola, H.A., "Flow-Injection Analysis Based on Two Consecutive Reactions at a Gas-Solid Interface for Determination of Bromine and Chlorine", Anal. Chem., **52**, pg. 2062, 1980.
53. Krauskopf, K.B., "The Solubility of Gold", Economic Geology, **46**, pp. 858-870, 1951.
54. Bard, A.J., Parsons, R. and Jordan, R.M., Standard Potentials in Aqueous Solution, Marcel Dekker, Inc., New York, 1985.
55. Garrels, R.M. and Christ, C.L., Solutions, Minerals, and Equilibria, Freeman, Cooper, & Company, San Francisco, 1965.
56. Langmuir, D., Thermodynamic Data on Gold, Unpublished Compilations, 1978.
57. Wadsworth, M.E., "Hydrometallurgical Processes", in Rate Processes of Extractive Metallurgy, Sohn, H.V. and Wadsworth, M.E., Eds., Plenum Press, New York, 1979.
58. Laidler, K.J., Chemical Kinetics, 2nd Ed., McGraw-Hill Book Company, New York, 1965.
59. Mortimer, C.E., Chemistry. A Conceptual Approach, 3rd Ed., D. Van Nostrand, New York, 1975.
60. Calvert, J.G. and Pitts, J.N., Jr., Photochemistry, John Wiley & Sons, Inc., New York, 1966.
61. Okabe, H., Photochemistry of Small Molecules, John Wiley & Sons, Inc., New York, 1978.
62. Cundall, R.B. and Gilbert, A., Photochemistry, Appleton-Century-Crofts, New York, 1970.

63. Arnold, D.R., et al, Photochemistry: An Introduction, Academic Press, Inc., New York, 1974.
64. Legget, D.L., Chen, N.H. and Mahadevappa, D.S., "Rapid Determination of Residual Chlorine by Flow Injection Analysis", Analyst, 107, pg. 433, April, 1982.
65. Vogel, A.I., A Text-book of Quantitative Inorganic Analysis Including Elementary Instrumental Analysis, 3rd Ed., John Wiley & Sons, Inc., New York, 1961.
66. Braunstein, P. and Clark, R.J.H., "The Preparation, Properties, and Vibrational Spectra of Complexes Containing the AuCl_2^- , AuBr_2^- , and the AuI_2^- Ions", Journal of the Chemical Society, the Dalton Transactions, pg. 1845, 1973.
67. Perkin-Elmer Corporation, Operating Manual for the 2380 Atomic Absorption Spectrophotometer, 1982.
68. Atwood, G.E. and Curtis, C.H., "Hydrometallurgical Process for the Production of Copper", U.S. Patent No.3,785,944, January 15, 1974.
69. Stensholt, E.O., Zachariassen, H. and Lund, J.H., "The Falconbridge Chlorine Leach Process", Extraction Metallurgy '85, Institute of Mining and Metallurgy, Great Brittain, 1985.
70. Jennings, P.H., Stanley, R.W. and Ames, H.L., "Process for Purifying Molybdenite Concentrates", Canadian Patent No. 878999, Brenda Mines Ltd., Toronto, 1971.
71. Titov, A.A., Krohin, V.A. and Elutin, A.V., "Chlorination Method for Decomposing and Processing Titanoniobates of Rare-earth Metals", Extraction Metallurgy '89, Institution of Mining and Metallurgy, London, 1989.
72. Nelson, L.R. and Eric, R.H., "Kinetics and Mechanism of the Chlorination of Ferrochromium", Extraction Metallurgy '89, Institution of Mining and Metallurgy, London, 1989.
73. Habashi, F., "Kinetics and Mechanism of Gold and Silver Dissolution In Cyanide Solution", State of Montana Bureau of Mines and Geology, 1967.
74. Freeman, D.W. and Baglin, F.G. "A Raman Study of Gold-Oxygen Bonds From Several Tetracoordinate Complexes in Aqueous Solution", Inorganic Nuclear Chemistry Letters, 17, 161-167, 1981.

75. Cho, E.H. and Pitt, C.H. "The Adsorption of Silver Cyanide on Activated Charcoal", Metallurgical Transactions B, 10, 159-164, 1979.
76. McDougall, G.J. et al., "The Mechanism of the Adsorption of Gold Cyanide on Activated Carbon", J. South African Institute of Mining and Metallurgy, 80(9), 344-356, 1980.
77. Gallagher, N.P., Interaction of Gold Cyanide, Thiocyanate, Thiosulfate, and Thiourea Complexes with Carbon Matrices, University of Nevada, Reno, Masters Thesis, 1987.
78. Hiskey, J.B., Jiang, X.H. and Ramadorai, G., "Fundamental Studies on the Loading of Gold on Carbon in Chloride Solutions", paper presented at the Annual Meeting of the AIME-SME in Salt Lake City, February, 1990.
79. Nelson, J.H., personal communication of unpublished results.
80. Peters, E., "Applications of Chloride Hydrometallurgy to Treatment of Sulphide Minerals", Chloride Metallurgy, Benelux Metallurgie, Brussels, 1977.
81. Amadiantehrani, M., "Effects of Monochloride and Dichloride Salts on Ferric Chloride Leaching of Galena Concentrates", MS Thesis, University of Nevada--Reno, May, 1985.
82. Seidell, A., Solubilities of Inorganic and Organic Substances, 4th Ed., Linke, W.F., ed., American Chemical Society, Washington, D.C., 1958.
83. Marcus, R.A., "Chemical and Electrochemical Electron-transfer Theory", in Annual Review of Physical Chemistry, Vol. 15, Eyring, H., ed., Annual Reviews, Inc., Palo Alto, CA, pp. 155-196, 1964.
84. Klotz, I.M., Chemical Thermodynamics, W.A. Benjamin, Inc., New York, 1964.
85. Meissner, H.P. and Tester, J.W., "Activity Coefficients of Strong Electrolytes in Aqueous Solutions", Ind. Eng. Chem. Des. Proc. Dev., 11(1), 1972.
86. Meissner, H.P. and Kusik, C.L., "Activity Coefficients of Strong Electrolytes in Multicomponent Aqueous Solutions", AIChE Journal, 18(2), pg. 295, 1972.
87. Johnson, J.D. and Overby, R., "Stabilized Neutral Orthotolidine, SNORT, Colorimetric Method for Chlorine", Anal. Chem., 41(13), pp. 1744-1750, 1969.